ISSN 2500-0632 (ON-LINE)

ГОРНЫЕ НАУКИ И ТЕХНОЛОГИИ

MINING SCIENCE AND TECHNOLOGY

ТОМ VOL. 4, №2
2019

НАЦИОНАЛЬНЫЙ ИССЛЕДОВАТЕЛЬСКИЙ ТЕХНОЛОГИЧЕСКИЙ УНИВЕРСИТЕТ «МИСИС»
NATIONAL UNIVERSITY OF SCIENCE AND TECHNOLOGY MISIS

CONTENTS

ORIGINAL PAPERS

СОДЕРЖАНИЕ

ОРИГИНАЛЬНЫЕ СТАТЬИ

ORIGINAL PAPERS

DOI: 10.17073/2500-0632-2019-2-79-89

Effect of Operating Factors on Reliability of Stoping Complexes and Assessment of Reliability of their Elements

V. A. Troinich, A. A. Dubovsky, N. A. Vysotskaya

Joint Stock Company «Soligorsk Institute of Resources Saving Problems with Pilot ProductionSoligorsk, Minsk region, the Republic of Belarus, ✉onti@sipr.by

Abstract: For analyzing the dependence of face equipment failure on its length, two groups of elements are commonly considered. The first group includes all elements of shearer-loaders: conveyor drives, elements of pumping stations of powered supports, supports of face junctions with strikes and others. The second group includes all elements of powered support sections, linear sections of pan lines and scrapers of face scraper conveyors, electric cables of shearer-loaders, main pipelines of powered supports, etc. It is noted that the constancy of number of the first group elements linear variability of number of the second group elements do not uniquely determine the constancy or variability of the failure factor of the aggregate of the same type elements of the first or the second groups [1]. The plot of mean-time-between-failures (MTBF) of SL-500S stoping complex as function of face length is presented. Besides, the curve of the face (complex) length-dependence of average recovery) time (after failure of the SL-500S stoping complex time is shown. Analyzing the dependence of availability factor of stoping complexes on the face length showed that the length of stoping complexes is not a factor determining decrease in the MTBF and increase in the average recovery time. The plot of recovery time (after failure) of the SL-500S stoping complex as function of face length is shown. A formula is presented for assessing the cumulative effect, on the MTBF of SL-500S stoping complex, of its length and potash ore cuttability. The plot of correlation between the MTBF of SL-500S stoping complex and the face length/the potash ore cuttability is presented, which demonstrates that the complex length followed by the thickness of the extracted layer produce the greatest effect on the MTBF. The plot of the number of failures per day as a function of the maintenance factor of the SL-500C shearer-loader is presented. The plot demonstrates that the average number of failures of the SL-500C shearer-loader per day reaches a minimum and practically stabilize at values of the maintenance factor of 0.9–1.0, which correspond to three-shift production with one 6-hour maintenance shift per day.

Keywords: production face, stoping complex, face equipment, running hours, failure, recovery time, correlation coefficient, face length, thickness of extracted layer.

For citation: Troinich V. A., Dubovsky A. A., Vysotskaya N. A. Effect of operating factors on reliability of stoping complexes and assessment of reliability of their elements. *Mining Science and Technology*. 2019;4(2):79-89 (In Russ.). DOI: 10.17073/2500-0632-2019-2-79-89.

Влияние эксплуатационных факторов на надежность очистных комплексов и оценка надежности их элементов

Тройнич В. А., Дубовский А. А., Высоцкая Н. А.

Закрытое акционерное общество «Солигорский Институт проблем ресурсосбережения с Опытным производством», Солигорск, Минская область, Республика Беларусь,✉onti@sipr.by

Аннотация: В целях анализа зависимости на отказ забойного оборудования от его длины обычно рассматриваются две группы элементов. К первой группе отнесены все элементы очистных комбайнов: приводы конвейеров, элементы насосных станций механизированных крепей, крепей сопряжений лавы со штреками и другие. Ко второй группе относятся все элементы секций механизированной крепи, линейные секции рештачного става и скребки забойных скребковых конвейеров, электрические кабели комбайнов, магистральные трубопроводы механизированных крепей и т.п. Отмечено, что постоянство числа элементов первой группы или изменчивость по линейному закону числа элементов второй группы не определяют однозначно постоянство или изменчивость величины параметра потока отказов совокупности однотипных элементов первой (ω_{cI}) или второй (ω_{cII}) групп [1]. Представлен график зависимости времени наработки на отказ очистного комплекса СЛ-500С. В общем виде представлена зависимость величины среднего времени восстановления комплекса от его длины. Анализ зависимости коэффициента готовности очистных комплексов от длины лавы показал, что длина очистных комплексов не является фактором, определяющим степень снижения наработки на отказ и увеличения среднего времени восстановления. Проиллюстрирован график зависимости времени восстановления отказов очистного комплекса СЛ-500С от длины лавы. Представлена формула для оценки совместного влияния на наработку на отказ очистного комплекса, его длины и сопротивляемости калийной руды резанию. Приведен график корреляционной связи между наработкой на отказ комплекса СЛ-500С от длины лавы и сопротивляемостью калийных руд резанию, из которого видно, что наибольшее влияние на величину наработки на отказ очистных комплексов оказывает их длина, а затем и мощность вынимаемого пласта. Представлен график изменения количества отказов в сутки в зависимости от коэффициента технического обслуживания очистного комбайна СЛ-500С, из которого следует, что среднее количество отказов очистного комплекса СЛ-500С в сутки достигает минимума и практически стабилизируется при значениях коэффициента технического обслуживания 0,9–1,0, что соответствует трехсменному режиму по добыче и одной 6-часовой ремонтной смене в сутки.

Ключевые слова: очистной забой, очистной комплекс, забойное оборудование, наработка, отказ, время восстановления, коэффициент корреляции, длина лавы, мощность вынимаемого пласта.

Для цитирования: Тройнич В. А., Дубовский А. А., Высоцкая Н. А. Влияние эксплуатационных факторов на надежность очистных комплексов и оценка надежности их элементов. *Горные науки и технологии.* 2019;4(2):79-89. DOI: 10.17073/2500-0632-2019-2-79-89.

Introduction

Stoping mechanical equipment at potash mines has undergone significant quantitative and qualitative changes in recent years. Their development expanded from mechanization of certain basic operations of mineral extraction process in a face to complex mechanization and automation of the entire technical process. Integrated mechanization and automation of all processes of potash ore mining provides for the interaction and simultaneous operation of various machines and mechanisms united in a single technological process. Due to availability of many components and sequence of the equipment operation, insufficient reliability of individual machines and mechanisms leads to decreasing the useful (machine) operating time of the entire longwall set of equipment (LSE) [2]. The failure of any of the mechanisms of the LSE leads, as a rule, to complete stop of stoping in the face, therefore, the requirements for the reliability of each mechanism of the LSE are significantly increased.

Failures of stoping equipment (stoping machines, powered support, scraper conveyors) for the most part occurs during short-term single static and dynamic loading or long-term static loading. Fatigue failures caused by prolonged action of alternating-sign loads occur less frequently. This is due to the fact that stoping equipment is subject to high loads, which leads to the destruction of parts under stresses exceeding their endurance limit.

The main function of stoping facilities is the production of potash ore with the required productivity, determined based on the condition of ensuring a given load on ta production face and labor productivity of workers.

The effect of longwall face length on the level of reliability of longwall sets of equipment. Improving the mining sector and increasing the economic performance of potash mines is connected with permanent increasing length of the production faces, and, consequently, the length of longwall sets of equipment. As changing the length of the stoping equipment leads to changing length of the scraper chains of conveyors, the number of linear sections of their pan lines and sections of powered supports, as well as the operation mode of various elements, the reliability indicators of the same type face equipment will not remain constant [3].

For analyzing the dependence of face equipment mean-time-between-failures (MTBF) T on its length L, two or three groups of elements are usually considered [4], namely: elements whose number changes stepwise with significant change in the length of longwall sets of equipment, and elements whose number and length change in direct proportion to L.

The first group includes all elements of shearers (with the exception of electric cables), conveyor drives, elements of pumping stations for powered support, support for longwall face junction with drifts and other.

Total number of the first group elements:

$$N_{\mathrm{I}}(L)=\sum_{i=1}^{ч_{\mathrm{I}}} N_i=\mathrm{const}, \tag{1}$$

where N_i – is the number of elements of the i-th type; $ч_{\mathrm{I}}$ – the number of types of elements quantity of which is independent of L.

The second group includes all elements of powered support sections, linear sections of pan lines and scrapers of face scraper conveyors, electric cables of shearers, main pipelines of powered support, etc. [5].

The number of second group elements is dependent on the face equipment length by expression:

$$N_{\mathrm{II}}(L)=\sum_{j=1}^{ч_{\mathrm{II}}} K_j L, \tag{2}$$

where $K_j=\Delta N_j$ is coefficient of proportionality of changing total number of elements of the j-th type (for linear elements $K_j=1$); $ч_{\mathrm{II}}$ – the number of types of elements, quantity and length of which varies proportionally to L.

It should be noted that the constancy of number of the first group elements, or the linear variability of number of the second group elements do not uniquely determine the constancy or variability of the failure factor for the assembly of the same type elements of the first (ω_{cI})or second (ω_{cII}) groups [1]. The condition $\omega_{\mathrm{cI}}=\omega_i N_i=\mathrm{const}$ will be met if $\omega_i=\mathrm{const}$, which in turn is also determined by the mode of operation of the elements, which may deteriorate, improve, or remain unchanged with the growth of L [6].

The loading modes of the elements of shearers, with neglect of certain change in the their work dynamics can be considered practically independent of L, that is, in this case the condition $\omega_{\mathrm{cI}}=\omega_i N_i=\mathrm{const}$ is met. The value of the sudden failure factor of shearer electric cables normalized to 1 linear meter is also independent of L [7]. But due to the fact that the length of such elements varies in direct proportion to L, the failure factor for a combination of such elements is function of L, that is $\omega_{\mathrm{cII}}=\omega_j L$. The magnitude of the load of traction chains and drives of face scraper conveyors increases with growth of L, therefore, for the former, $\omega_{\mathrm{cII}}=\omega_j(L)$, and for the latter, $\omega_{\mathrm{cII}}=\omega_j(L)N_j$. With growth of L, the duration of the load on the elements of the powered support sections, which ensures operation of the roof-supporting sections, will increase. For this case, $\omega_{\mathrm{cII}}=\omega_j(L)\Delta N_j L$.

For elements of cyclic action, when the number of working cycles per unit time of effective operation of the longwall set of equipment [8] is inversely proportional to L, and the total number of elements increases in direct proportion to L, the failure factor of the aggregate of the same type elements remains unchanged. For example, the value ω_{c} for back-flow valves of the support valve of a hydraulic prop, the sections of which move after the shearer passage, does not depend on L and is equal to expression

$$\omega_{\text{c}} = \frac{60V_{\text{п}}}{\bar{n}_{\text{пер}}L}\Delta NL\,, \qquad (3)$$

where $V_{\text{п}}$ is the shearer axis velocity, m/min;

L – face length, m;

$\bar{n}_{\text{пер}}$ – MTBF of back-flow valve, measured by the number of movements of the support sections;

ΔN – the number of elements per 1 linear meter of the longwall set of equipment length.

In the general case, one can imagine

$$T(L) = \frac{1}{\sum_{i=1}^{ч_{\alpha}} \omega_{ci} + \sum_{j=1}^{ч_{\alpha}} \omega_{cj}(L)}, \qquad (4)$$

where ω_{ci} and ω_{cj} are the values of the failure factors for the assembly of elements of the i-th or j-th structural types;

$ч_{\alpha}$ – the number of types of elements for which $\omega_{ci} = \text{const}$;

ω_{cj} – the number of types of elements for which $\omega_{cj} = \phi(L)$.

In this case, it is understood that the ω_{ci} and ω_{cj} values are constant in time t.

The task of determining quantitative dependencies $T(L)$ for different types of face equipment systems was solved using correlation analysis. The obtained empirical dependences for longwall sets of equipment with narrow-web shearers for layer-by-layer and bulk (Fig. 1) extraction are described by the hyperbole equation of the form [9], min,

$$T(L) = \frac{\alpha}{L - C} + \text{в}. \qquad (5)$$

The values of indicators a, в and C (Table 1) were obtained by the algorithm and the computer program.

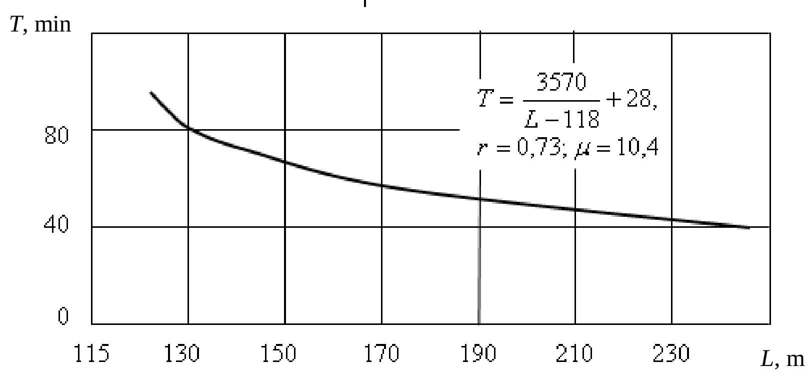

Fig. 1. Mean-time-between-failures of SL-500S stoping complex as function of face length

Table 1

Parameters of formula (5) and the correlation coefficient reliability indicators

Face equipment	Measurement limits L, m	Parameter value			Correlation ratio r	Reliability of correlation ratio μ
		α	в	C		
SL-500S	150…250	1070	28	118	0.73	10.4

The values of the obtained correlation ratios given in Table 1 indicate good correlation between T and L.

According to Lyapunov's theorem [3, 4], if $\mu \geq 3$, it can be argued that the relationship between the studied quantities is reliable and the $T(L)$ dependence is objective.

To establish the nature of the dependence of the average recovery time of a longwall set of equipment on its length, it is also advisable to consider two types of failures, the duration of the elimination of which does not depend on L. The time for eliminating failures of the end elements of longwall set of equipment on the side of the stoping face, where the repairman (duty wireman) is usually located, does not depend on the length [10, 11]. The time for eliminating failures of the longwall set of equipment elements, when no spare parts or special tools are required, also practically does not depend on L. This may include failures such as "a shearer – conveyor misalignment", "tilt" and "skew" of a support section. Such failures are usually eliminated by the stoping face workers, or they are liquidated without waiting for the repairman to arrive.

In general terms, the dependence of the average recovery time of a longwall set of equipment on its length is given by

$$T_{\text{в}}(L) = \frac{\sum_{i=1}^{n_i} t_{\text{в}i} + \sum_{j=1}^{n_j} t_{\text{в}j\text{пост}} + \sum_{j=1}^{n_j} t_{\text{в}j}(L)}{n_i + n_j}, \quad (6)$$

where $t_{\text{в}i}$ – is the time of eliminating the i-th failure, when the time is independent of L;

$t_{\text{в}j\text{пост}}$ – a constant component of the failure eliminating time, when the time depends on L;

$t_{\text{в}j}(L)$ – the variable component of the j-th failure eliminating time;

n_i, n_j – the total number of failures of the i-th and j-th types.

The constant component of the j- th failure eliminating time $t_{\text{в}j\text{пост}}$ includes the time of repair or replacement of an element, as well as the time spent on testing equipment after the repair and downtime for organizational reasons.

The variable component $t_{\text{в}j}(L)$ takes into account the time spent on failure detection, consisting of the time the repairman moves along the face and the failure search, and the time for the necessary spare part delivery. Changing the variable component of the j-type failure elimination time is described by the following expression:

$$t_{\text{в}j}(L) = \frac{\alpha}{V_{\text{раб}}} L + \Delta t_{\text{в}j}(L), \quad (7)$$

where $V_{\text{раб}}$ – the average repairman velocity of travel along the face;

$\Delta t_{\text{в}j}(L)$ – additional time for the spare part delivery, not combined with the repairman traveling;

α – coefficient taking into account the most probable way of the repairman traveling.

For existing longwall sets of equipment, for the face equipment element failure elimination, the value α can be taken equal to 0.5.

Experimental studies have shown that for longwall set of equipment the dependence of the average recovery time on the longwall face length is rectilinear (Fig. 2), min,

$$T_{\text{в}} = \alpha + eL. \quad (8)$$

The values of α and e parameters in formula (8) for the investigated types of the face equipment, as well as the obtained values of the correlation coefficients r and reliability indicators of the correlation coefficients μ are shown in Table 2.

Table 2

Parameters of formula (8) and the correlation coefficient reliability indicators

Face equipment	Measurement limits L, m	Parameter value		Correlation coefficient r	Correlation coefficient reliability μ
		α	e		
SL-500S	150…250	−22	0.31	0.53	3.7

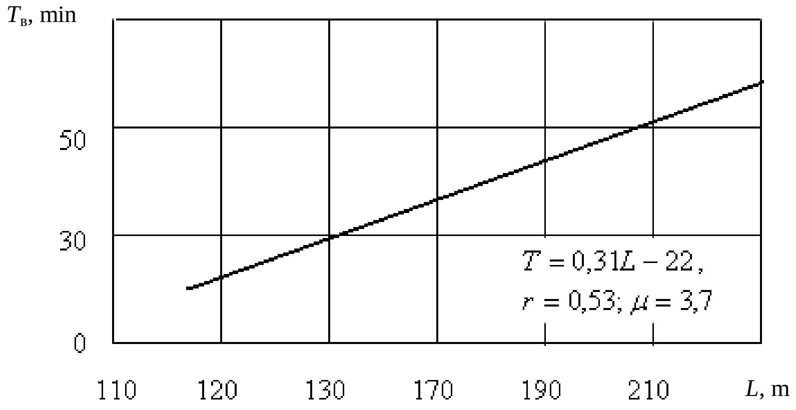

Fig. 2. SL-500S stoping complex recovery time ($T_в$) (after failure) as function of face length (L)

Decreasing the MTBF and an increasing the average recovery time with growth of L results in decreasing the availability factor (9), as

$$K_r(L) = \frac{T(L)}{T(L) + T_в(L)}. \qquad (9)$$

An analysis of the dependence of the availability factor of longwall sets of equipment on the face length showed that the LSE length is not a factor that uniquely determines the degree decreasing the MTBF and increasing the average recovery time.

Influence of potash ore cuttability and layer thickness on the face equipment reliability.

When extracting potash ore by longwall set of equipment, the main factor restraining the production development is rock cuttability A, kN/m [13].

Using the pair correlation method allowed determining a relationship between the MTBF and the average recovery time of face equipment on the one hand, and individual mining, geotechnical, and geological factors on the other hand.

To determine the joint effect of a number of factors on one dependent variable, the multiple correlation method was used, which makes it possible to identify the joint effect of a combination of the listed factors on face equipment reliability, to separate the major factors from the minor ones, and to determine the contribution of different factors in the formation of reliability indicators.

The SL-500S longwall set of equipment factors variation limits, their average values, and standard deviations are given in Table 3.

The joint effect of a longwall set of equipment length and potash ore cuttability on the MTBF is estimated by formula, min,

$$T = \frac{17100}{L} + \frac{2200}{A - 75} - 59, \qquad (10)$$

at $R_{T,L,A} = 0{,}65 \pm 0{,}065$; $R_{T,\,L,\,A} = 0{,}65 \pm 0{,}065$; $d = 0{,}42$; $\mu = 9{,}6$.

Table 3

Determination of the SL-500S stoping complex factors variation limits

Factor description	UoM	Average factor value	Factor variation range
Face length $L_{л}$, m	150	126–250	33
Potash ore cuttability A, kN/m	265	128–196	20

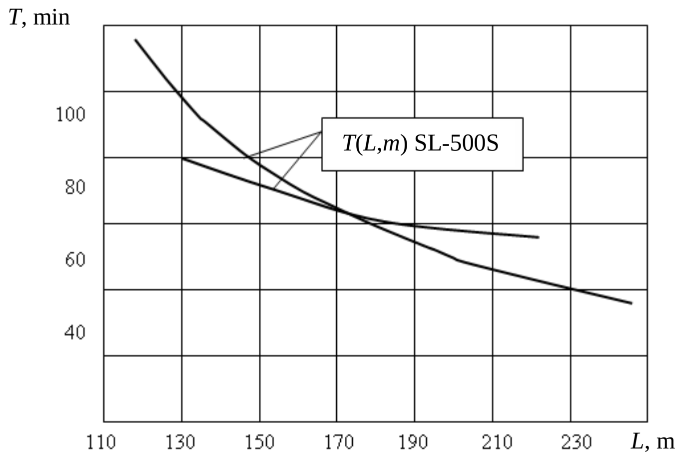

Fig. 3. Correlation between the mean-time-between-failures of SL-500S stoping complex and the face length/the potash ore cuttability

The high values of the multiple correlation coefficients R and the determination coefficients d in the equations indicate that the major factors that influence the MTBF of the considered types of face equipment are taken into account and the relationship T with mining, geotechnical, and geological conditions of LSE operation are effectively reflected [14].

To determine the degree of influence of each of the considered factors on the MTBF of the SL-500S longwall set of equipment based on correlation equations (10), specific correlation equations of the relationship between the studied attributes were found [15]. At average values of the arguments (attributes) listed in Table 3, the specific equations for the SL-500S LSE are as follows, min,

$$T(L)=\frac{3050}{L-93}+10, \qquad (11)$$

$$T(A)=\frac{2100}{A-80}+12. \qquad (12)$$

The graphs constructed based on equations (11), (12) are shown in Fig. 3.

The graph obviously demonstrates that the LSE length followed by the thickness of the extracted layer produce the greatest effect on the MTBF.

The joint influence of the considered factors on the average recovery time for the SL-500S LSE is characterized by correlation equations, min,

$$T_{в}=0{,}3L-23m-1, \qquad (13)$$

at $R=0{,}65\ldots0{,}14$; $\mu=6{,}2$; $d=0{,}42$.

From equation (13), specific correlation equations can be obtained, which have the following form for the SL-500S LSE, min,

$$T_{в}(L)=0{,}3L-16, \qquad (14)$$

$$T_{в}(m)=66-23m. \qquad (15)$$

An analysis of equations (14), (15) shows that, same to the case of MTBF, the face length is the factor that has the most significant effect on the average recovery time of the face equipment.

Influence of a stoping face operation condition on reliability of the face equipment.

It was found that the probability of failure-free operation of a LSE decreases with increasing intermaintenance period. In [16], it is indicated that the number of gradual failures of the face equipment is significantly affected by the intermaintenance period and the labor input of a maintenance team (man-hour). The probability of wear-out failures at different maintenance team man-hour values and maintenance frequency for the SL-500S longwall set of equipment can be assessed using the data given in Table 4.

Processing of statistical data for the SL-500S LSE made it possible to obtain a maintenance factor $K_{\text{ТО}}$ and determine the number of failures [17] that occur for a day, the analysis of which showed that the stoping face operation condition/mode significantly affects the LSE reliability.

The correlation equation for the relationship between the number of failures per day $n_{\text{сут}}$ and the factor $K_{\text{ТО}}$ value is given by:

$$n_{\text{сут}} = \frac{5{,}1}{K_{\text{то}} + 0{,}5} - 0{,}6, \qquad (16)$$

at $K_{\text{то}} = 0 - 1{,}22$; $r = 0{,}74$; $\mu = 8{,}3$ and maintenance labor input equal to 18–24 man-hour.

The number of failures per day as function of maintenance factor of SL-500S longwall set of equipment is shown in Fig. 4.

Table 4

Probability of wear-out failures at different maintenance man-hour values and maintenance frequency for the SL-500S stoping complex

Maintenance team labour input, man-hours	Probability of wear-out failures during intermaintenance period $t_{\text{мр}}$, h			
	18	42	66	144
18	0.030	0.080	0.145	0.495
30	0.010	0.035	0.095	0.245
42	0.001	0.010	0.020	0.115

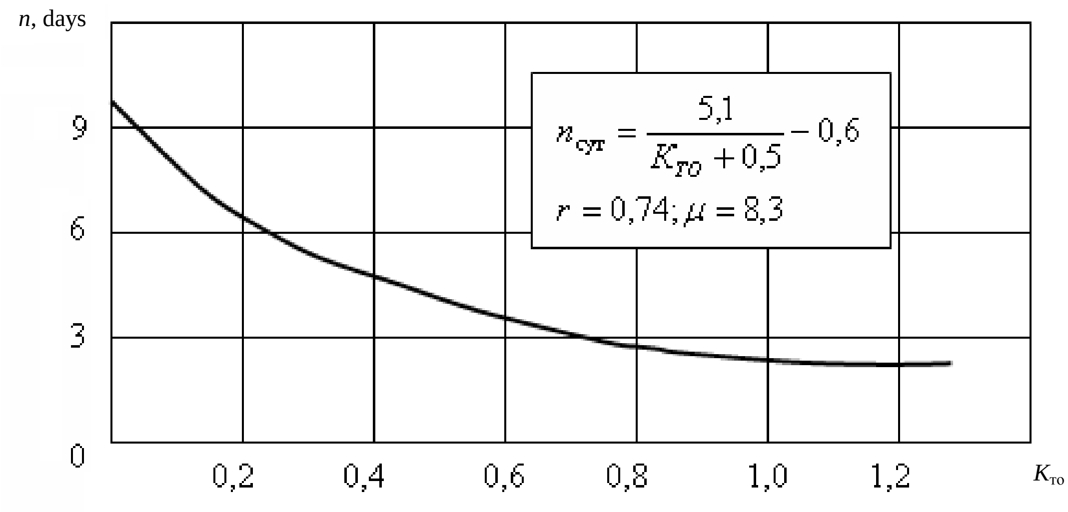

Fig. 4. Number of failures per day as function of maintenance factor of SL-500S stoping complex

The graph in Fig. 4 demonstrates that the average number of failures of the SL-500S LSE per day reaches a minimum and practically stabilizes at values of the maintenance factor $K_{\text{ТО}} = 0.9 - 1.0$ that correspond to three-shift production mode with one 6-hour maintenance shift per day. The studies allowed establishing that for different types of face equipment there exist a limit of increasing the average intermaintenance period at the expense of increasing the maintenance team labor input (man-hour). This limit depends on complexity of the equipment used [18, 19].

Conclusion

Among the mining and geological factors, the most significant impact on LSE shearer faultless performance is produced by the potash ore cuttability, and on reliability of the LSE as a whole, by the thickness. Increasing these parameters results in decreasing the face equipment MTBF. The average face equipment recovery time decreases with increasing the layer thickness.

The change in the failure factor of complex face equipment depending on its mechanical life is characterized in the general case by a sequence of typical diagrams with increasing value of the failure factor in stationary sections.

Analyzing the dependence of availability factor of longwall set of equipment on the face length showed that the LSE length is not a factor determining decrease in the MTBF and increase in the average recovery time [20].

The studies allowed establishing that for different types of face equipment there exists a limit of increasing the average intermaintenance period at the expense of increasing the maintenance team labor input (man-hour).

References

1. Kurbatova O. A. Reliability of mining machinery. Textbook / Kurbatova O. A., Ksendzenko L. S., Nikolaychuk D. N. DVSTU, DVSTU Publ., 2005, 88 p. (in Russ.).

2. [Electronic source] Available at: http://jc.surgu.ru/attachments/article/133/2-kom.pdf) (acc. 30.10.2017).

3. Topchiev A. V. The effect of length of stoping complexes on their reliability. / Topchiev A. V. [et al.]. Proceedings. Moscow, MGI Publ., 1978, pp. 3-65 (in Russ.).

4. Ryzhov P. A. Some applications of probability theory and mathematical statistics in mining. Coal of Ukraine. Moscow, 1977, no. 5, pp. 7-12 (in Russ.).

5. Meares P. Ion membranes: principles, production and processes / Ion Exchange: Sci. and Techol.: Proc. NATO Adv. Study Inst., Troja, July 14-26, 1985. Dordrecht e. a., 1986, pp. 529-558.

6. Gorindan K. R., Nazayanan P. K. Bench scale studies of demineralysation by electrodialysis. Proc. 7th Int. Symp. Fresh Water Sea. Amsterdam, 1980, № 2, Athens, 1980, p. 59.

7. Shklyar V. N. Reliability of control systems: Textbook. Federal Agency for Education, "Tomsk Polytechnic University", Tomsk Polytechnic University Publ., 2009, 126 p. (in Russ.).

8. Kin T. Materials Science of Syntetic Membranes ACS, Washington, 1985, pp. 365-405.

9. Dukhin S., Mishuk N. Intensifikation of electrodialysis based on electroosmosis of second kind III. Membr. Sci., 1993, vol. 79, pp. 199-210.

10. Selvey C., Reiss H. Ion transport in inhomogeneous ion exchange membranes // Ibid., 1985, vol. 23, pp. 11-27.

11. Kakharov S.K. Improving reliability of hydraulic equipment of drilling rigs for drilling geotechnical boreholes. Cand. Sci. (25.00.14 Engineering) Dissertation. Moscow, 2015, 104 p. (in Russian).

12. Ryzhov P. A. Mathematical statistics in mining. Moscow, MIRGEM Publ., 1972, 153 p. (in Russ.).

13. Shcherba V. Ya. The study of the effect of cutting tool parameters on cutting forces. / Shcherba V. Ya., Starovoitov V. S., Starovoitov Yu. V. Hardening, recovery, and maintenance at the turn of the century. Proceedings of International. scientific and technical conference. Novopolotsk, 2001, pp. 710-713 (in Russ.).

14. Bergner D. Reduction of by-product formation in alkali chloride membrane electrolysis // J. ApLL. Electrochem., 1990, vol. 20, № 5, pp. 716-722.

15. Sarradzin J. Le developpement industriel contemporain des membranes exchangeuses dliones. Bull, union Phys., 1986, vol. 80, № 688, pp. 1427-1447.

16. Lipkovich S. M. Rational daily operating mode of KM-87 complex based on the conditions of operational reliability. / Lipkovich S. M., Miroshnikov S. I. Coal of Ukraine. Moscow, 1977, no. 5, pp. 7-12 (in Russ.).
17. Mouritz K. A., Hopfinger A. J. II J. Modern aspects of electrochem. 1982. Vol. 14. Pp. 425-433.
18. Kuleshov A. A. Reliability of mining machinery and equipment. Textbook. / Kuleshov A. A., Dokukin V. P. Federal Agency for Education, State Educational Institution of Higher Professional Education St. Petersburg State Mining Institute named after G.V. Plekhanov (Technical University) Publ. St. Petersburg, 2004, 104 p. (in Russ.).
19. Zhilinsky V. V. Electrochemical wastewater treatment and water treatment: Summary of lectures for students of specialty 1-48 01 04 "Technology of electrochemical production". BSTU Publ. Minsk, 2013, 191 p. (in Russ.).
20. Gronovski A. A., Yeager A. L. Factors which affect the permselectivity of Nation membranes in chlor-alcali ellectrolysis // J. Electrochem. Soc., 1991, 138, № 9, pp. 2690-2697.

Библиографический список

1. Курбатова О. А. Надежность горных машин: учеб.-метод. пособие / О. А. Курбатова, Л. С. Ксендзенко, Д. Н. Николайчук. ДВГТУ: Изд-во ДВГТУ, 2005. 88 с.
2. [Электронный ресурс]. Режим доступа: http://jc.surgu.ru/attachments/article/133/2-kom.pdf. Дата доступа: 30.10.2017.
3. Топчиев А. В. Влияние длины очистных комплексов на надежность / А. В.Топчиев [и др.]: Сб. трудов. М.: МГИ, 1978. С. 53-65.
4. Рыжов П. А. Некоторые приложения теории вероятностей и математической статистики в горном деле / П. А. Рыжов // Уголь Украины. 1977. № 5. С. 7-12.
5. Meares P. Ion membranes: principles, production and processes / Ion Exchange: Sci. and Techol.: Proc. NATO Adv. Study Inst., Troja, July 14-26, 1985. Dordrecht e. a., 1986. Pp. 529-558.
6. Gorindan K. R., Nazayanan P. K. Bench scale studies of demineralysation by electrodialysis. Proc. 7^{th} Int. Symp. Fresh Water Sea. Amsterdam, 1980, № 2, Athens, 1980. P. 59.
7. Шкляр В. Н. Надежность систем управления : учеб.пособие / В. Н. Шкляр; Федеральное агентство по образованию «Томский политехнический университет». Изд-во Томский политехн. ун-т, 2009. 126 с.
8. Kin T. Materials Science of Syntetic Membranes ACS, Washington. 1985. Pp. 365-405.
9. Dukhin S., Mishuk N. Intensifikation of electrodialysis based on electroosmosis of second kind III. Membr. Sci., 1993. Vol. 79. Pp. 199-210.
10. Selvey C., Reiss H. Ion transport in inhomogeneous ion exchange membranes // Ibid., 1985, vol. 23, pp. 11-27.
11. Кахаров С. К. Повышение надежности гидравлического оборудования буровых установок для сооружения геотехнологических скважин: дис. … канд. техн. наук: 25.00.14 / С. К. Кахаров. Москва, 2015. 104 с.
12. Рыжов П. А. Математическая статистика в горном деле / П. А. Рыжов. М.: МИРГЭМ, 1972. 153 с.
13. Щерба В. Я. Исследование влияния параметров режущего инструмента на усилия резания / В. Я. Щерба, В. С. Старовойтов, Ю. В. Старовойтов // Упрочнение, восстановление и ремонт на рубеже веков: Сб. научн. трудов междунар. науч.-техн. конф. Новополоцк, 2001. С. 710-713.
14. Bergner D. Reducation of by-product formation in alkali chloride membrane electrolysis // J. ApLL. Electrochem., 1990, vol. 20, № 5, pp. 716-722.
15. Sarradzin J. Le developpement industriel contemporain des membranes exchangeuses dliones. Bull, union Phys., 1986, vol. 80, № 688, pp. 1427-1447.
16. Липкович С. М. Рациональный суточный режим работы комплекса КМ-87 из условий эксплуатационной надежности / С. М. Липкович, С. И. Мирошников // Уголь Украины. 1977. № 5. С.7-12.
17. Mouritz K. A., Hopfinger A. J. II J. Modern aspects of electrochem. 1982, vol. 14, pp. 425-433.
18. Кулешов А. А.Надежность горных машин и оборудования: учеб. пособие / А. А. Кулешов, В. П. Докукин. Федеральное агентство по образованию, государственное образовательное учреждение высшего профессионального образования Санкт-Петербургский государственный горный институт им. Г.В. Плеханова (технический университет). СПб., 2004. 104 с.
19. Жилинский В. В. Электрохимическая очистка сточных вод и водоподготовка: Конспект лекций для студентов специальности 1-48 01 04 «Технология электрохимических производств» / В.В. Жилинский. БГТУ. Минск, 2013. 191 с.
20. Gronovski A. A., Yeager A. L. Factors which affect the permselectivity of Nation membranes in chlor-alcali ellectrolysis // J. Electrochem. Soc., 1991. 138, № 9, pp. 2690-2697.

Information about the Authors

V. A. Troinich – First Deputy Technical Director, Joint Stock Company «Soligorsk Institute of Resources Saving Problems with Pilot Production»; Soligorsk, Minsk region, the Republic of Belarus.

A. A. Dubovsky – Assistant of Technical Director for Material and technical supply, Joint Stock Company «Soligorsk Institute of Resources Saving Problems with Pilot Production»; Soligorsk, Minsk region, the Republic of Belarus.

N. A. Vysotskaya – Deputy Head of Department of scientific and technical information, Joint Stock Company «Soligorsk Institute of Resources Saving Problems with Pilot Production»; Soligorsk, Minsk region, the Republic of Belarus, onti@sipr.by.

Информация об авторах

Тройнич В. А. – первый заместитель технического директора, Закрытое акционерное общество «Солигорский Институт проблем ресурсосбережения с Опытным производством», г. Солигорск, Минская область, Республика Беларусь.

Дубовский А. А. – помощник технического директора по материально-техническому снабжению, Закрытое акционерное общество «Солигорский Институт проблем ресурсосбережения с Опытным производством», г. Солигорск, Минская область, Республика Беларусь.

Высоцкая Н. А. – заместитель начальника отдела научно-технической информации, Закрытое акционерное общество «Солигорский Институт проблем ресурсосбережения с Опытным производством», г. Солигорск, Минская область, Республика Беларусь, onti@sipr.by.

ORIGINAL PAPERS

DOI: 10.17073/2500-0632-2019-2-90-102

Experimental Studies of Effect of Shearer Auger Operating Device Effective Width on Effectiveness of Loading Process

O. E. Shabaev[1], P. P. Zinchenko[1], A. V. Meznikov[2]

[1]Donetsk National Technical University, Donetsk, Ukraine, ✉ pawel.zin4encko@yandex.ru;
[2]State Enterprise "Donuglemash", Donetsk, Ukraine

Abstract: Intensification of coal mining from mine seams of 0.55–1.20 m thick requires increasing efficiency of loose coal loading that may be achieved by selecting the optimal parameters of auger operating device of a shearer. The most reliable way to determine effect of the auger parameters on the energy parameters of the shearer operation is experimental research in actual operating conditions. As the subjects of the research, we selected up-to-date UKD400 and UKD200-500 shearers, operating in representative conditions of the Krasny Partizan mine of SE SVERDLOVANTRATSIT and Ternovskaya mine of DTEK PAVLOGRADUGOL PJSC. An adaptive method for specific mining operating conditions is proposed for determining the specific energy consumption of the shearers on material disruption and loading for thin seams in actual operating conditions based on fixing the values of currents of the cutting drive motors. Based on processing of the experimental data, an indicative dependence of the power for rock mass loading on the feed rate and the effective width of the operating device is determined. Increasing the auger effective width results in increasing the loading power and specific energy consumption. At the same time, the higher the shearer feed rate, the greater the growth of the loading power and specific energy consumption. This is due to the beginning of the process of loose rock mass circulation, and the larger the auger effective width, the more intensive the circulation process, and at the lower feed rate of the shearer the process starts. A method is proposed for selecting the auger optimum effective width based on the criteria of minimum specific energy consumption and maximum commercial productivity.

Keywords: shearer, auger operating device, productivity, shearer feed rate, specific energy consumption, loading power, effective width.

For citation: Shabaev O. E., Zinchenko P. P., Meznikov A. V. Experimental studies of effect of shearer auger operating device effective width on effectiveness of loading process. *Mining Science and Technology*. 2019;4(2):90-102 (In Russ.). DOI: 10.17073/2500-0632-2019-2-90-102.

Экспериментальные исследования влияния ширины захвата шнекового исполнительного органа комбайна на эффективность процесса погрузки

Шабаев О. Е.[1], Зинченко П. П.[1], Мезников А. В.[2]

[1]ГОУ ВПО «Донецкий национальный технический университет», Донецк, Украина,
✉pawel.zin4encko@yandex.ru;

[2]ГП «Донуглемаш», Донецк, Украина

Аннотация: Интенсификация добычи угля из шахтопластов мощностью 0,55–1,20 м требует повышения эффективности процесса погрузки разрушенного угля, что может быть обеспечено путем выбора оптимальных параметров шнекового исполнительного органа очистного комбайна. Наиболее достоверным способом установления влияния параметров шнека на энергетические параметры работы очистного комбайна являются экспериментальные исследования в реальных условиях эксплуатации. Объектами исследования выбраны очистные комбайны нового технического уровня УКД400 и УКД200-500, эксплуатирующиеся в представительных условиях шахт «Красный партизан» ГП «СВЕРДЛОВАНТРАЦИТ» и «Терновская» ПАО «ДТЭК ПАВЛОГРАДУГОЛЬ» соответственно. Предложена адаптивная под горнотехнические условия работы методика определения удельных энергозатрат разрушения и погрузки очистных комбайнов для тонких пластов в реальных условиях эксплуатации на основе фиксации значений токов двигателей приводов резания. После обработки экспериментальных данных установлена зависимость мощности на погрузку горной массы от скорости подачи и ширины захвата исполнительного органа показательного вида. С увеличением ширины захвата шнека мощность и удельные энергозатраты на погрузку возрастают тем интенсивнее, чем выше скорость подачи очистного комбайна. Это обусловлено началом процесса циркуляции разрушенной горной массы, при этом, чем больше ширина захвата шнека, тем процесс циркуляции интенсивнее и наступает при меньших значениях скорости подачи очистного комбайна. Предложен метод выбора рациональной ширины захвата шнека по критериям минимальных удельных энергозатрат и максимальной технической производительности.

Ключевые слова: очистной комбайн, шнековый исполнительный орган, производительность, скорость подачи комбайна, удельные энергозатраты, мощность на погрузку, ширина захвата.

Для цитирования: Шабаев О. Е., Зинченко П. П., Мезников А. В. Экспериментальные исследования влияния ширины захвата шнекового исполнительного органа комбайна на эффективность процесса погрузки. *Горные науки и технологии.* 2019;4(2):90-102. DOI: 10.17073/2500-0632-2019-2-90-102.

Articulation of issue

The main energy resource of the Donetsk region is coal, whose reserves, according to the DonUGI, are about 6.84 billion tons. The bulk of these reserves (about 83.2 %) is concentrated in seams 0.55–1.2 m thick [1].

Almost all of the Donbass coal seams have adverse mining & geological and geotechnical conditions and mode of occurrence. They are characterized by variable hypsometry, the presence of rock partings and solid inclusions in a coal mass [1]. These factors almost completely exclude the possibility of coal extraction using plow and modular complexes that leads to widespread use of shearers with auger operating devices as parts of powered complexes [1–5]. All of the above suggests the need for researches in the field of design and construction of shearers of a new generation, capable of working effectively in conditions of thin shallow seams.

The process of coal mining from seams 0.55–1.2 m thick by shearers can be described as highly energy-intensive [2–3]. This is due to the low loading capacity of the auger operating devices, which limits the shearer axis velocity within 2–5 m/min and as a result leads to low productivity of the shearer [2–3]. Intensification of coal mining from mine seams 0.55–1.2 m thick requires increasing efficiency of loosened coal loading that may be achieved by selecting the optimal parameters of auger operating device of a shearer.

Review of researches and publications

The issue of creating highly efficient stoping equipment was studied by many scientists [2–22]. The issues considered in [2, 3] relate to the design of narrow-web shearers operating in conditions of thin shallow seams extraction. In [4], the principles of designing the shearer traveling mechanisms are described. In work [5], the general tasks and principles of designing and engineering of mining machines and complexes of a new technical level are given. It was found [6–13] that auger operating devices, used in shearers for extracting thin and very thin seams, have greater breaking-down productivity than loosened rock mass loading productivity. The authors of works [14–22] were engaged in solving the problem of optimizing the loading process with auger operating devices based on determining the rational values of the geometric parameters of the augers and operating parameters of the shearer. The works [23–26] are aimed at solving the problems of automation of coal mining by shearers. In [27–36], an experience was described in the use of pulsed jets of a working fluid for breaking-down of a rock mass. However, there is no reliable data on the regularities of changing the energy parameters of a shearer operation when extracting thin shallow seams depending on the auger operating device width. The most reliable way to obtain the actual values of the energy parameters of the stoping equipment operation is experimental study in actual operating conditions.

The research aim (tasks)

Thus, the aim of this study is to determine regularities of effect of the auger operating device parameters on coal loading energy performance when extracting thin shallow seams.

The experiment description and findings

As the subjects of the study, up-to-date drum shearers UKD400 and UKD200-500 were selected, operating in representative conditions of the Krasny Partizan mine of the SE SVERDLOVANTRATSIT (Dolzhansky k^1_5 seam) and Ternovskaya mine of DTEK PAVLOGRADUGOL PJSC (C^B_5 seam). Summary on technical specifications of the considered shearers are given in Table 1.

In Fig. 1, breaking-down schematics and seam structures in conditions of the experimental studies of UKD400 and UKD200-500 shearers operation are shown.

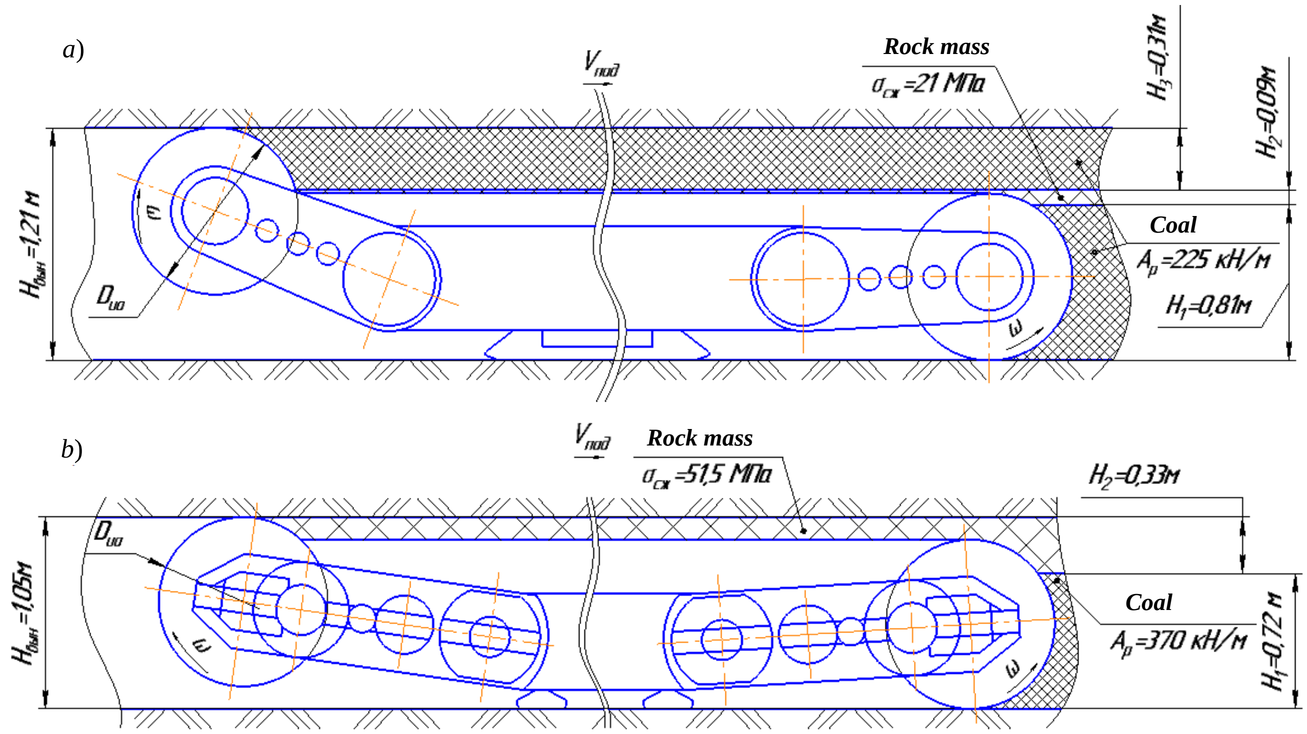

Fig. 1. Schematics of rock mass loosening by UKD400 (*a*) and UKD200-500 (*b*) shearers

Table 1

Technical specifications of the considered shearers

Parameter	Shearer type	
	UKD400	**UKD200-500**
Type of motor of operating device drive	EKV4-200V	SG7W490L-4
Rated power of cutting drives $P_{ном}$, kW	2×200	2×250
Motor rated current $I_{ном}$, A	129	155
Power factor cos φ, relative units	0.837	0.880
Operating device diameter $D_{ио}$, m	0.9	
Cut (web) width $B_з$, m	0.7	0.8
Auger blade angle of lead (by blade) $\alpha_п$, degrees	15°38′	13°54′
Auger angular rate ω, sec^{-1}	8.17	8.31

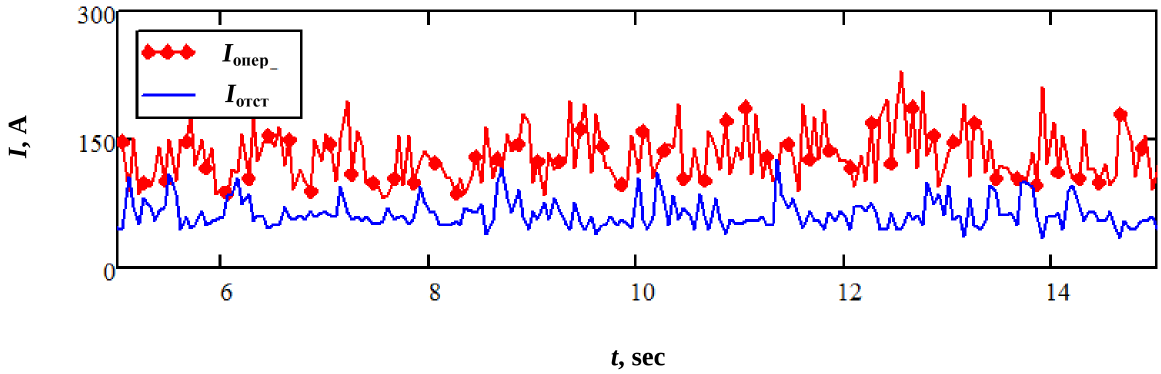

Fig. 2. A fragment of recording the values of motor currents of leading ($I_{опер}$) and lagging ($I_{отст}$) behind drives of UKD400 shearer operating devices

Table 2

Data of the experimental studies of UKD400 and UKD200-500 shearers operation

Parameter	Shearer type						
	UKD400			**UKD200-500**			
Discretization interval Δ*t*, sec	0.05			0.2			
Number of sections *n*	3			4			
Measured section length *l*, m	1.5			6.0	7.5		
Time of passing a measured section length t_j, min	0.400	0.330	0.283	1.500	1.800	1.700	1.180
Axis velocity V_n, m/min	3.75	4.50	5.30	4.00	4.20	4.40	6.40
The value of the electric motor off-load current according to the experimental data $I_{хол.ход}$, A	45			65			
The average value (for the measuring period) of the current of the leading operating device motor $I_{ср.опер}$, A	73.6	129.5	114.2	166.1	190.1	183.2	190.9
The average value (for the measuring period) of the current of the lagging operating device motor $I_{ср.отст}$, A	50.1	64.0	57.9	7.9	10.1	9.3	7.3

According to [41], the load on the shearer operating devices is determined taking into account the coal cuttability. Therefore, hardness factors of a rock mass to be broken down (cut) were brought to $\overline{A}_p$ value based on the data presented in [1, 37].

The weighted average value of coal cuttability when cutting by each k-th operating device, kN/m,

$$\overline{A}_{\text{р},k} = \frac{\sum_{i=1}^{m_k} \overline{A}_i H_i}{H_{k.\text{ио}}},$$

where $\overline{A}_i$, H_i – coal cuttability and thickness of the i-th member of rock mass cut by the k-th auger operating device;

$H_{k.\text{ио}}$ – the extracted thickness of rock mass cut by the k-th auger;

m_k – the number of members cut by the k-th auger operating device.

In the course of experimental studies of the shearer operation, the average current values of the electric motors of each shearer cutting drive in increments Δt were recorded using a multichannel energy quality recorder-analyzer [38]. The face was conditionally divided into n sections differing in length l m. At the same time, the time of the passage of each section t_j was recorded, sec ($j = 1..n$).

As an example, Figure 2 shows a fragment of recording the values of the UKD400 shearer auger operating device drive currents when passing a face section 1.5 m long at a speed of 4.5 m/min.

The results of preliminary processing of the experimental research data are given in Table 2.

Shearers of a new technical level have an individual motor for each operating device drive. Then, according to the methodology proposed in [39], the actual value of the power of cutting and loading of rock mass on each k-th operating device drive motor can be determined from the expression, kW:

$$P_k = P_{\text{ном}} \frac{I_{\text{ср}.k} - I_{\text{хол.ход}}}{I_{\text{ном}}} \cos\varphi.$$

According to the operating conditions of shearers with auger operating device for thin shallow seams, the leading auger cuts a coal member adjacent to the seam bottom and loads the broken-down mass, while the lagging auger performs mainly the function of cutting the remaining coal member (Fig. 1). With this in mind, the value of the cutting power on the leading auger $P_{\text{рез.опер}}$ can be determined based on the power values on the lagging auger $P_{\text{отст.}}$ taking into account cutting the coal mass of different average coal cuttability, the factors of coverage of auger face and decreasing stability of the coal mass, kW:

$$P_{\text{рез.опер}} = \frac{P_{\text{отст.}} \overline{A}_{\text{р.отст.ио}}}{k_{\text{осл}} k_{\gamma.\text{охв}} \overline{A}_{\text{р.опер.ио}}},$$

where $k_{\text{осл}}$ – factor of decreasing stability of coal mass; $k_{\gamma.\text{охв}}$ – factor of coverage of auger face.

Then the value of the loading power on the leading operating device $P_{\text{погр.опер}}$ can be found from the expression, kW:

$$P_{\text{погр.опер}} = P_{\text{опер}} - P_{\text{рез.опер}},$$

Determining the value of specific energy consumption requires determining the actual productivity on the extraction for the period under consideration. The performance of the k-th operating device can be determined from the expression, t/min:

$$Q_k = H_{k.\text{ио}} B_{\text{з}} V_{\text{п}} \rho,$$

where $B_{\text{з}}$ – cut width of the shearer operating device, m;

$V_п$ – axis velocity of the shearer, m/min;

ρ – coal density, t/m^3.

With this in mind, the value of specific energy consumption at the *k*-th auger can be determined as, kWh/t:

$$W_k = \frac{P_{ном}(I_{ср.k} - I_{хол.ход})\cos\varphi}{60 I_{ном} H_{k.ио} B_з V_п \rho}.$$

Based on the above-mentioned features of the modern shearer operation flow sheet for extracting thin seams, the cutting specific energy consumption at the lagging auger can be determined as, kWh/t,

$$W_{разр} = \frac{W_{отст}\bar{A}_{р.отст.ио}}{k_{\gamma.охв} k_{осл} \bar{A}_{р.опер.ио}},$$

and the cutting specific energy consumption at the leading auger $W_{погр}$ can be determined as, kWh/t,

$$W_{погр} = W_{опер} - W_{разр} = \frac{P_{погр.опер}}{Q_{опер} \cdot 60}.$$

The performance parameters of the UKD400 and UKD200-500 shearers obtained based on processing of the experimental study data are given in Table 3.

Based on the data presented in Table 3 regression equations were obtained for determining the power for loading ($R^2{}_{Pпог} = 0.91$) of the studied shearers, kW:

$$P_{пог}(V_п, B_з) = 3{,}612\, B_з e^{0{,}619 B_з V_п}.$$

A plot of power and specific energy consumption for loading as function of operating device effective width and axis velocity of the shearers under consideration is presented in Fig. 3.

The analysis of the given dependences (Fig. 3) shows that the loading power and specific energy consumption increase with increasing the auger effective width in line with increasing the shearer axis velocity: the higher the velocity, the higher the power and specific energy consumption. For instance, at $V_n = 4$ m/min, increasing the auger effective width of the executive body from 0.7 to 0.8 m leads to increasing the power from 14 to 21 kW, i.e. 1.5 times, and the loading specific energy consumption from 0.07 to 0.09 kWh/ t, i.e. 1.3 times. Achieving the axis velocity of $V_n = 6$ m/min leads to increasing the power from 34 to 56 kW, i.e. 1.7 times, and the loading specific energy consumption from 0.11 to 0.16 kWh/t, i.e. 1.5 times. This is due to the beginning of the process of loose rock mass circulation, and the larger the auger effective width, the more intensive the circulation process, and at the lower axis velocity of the shearer the process starts.

Table 3

The findings of processing of the experimental data on UKD400 and UKD200-500 shearers operation

Parameter	Shearer type						
	UKD400			UKD200-500			
Axis velocity, m/min	3.75	4.5	5.3	4.0	4.2	4.4	6.4
Productivity, t/min:							
leading auger	3.307	3.969	4.675	4.032	4.234	4.435	6.451
lagging auger	1.139	1.367	1.61	0.672	0.706	0.739	1.075
Specific energy consumption, kWh/t:							
leading auger	0.187	0.461	0.320	0.593	0.699	0.63	0.462
lagging auger	0.125	0.390	0.227	0.506	0.613	0.537	0.290
for rock mass loading	0.062	0.071	0.093	0.087	0.086	0.093	0.172
Power for loading, kW	12.28	16.73	26.19	21.14	21.92	24.77	66.39

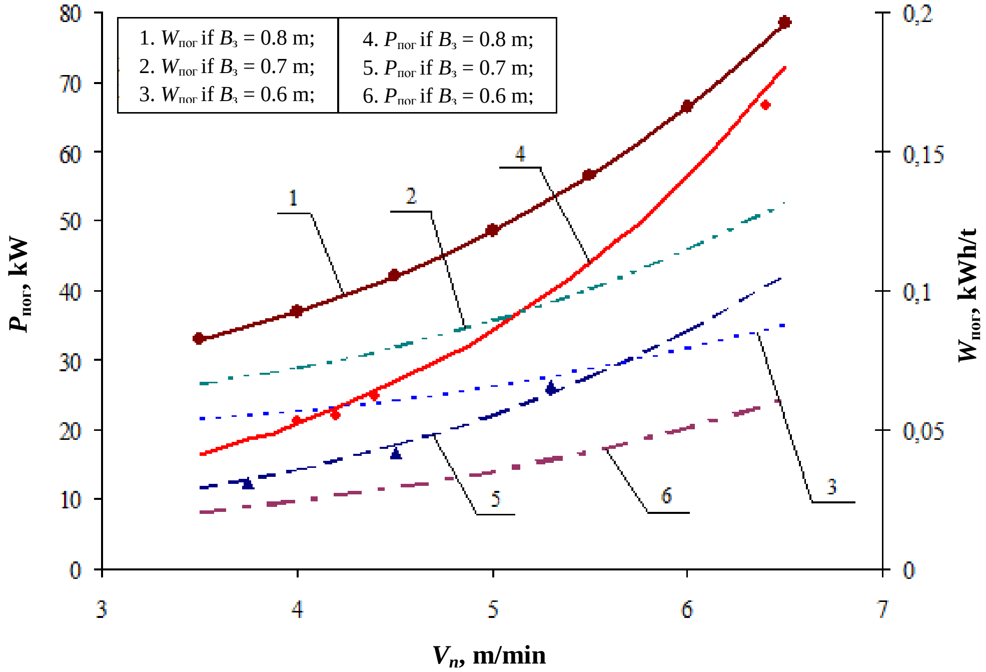

Fig. 3. Plot of power and specific energy consumption for loading as function of operating device effective width and feed rate

To assess the effect of the auger operating device effective width on the efficiency of the shearer operation in thin seams, a nomogram was built based on the proposed methodology [39] (Fig. 4). The nomogram was built for the following mining & geological and geotechnical conditions: the average thickness of the extracted seam of 1.0 m; the longwall face 200 m long; density of the coal to be cut of 1.41 t/m^3; coal cuttability in an uncompressed mass of 220 kN/m; the seam brittleness factor when cutting of 1.65. Arrangement of the cutter set of UKD200-500 shearer was adopted and adjusted taking into account the effective width.

Figure 4 presents the graphs of following dependencies: cutting and loading power of the leading auger operating device P, obtained using the regression dependencies for loading and [40] for cutting, versus the axis velocity (V_n); the specific energy consumption for cutting and loading at the leading auger operating device W, defined as the ratio of the cutting and loading power on the leading auger to its theoretical productivity, versus the axis velocity (V_n); the technical performance $Q_{тех}$ versus the axis velocity (V_n).

Based on the analysis of a new-level shearer fleet designed for coal extraction from thin gently sloping seams, the cutting drive power is at the level of 200 kW, that, taking into account the efficiency of the auger operating device drive gear unit, means about 160 kW at the auger.

Based on the adopted power value at the shearer auger operating device, using the nomogram enabled determining the optimal values of the auger effective width, which are in the range of 0.6–0.7 m, providing maximum performance with minimal specific energy consumption (compared to larger effective values, decreasing the specific energy consumption is about 15–30 %).

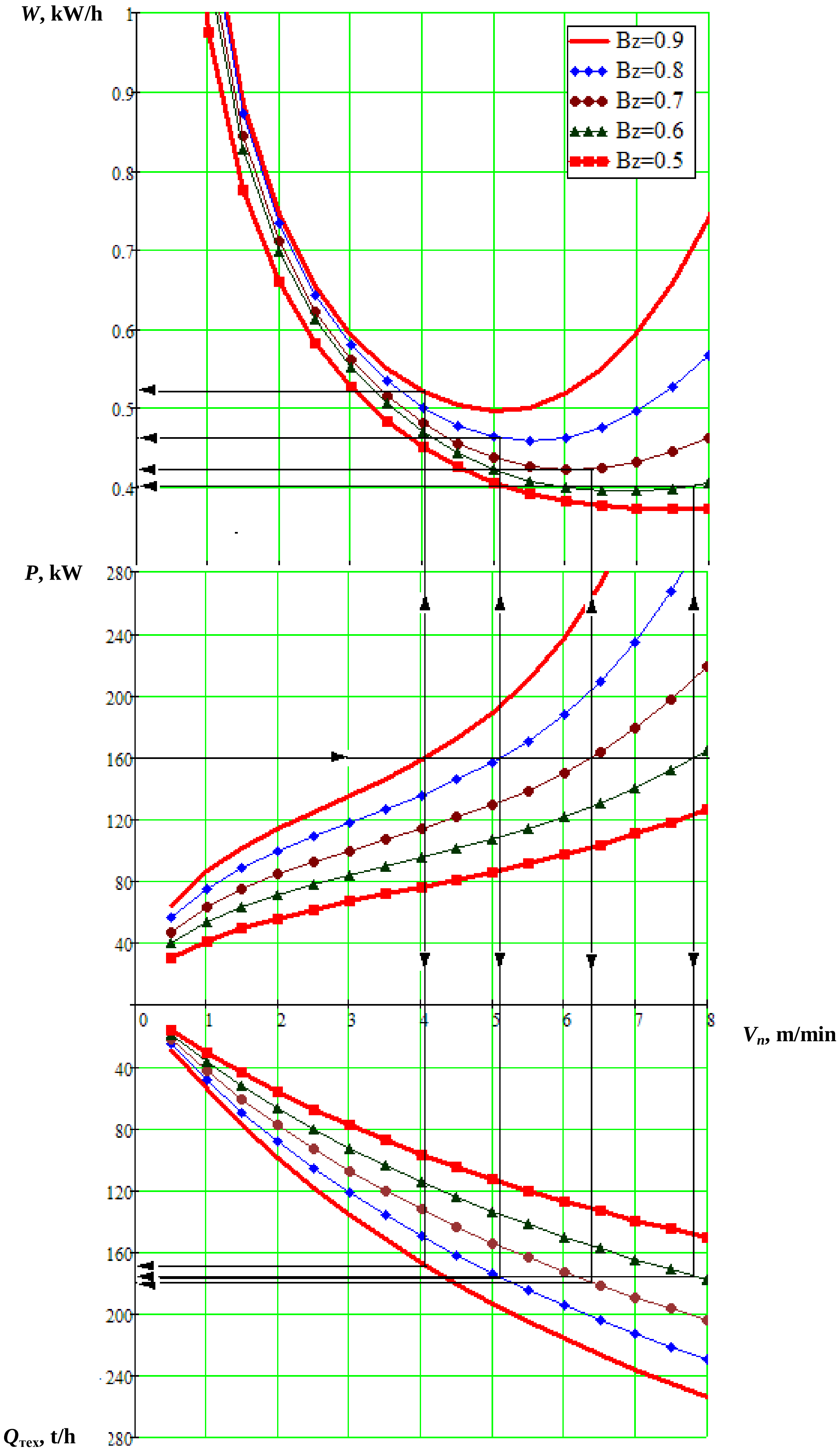

Fig. 4. The findings of processing of the experimental data on UKD400 and UKD200-500 shearers operation

Thus, it seems expedient to determine the optimal values of the auger effective width based on the criterion of the minimum energy parameters of a shearer operation for specific mining & geological and geotechnical conditions, that will significantly improve the efficiency of shearer with the auger operating device operation for extracting thin gently sloping seams, taking into account possible limiting factors for shearer travel speed.

Conclusions and direction of further research

1. An adaptive method for specific mining and geological operating conditions is proposed for determining the specific energy consumption of shearers on cutting and loading for thin seams in actual operating conditions based on fixing the values of currents of the cutting drive motors.

2. Processing of the experimental study data on the operation of UKD400 and UKD200-500 shearers in representative conditions enabled obtaining a dependence of the form $P_{пог}(V_п, B_з) = 3.612 \cdot B_з \cdot e^{0.619 \cdot B_з \cdot V_п}$ of the power for rock mass loading on the axis velocity and the effective width of the operating device. Increasing the auger effective width leads to increasing the loading power and specific energy consumption. In this case the higher the shearer axis velocity, the greater the growth of the loading power and specific energy consumption. This is due to beginning of the process of loose rock mass circulation, and the larger the auger effective width, the more intensive the circulation process and the lower the shearer axis velocity at which the process starts.

3. It was found that the specific energy consumption for coal cutting and loading by the auger operating device can be significantly reduced by selecting a rational auger effective width for the mining & geological and geotectnical conditions under consideration, while maintaining the preset technical performance.

References

1. Gorbatov P. A., Petrushkin G. V., Lysenko N. M., Pavlenko S. V., Kosarev V. V. Mining machinery for underground coal production. College-level Textbook. Ed. Gorbatov, P.A., 2nd revised and enlarged edition, Donetsk, Nord Computer Publ., 2006, 669 p. (in Russ.).

2. Nechepaev V. G. Mechanical-hydraulic auger systems for unloading and transportation. Donetsk, DonNTU Publ., 2005, 215 p. (in Russ.).

3. Boiko N. G. Shearers for thin seams. DVNZ "DonNTU" Publ., 2010, 476 p. (in Russ.).

4. Kondrakhin V. P., Kosarev V. V., Stadnik N. I. Electric mechanisms for moving shearers. Ed. Kondrakhin, V.P. Donetsk, "DonNTU Technopark "UNITEKh" Publ., 2010, 257 p. (in Russ.).

5. Kosarev I. V., Meznikov A. V. Improving the performance of shearers with remote feed system. International Scientific and Technical Journal Bulletin of Donetsk National Technical University, no. 6, 2016, pp. 19-23 (in Russ.).

6. Gulyaev V. G. Design and construction of mining machinery and complexes. Part 1. Shearer loaders. (Theory of work processes and methods for improving reliability). Textbook. Donetsk, "DonNTU Technopark "UNITEKh" Publ., 2011, 322 p., illustrated (in Russ.).

7. Nechepaev V. G. Studying and determination of parameters of shearer variable-pitch augers for thin seams for increasing their loading capacity. Cand. Sci. (Engineering) Dissertation. Donetsk, 1982, 240 p. (in Russ.).

8. Boiko N. G. Theory of work processes of shearers for extraction of coal from thin flat seams: Extended Abstract of Cand.Sci. (05.17.06 Engineering) Dissertation. Donetsk, 1985, 31 p. (in Russ.).

9. Boiko N. G., Boltyan A. V., Shevtsov V. G., Markov N. A. Operating devices of shearers for thin flat seams. Donetsk, "Donechchina" Publ., 1996, 223 p. (in Russ.).

10. Maleev G. V., Gulyaev V. G., Boiko N. G., Gorbatov P. A., Mezhakov V. A. Design and construction of mining machinery and complexes. Moscow, Nauka Publ., 1988, 368 p. (in Russ.).

11. Solod V. I., Getopanov V. M., Rachek V. M. Design and construction of mining machinery and complexes. Moscow, Nedra Publ., 1982, 350 p. (in Russ.).

12. Solod V. I., Zaykov V. I., Pervov K. M. Mining machinery and automated complexes. Moscow, Nedra Publ., 1981, 503 p. (in Russ.).

13. Kantovich L. I., Getopanov V. I. Mining Machinery. Moscow, Nedra Publ., 1989, 304 p. (in Russ.).

14. Minichev V. I. Coal shearers. Moscow, Mechanical Engineering Publ., 1976, 248 p. (in Russ.).

15. Dokukin A. V., Modinov V. V., Pshenichny I. D. Study of the loading capacity of auger operating devices. Moscow, IGD named after A. A. Skochinsky Publ., 1967, 36 p. (in Russ.).

16. Pshenichny I. D., Modinov V. V. Investigation of the effect of auger surface shape on loading capacity of auger device. In: The scientific basis for determining rational parameters of operating devices for extraction and transportation of minerals. Moscow, Nauka Publ., 1969, pp. 59-69 (in Russ.).

17. Pshenichny I. D., Modinov V. V. The study of material movement along the helical surface of auger operating device of shearer. Proceedings of IGD named after A. A. Skochinsky. Moscow, IGD named after A. A. Skochinsky Publ., 1969, no. 66, pp. 30-39 (in Russ.).

18. Korzyukov E. K., Zatonskikh A. T., Matveev N. V. Determination of loading capacity of shearer operating device when working with lateral pitch. In: Problems of mining mechanization. Kemerovo, KuzPI Publ., 1972, no. 46, pp. 46-51 (in Russ.).

19. Voronovsky K. F. Research and determination of rational parameters of auger operating device of coal shearer for thin seams. Cand. Sci. (Engineering) Dissertation. Moscow, Moscow Mining Institute Publ., 1970, 182 p. (in Russ.).

20. Chefranov V. V., Brilling V. N., Miller K. O. et al. Research and selection of optimal shape of helical surface of helical surface of shearer auger operating device at down-dip extracting coal seam. In: KNIUI Proceedings, Karaganda, 1972, no. 38, pp. 68-72 (in Russ.).

21. Loginov L. A., Makarov I. V. On moving a particle by auger operating device blade. In: Problems of mining mechanization, Kemerovo, 1975, no. 75, pp. 59-62 (in Russ.).

22. Belikov K. N. Experimental studies of the loading capacity of shearer auger operating device. In: Improving the efficiency of development of Moscow lignite basin coal deposits. Moscow, IGD named after A.A. Skochinsky Publ., 1973, no. 16, pp. 135-146 (in Russ.).

23. Nechepaev V. G. Determination of rational parameters of shearer variable-pitch augers for thin seams for increasing their loading capacity. 1981, no. 3127, 25 p. Deposited manuscript / UkrNIINTI Publ. (in Russ.).

24. Hackelboerger B. Automation of the shearer loader technique – an overview / Hackelboerger B., Hoelling B. // Glueckauf. 2007, № 9, pp. 404-413.

25. Kowal J. Control systems for multiple tool heads for rock mining / Kowal J., Podsiadlo A., Pluta J., Sapinski B. // Acta montanistica slovaca rocnik, 2003, no. 8, pp. 162-167.

26. Tkachov V. Control automation of shearers in term of auger gumming criterion / V. Tkachov, A. Bublikov, M. Isakova // Energy efficiency improvement of geotechnical systems. Dnipropetrovs'k: Taylor & Francis Group, 2013, pp. 137-145.

27. Tkachev V. Automatic control of coal shearer providing effective use of installed power / V. Tkachev, A. Bublikov, N. Stadnik // Power Engineering Control & Information Technologies. Dnipropetrovs'k: Taylor & Francis Group, 2014, pp. 73–87.

28. Atanov G. A. Interior ballistics of impulsive water jet. Proc. Sixth Intern. Symp. Jet Cutting Technol. Guildford. 1982, Apr. 6-8, pp. C5-141–C5-159.

29. Atanov G. A., Petrakov A.I. Impulsive hydrodynamic method of rock breaking. Proc. 6-th Intern. Cont. on Erosion by Liquid and Solid Impact, 1983, pp. 32-1–32-8.

30. Daniel I.M. Experimental studies of water jet impact on rock and rocklike materials. - Third Intern. Symp. Jet Cutting Technol. Chicago. 1976, pp. B3/27–D3/46.

31. Edney B.E. Experimental studies of pulsed water jets. Proc. Third Intern. Symp. Jet Cutting Technol. Chicago, 1976, pp. B2/11–B2/26.

32. Petrakov A. I., Krivorotko O. D. Some experience in developing mining roadways using experimental heading machine with pulsed water jets. - Proc. Fourth Intern. Symp. Jet Cutting Technol. Canterbury, 1978, Apr. 12-14, pp. J3-23–J3-36.

33. Atanov G. A., Powder impulsive water jetter. Proceeding of the 11th International Conference on Jet Cutting Technology, St Andrews, Scotland, 8-10 September, 1992, pp. 295-303.

34. Atanov G. A., The Impulsive Water Jet Device: A new machine for breaking rock. International journal of water jet technology, 1991, v.1, N2, pp. 85-91.

35. Atanov G. A. Impulsive hydrodynamic method of breaking rocks and concrete. Water Jet Applications in Construction Engineering, 1998, pp. 73-89.

36. Atanov G. A. & Beshevly B. I. A model of the impulsive water jet device jet. Int. J. of Water Jet Technology, 1994, 2:72–77.

37. Atanov G. A., Indexes of breaking rocks by impulsive water jet device. Proceeding of the International Conference Geomechanics 96, Rožnov P.R. / Czech Republic / 3-6 September, 1996. Pp. 407–410.

38. Protodyakonov M. M., Teder R. I., Ilnitskaya E. I. et al. Distribution and correlation of rock physical properties indicators. Reference manual. Moscow, Nedra Publ., 1981, 192 p. (in Russ.).

39. Kudlay R. A. Block for event registration at roadheader./ In: Kudlay, R.A., Meznikov, A.V., Stadnik, N.I. Solution of scientific and technical problems in creation and implementation of modern mining equipment. Donetsk, Astro Publ., 2008, pp. 647-660 (in Russ.).

40. Shabaev O. E. Techniques for determining the specific energy consumption of destruction and loading of shearers for thin layers in real operating conditions./ Shabaev O. E., Nechepaev V. G., Zinchenko P. P., Meznikov A. V., Kovalenko A. V. Bulletin of Donetsk National Technical University, no. 4, 2017, pp. 28-33 (in Russ.).

41. Shabaev O. E. Techniques for determining the optimal width of shearer auger operating device. / Shabaev O. E., Nechepaev V. G., Zinchenko P. P. In: Mechanical Engineering and Technosphere of the XXI Century. Proceedings of the XXV International Scientific and Technical Conference in Sevastopol, Donetsk, 2018, v. 2, pp. 237-243 (in Russ.).

42. KD 12.10.040-99. Coal machine building products. Shearers. Methods for selecting parameters and calculating cutting and feeding forces at operating devices (replaces OST12.44.258-84). Effective from 01.01.2000. Donetsk, Minugleprom of Ukraine, 1999, 75 p. (in Russ.).

Библиографический список

1. Горные машины для подземной добычи угля: учеб. пособие для вузов / П. А. Горбатов, Г. В. Петрушкин, Н. М. Лысенко, С. В. Павленко, В. В. Косарев; под общей редакцией П. А. Горбатова. 2-е изд., перераб. и доп. Донецк: Норд Компьютер, 2006. 669 с.

2. Нечепаев В. Г. Механо-гидравлические шнековые системы выгрузки и транспортирования. Донецк: ДонНТУ, 2005. 215 с.

3. Бойко Н. Г. Очистные комбайны для тонких пластов. Донецк: ДВНЗ «ДонНТУ», 2010. 476 с.

4. Электрические механизмы перемещения очистных комбайнов В.П. Кондрахин, В.В. Косарев, Н.И. Стадник; под общ. ред. В. П. Кондрахина. Донецк: «Технопарк ДонНТУ «УНИТЕХ», 2010. 257 с.

5. Косарев И. В., Мезников А. В. Повышение производительности очистных комбайнов с вынесенной системой подачи. Международный научно-технический журнал Вестник Донецкого национального технического университета. 2016. №6. С. 19-23.

6. Гуляев В. Г. Проектирование и конструирование горных машин и комплексов. Ч. 1. Выемочные комбайны. (Теория рабочих процессов и методы повышения надежности): учеб. пособие. Донецк: «Технопарк ДонНТУ «УНИТЕХ», 2011. 322 с.

7. Нечепаев В. Г. Исследование и определение параметров шнеков с переменным шагом очистных комбайнов для тонких пластов с целью повышения их погрузочной способности: дис... канд. техн. наук. Донецк, 1982. 240 с.

8. Бойко Н. Г. Теория рабочих процессов комбайнов для добычи угля из тонких пологих пластов: автореф. дис… д-ра техн. наук. Донецк, 1985. 31 с.

9. Исполнительные органы очистных комбайнов для тонких пологих пластов / Н. Г. Бойко, А. В. Болтян, В. Г. Шевцов, Н. А. Марков. Донецк: «Донеччина»,1996. 223 с.

10. Проектирование и конструирование горных машин и комплексов / Г. В. Малеев, В. Г. Гуляев, Н. Г. Бойко, П. А. Горбатов, В. А. Межаков. М.: Наука, 1988. 368 с.

11. Солод В. И., Гетопанов В. М., Рачек В. М. Проектирование и конструирование горных машин и комплексов. М.: Недра, 1982. 350 с.

12. Солод В. И., Зайков В. И., Первов К. М. Горные машины и автоматизированные комплексы. М.: Недра, 1981. 503 с.

13. Кантович Л. И., Гетопанов В. И. Горные машины. М.: Недра, 1989. 304 с.

14. Миничев В. И. Угледобывающие комбайны. М.: Машиностроение, 1976. 248 с.

15. Докукин А. В., Модинов В. В., Пшеничный И. Д. Исследование погрузочной способности шнековых исполнительных органов. М.: ИГД им. А.А. Скочинского, 1967. 36 с.

16. Пшеничный И. Д., Модинов В. В. Исследование влияния формы винтовой поверхности на погрузочную способность шнекового органа. В кн.: Научные основы установления рациональных параметров средств выемки и доставки полезных ископаемых. М.: Наука, 1969. С. 59-69.

17. Пшеничный И. Д., Модинов В. В. Исследование движения материала по винтовой поверхности шнекового органа комбайна. В кн.: Научные сообщения ИГД им. А.А. Скочинского. М.: ИГД им. А.А. Скочинского, 1969. Вып. 66. С. 30-39.

18. Корзюков Е. К., Затонских А. Т., Матвеев Н. В. Определение погрузочной способности исполнительного органа комбайна при работе с боковым креном. В кн.: Вопросы механизации горных работ. Кемерово: КузПИ, 1972. № 46. С. 46-51.

19. Вороновский К. Ф. Исследование и установление рациональных параметров шнекового исполнительного органа угольного комбайна для маломощных пластов: дис… канд. техн. наук. М.: Московский горный институт, 1970. 182 с.

20. Исследование и выбор оптимальной формы винтовой поверхности шнекового исполнительного органа комбайна, работающего по падению пласта / В. В. Чефранов, В. Н. Бриллинг, К. О. Миллер и др. В кн.: Научные труды КНИУИ. Караганда, 1972. № 38. С. 68-72.

21. Логинов Л. А., Макаров И. В. О перемещении частицы лопастью шнекового исполнительного органа. В кн.: Научные труды КузПИ. Вопросы механизации горных работ. Кемерово, 1975. № 75. С. 59-62.

22. Беликов К. Н. Экспериментальные исследования погрузочной способности шнекового исполнительного органа выемочных машин. В кн.: Повышение эффективности разработки угольных месторождений Подмосковного бассейна. М.: ИГД им. А.А. Скочинского, 1973. № 16. С. 135-146.

23. Нечепаев В. Г. Определение рациональных параметров шнеков с переменным шагом очистных комбайнов для тонких пластов, обеспечивающих повышение их погрузочной способности. 1981, № 3127. 25 с. Деп. рукопись / УкрНИИНТИ.

24. Hackelboerger B. Automation of the shearer loader technique – an overview / Hackelboerger B., Hoelling B. // Glueckauf. 2007, № 9, pp. 404-413.

25. Kowal J. Control systems for multiple tool heads for rock mining / Kowal J., Podsiadlo A., Pluta J., Sapinski B. // Acta montanistica slovaca rocnik. 2003, no. 8, pp. 162-167.

26. Tkachov V. Control automation of shearers in term of auger gumming criterion / V. Tkachov, A. Bublikov, M. Isakova // Energy efficiency improvement of geotechnical systems. Dnipropetrovs’k: Taylor & Francis Group, 2013, pp. 137-145.

27. Tkachev V. Automatic control of coal shearer providing effective use of installed power / V. Tkachev, A. Bublikov, N. Stadnik // Power Engineering Control & Information Technologies. Dnipropetrovs’k: Taylor & Francis Group, 2014, pp. 73–87.

28. Atanov G. A. Interior ballistics of impulsive water jet. Proc. Sixth Intern. Symp. Jet Cutting Technol. Guildford. 1982, Apr. 6-8, pp. C5-141–C5-159.

29. Atanov G. A., Petrakov A. I. Impulsive hydrodynamic method of rock breaking. Proc. 6-th Intern. Cont. on Erosion by Liquid and Solid Impact, 1983, pp. 32-1–32-8.

30. Daniel I. M. Experimental studies of water jet impact on rock and rocklike materials. Third Intern. Symp. Jet Cutting Technol. Chicago, 1976, pp. B3/27–D3/46.

31. Edney B. E. Experimental studies of pulsed water jets. Proc. Third Intern. Symp. Jet Cutting Technol. Chicago, 1976. Pp. B2/11–B2/26.

32. Petrakov A. I., Krivorotko O. D. Some experience in developing mining roadways using experimental heading machine with pulsed water jets. Proc. Fourth Intern. Symp. Jet Cutting Technol. Canterbury, 1978, Apr. 12-14, pp. J3-23–J3-36.

33. Atanov G. A. Powder impulsive water jetter. Proceeding of the 11th International Conference on Jet Cutting Technology, St Andrews, Scotland, 8-10 September, 1992, pp. 295-303.

34. Atanov G. A. The Impulsive Water Jet Device: A New Machine for breaking rock. International journal of water jet technology, 1991, v.1, no. 2, pp. 85-91.

35. Atanov G. A. Impulsive hydrodynamic method of breaking rocks and concrete. Water Jet Applications in Construction Engineering, 1998, pp. 73-89.

36. Atanov G. A. & Beshevly B. I. A model of the impulsive water jet device jet. Int. J. of Water Jet Technology, 1994, 2:72–77.

37. Atanov G. A. Indexes of breaking rocks by impulsive water jet device. Proceeding of the International Conference Geomechanics 96, Rožnov P.R. / Czech Republic / 3-6 September, 1996. Pp. 407–410.

38. Распределение и корреляция показателей физических свойств горных пород: Справочное пособие / М. М. Протодьяконов, Р. И. Тедер, Е. И. Ильницкая и др. М.: Недра, 1981. 192 с.

39. Кудлай Р. А. Блок регистрации произошедших событий на проходческом комбайне / Р. А. Кудлай, А. В. Мезников, Н. И. Стадник // Решение научно-технических проблем при создании и внедрении современного горношахтного оборудования. Донецк: Астро, 2008. С. 647-660.

40. Шабаев О. Е. Методика определения удельных энергозатрат разрушения и погрузки очистных комбайнов для тонких пластов в реальных условиях эксплуатации / О. Е. Шабаев, В. Г. Нечепаев, П. П. Зинченко, А. В. Мезников, А. В. Коваленко // Вестник Донецкого национального технического университета. № 4. 2017. С. 28-33.

41. Шабаев. О. Е. Методика определения оптимальной ширины захвата шнекового исполнительного органа очистных комбайнов / О. Е. Шабаев, В. Г. Нечепаев, П. П. Зинченко // Машиностроение и техносфера XXI века: сб. тр. XXV междунар. науч.-техн. конф. в г. Севастополе, Донецк. 2018. Т. 2. С. 237-243.

42. КД 12.10.040-99. Изделия угольного машиностроения. Комбайны очистные. Методика выбора параметров и расчета сил резания и подачи на исполнительных органах (взамен ОСТ12.44.258-84). Введен с 01.01.2000. Донецк: Минуглепром Украины, 1999. 75 с.

ОРИГИНАЛЬНЫЕСТАТЬИ / ORIGINALPAPERS

DOI: 10.17073/2500-0632-2019-2-103-110

Rock Burst and Actually Effective Bolting for Rock Burst Prevention

Ngoc Minh Nguyen[1], Duc Thang Pham[2]

[1]Central South University, Changsha, Hunan, China; Quang Ninh University of Industry, QuangNinh, Vietnam, minhnguyen1986vn@csu.edu.vn;
[2]Quang Ninh University of Industry, Quang Ninh, Vietnam, ✉hamducthangmct@gmail.com

Abstract: Rock burst represents a very dangerous phenomenon in deep underground mining, as well as for underground structures in unfavourable conditions (great depth, high horizontal stress, proximity of major tectonic structures, etc.). The rock burst problem relates to the natural and mining conditions of the rock mass. The evaluation of rock burst is becoming increasingly important as mining activities reach greater depths. In the literature, rock burst assessment challenge was tackled by many researchers using various methods. However, no study providing review and comparison of different rock burst assessment methods is available. In this paper, rock burst classification is briefly summarized. This includes a classification based on rock burst type, and another classification based on rock burst severity. As an important method for rock burst prevention, some novel energy-absorbing bolts were developed. These bolts demonstrate constant resistance under both static and shock loads and large elongation ability enabling them to withstand large deformations of rock masses under rock burst-prone conditions. Among the novel energy absorbing bolts, Modified Cone Bolt (MCB) and Constant Resistance at Large Deformation (CRLD) Bolt are selected to be presented in this paper.

Keywords: rock burst, bolting, rock burst prevention, deep mines, shock loads, rock strain.

For citation: Nguyen Ngoc Minh, Pham Duc Thang. Rock Burst and Actually Effective Bolting for Rock Burst Prevention. *Mining Science and Technology*. 2019;4(2):103-110. DOI: 10.17073/2500-0632-2019-2-103-110.

Эффективное анкерное крепление для предотвращения горного удара

Нгуен Нгок Минь[1], Фам Дык Тхань[2]

[1]Центральный Южный Университет, Чанша, Хунань, Китай; Промышленный Университет Куанг Нинь, Куанг Нинь, Вьетнам, minhnguyen1986vn@csu.edu.vn;
[2]Промышленный Университет Куанг Нинь, Куанг Нинь, Вьетнам, ✉phamducthangmct@gmail.com

Аннотация: Горный удар представляет собой очень опасное явление при подземных горных работах на больших глубинах, а также для подземных сооружений в неблагоприятных условиях (большие глубины, высокие горизонтальные напряжения, близость крупных разломов и т. д.). Проблема горного удара связана с природными и горнотехническими условиями горного массива. Оценка горного удара становится все более важной, поскольку горные работы достигают всё больших и больших глубин. В литературе попытки решения проблемы оценки горных ударов предпринимались многими исследователями с использованием различных методов. Тем не менее до сих пор не представлено исследование, которое рассматривало бы и сравнивало различные методы оценки горных ударов. В этой статье кратко изложена классификация горных ударов. Предлагаемый подход включает классификацию, основанную на типах горных ударов, а также учитывающую степень тяжести последствий горного удара. В качестве важного подхода к предотвращению горного удара были разработаны новые энергопоглощающие анкеры, которые демонстрируют постоянное сопротивление как при статических, так и при ударных нагрузках, и обладают большой способностью к удлинению, позволяющей выдерживать значительные деформации массивов горных пород. Для представления в этой статье выбраны два таких новых энергопоглощающих анкера, а именно: модифицированный конусный анкер (МКА) и анкер с постоянным сопротивлением при большой деформации (ПСБД).

Ключевые слова: горный удар, анкерная крепь, предотвращение горного удара, глубокие рудники, ударные нагрузки, деформация/механическое напряжение пород.

Для цитирования: Минь Нгуен Нгок, Фам Дык Тханг. Эффективное анкерное крепление для предотвращения горного удара. *Горные науки и технологии.* 2019;4(2):103-110. DOI: 10.17073/2500-0632-2019-2-103-110.

1. Introduction

Rock burst is an unstable rock failure and one of the most hazardous problems in deep mines and civil tunnels. It is a sudden failure of rock in the form of rapid ejection of failed rocks, accompanied by the release of a large amount of energy [1]. Rock burst frequently occurs at excavation faces or in a working panel of an underground excavation at great depth. It can cause mechanical damage, delays of projects, and economic losses. As an example, hundreds of rock bursts occurred during the construction of the extra-long seven tunnels at the Jinping II hydropower station in China. On 28 November 2009, an extremely severe rock burst caused seven deaths and one injury, as well as total destruction of a tunnel boring machine (TBM) [2].

In the latest years, rock burst phenomena have been investigated by many researchers through theoretical, numerical, and experimental approaches [3]. Due to the complex nature of rock burst phenomenon, precise rock burst prediction is rather difficult. Since Cook et al. (1966) first proposed the method for evaluating the rock burst in mining conditions, a variety of methods, either elaborated or simplified, ranging from empirical to theoretical and mathematical approaches for predicting rock burst potential have been developed in the past few decades. However, due to the complexity of rock burst assessment systems, including multivariable and strong interference, there is no universally accepted method to predict the moment of rock burst, and the best we can achieve today is to identify rock burst hazard areas using empirical criteria, numerical models or personal experience [4].

In addition to understanding rock burst mechanisms, controlling rock burst damage is important for providing safety of mining operations and underground structures. Rock support using bolts and anchors, providing fractured rock reinforcement and retaining, is an efficient measure for rock burst control in underground mining [5]. Researchers worldwide have developed some dynamic rockbolts [6, 7]. The MCB conebolt developed in Canada has been successfully used in Canadian hard rock mines and in some other countries. The "constant resistance at large deformation (CRLD)" bolt, developed by the State Key Laboratory for Geo-mechanics and Deep Underground Engineering at China University of Mining and Technology, Beijing (GDUE), is successfully tested in a coalmine in China to demonstrate the effectiveness of the CRLD cable [3].

This paper focuses on providing the reader with a complete review of rock burst classification and some dynamic rockbolts to control rock burst.

2. Rock burst classification

2.1. Classification based on rock burst type

A classification system was developed and applied worldwide to record and report rock bursts using the terms of induced bursts, residual bursts, inherent bursts, and combination bursts were adapted by Colson (1950) [8] based on the origin of the burst. Later scientists have been recognized and developed some new methods of rock burst classifications such as:

+ Ortlepp (1997) [9] made a distinction between the seismic source mechanism and the rock burst crushing mechanism, while Kaiser et al. (1992) [10] used the term "modes of failure", to describe the same cases, and a rock burst may be further classified by Kaiser et al. (1996) [11] as bulking, ejection, and seismically-induced caving ground based on the damage mechanism (See Fig. 1a);

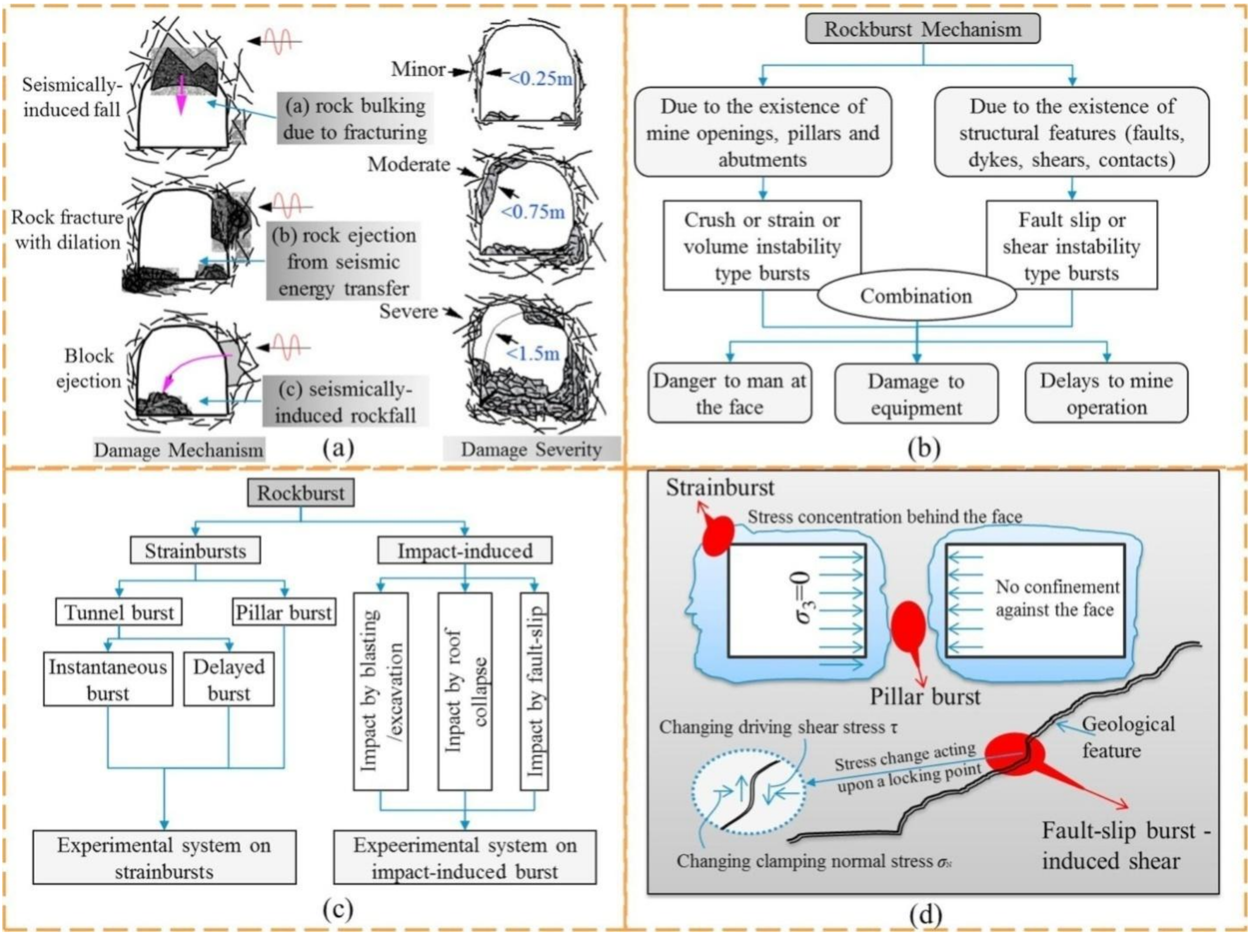

Fig. 1. Rock burst type classification: (a) by rock burst damage mechanism and damage severity; (b) by rock burst mechanism; (c) by rock burst triggering mechanism; (d) by rock burst potential and confinement effect

+ Rock burst mechanisms are grouped by Tang (2000) [12] into three broad categories: strainbursts, slip fault bursts and combined mechanism bursts (see Fig. 1b), and he pointed out that the majority of rock bursts are of the strainburst type in deep hard rock mines;

+ Based on stress paths and using experimental methods, He et al. (2012) [13] classified rock bursts into two major types: strainbursts and impact-induced bursts as shown in Fig. 1c. Strainburst: frequently encountered in tunnelling and mining environment; they are associated with pillar and room mining cavities. In relation to different stress paths and failure locations, strainbursts can be divided into three sub-types: instantaneous burst, delayed burst, and pillar burst. The impact-induced burst: after excavation, the surfaces of the cavities and the pillars may also suffer rock burst due to the impact waves generated by mining-induced disturbances. Based on generation mechanism, the impact-induced burst can be divided into three subtypes, i.e. the rock burst induced by blasting or excavation, by roof collapse, and by slip fault.

+ Based on the analysis of classification of the rock burst mechanisms conducted by Kaiser et al. (1996) [11] the manifestations of potential rock burst phenomena with high levels of strain energy, which are usually classified as strainburst, pillar burst or slip fault bursts (Castro et al., 2012 [14]), are illustrated in Fig. 1d.

2.2. Classification based on rock burst severity

Numerous research works concerning the potential of rock burst have been performed. For example, Russnes's method (Russenes, 1974) [15], which classifies the rock burst intensity into four levels (none, weak, moderate, and severe based on noise, shape, and features of failure after rock burst); Tan's method [16] which classifies rock burst into four groups based on the large number of laboratory tests and investigations in situ, and considers mechanical characteristics, type and shape of the failure, intensity of breakdown failure, and the sound of the rock burst; Brauner's method [17], which classifies rock burst into three groups based on the intensity of breakdown failure of the surrounding rock mass; the Canadian Rock burst Research Program's (CRRP) [18] method, which classifies the severity of rock burst damage into minor, moderate, and major damage, and estimates the severity of rock burst damage based on observations and empirical evidences, the depth of the damage zone in the rock mass and geometric considerations. Recently a new rock burst classification method was introduced by Chen et al. (2013) [19] for quantitative evaluating rock burst intensity on the basis of the released energy of the rock burst, monitored by micro-seismic technique, and surrounding rock damage severity.

3. Rock burst support

Rock support in burst-prone rock mass differs from conventional rock support in shallow rock mass where controlling gravity-induced rock caving is the main concern. Rock support in burst-prone rock mass needs to resist dynamic loading and large rock dilation due to rock failure. Manystudies have been performed to address the rock burst problem [20]. These studies recommend and provide design of rock burst support to mitigate rock burst damage. MCB conebolt and CRLD bolt are proposed to control rock burst problem.

3.1. MCB conebolt

The concept of conebolt was firstly developed in South Africa. The conebolts were groutable yielding tendons developed by the Chamber of Mines Research Organization (COMRO) in 1987 [21] for use in cement grouted holes.

The South African conebolts were first tested in Canada in 1994 [22] using cement grout and polyester resin (injected with quick-setting resin grout). The cement grouted conebolt had a maximum displacement of 240 mm and the load-displacement curve similar to that of steel stretching curve, indicating that there was insignificant cone movement during pull-out test. In resin grout testing, the conebolt could not shear through the resin and failed after about 100 mm of displacement only. But no mine in Canada systematically used the South African conebolts in its operation. The main reason was that the resin injection was not practical for use that time, and cement grouting was time consuming and required a third pass to screw in the bolts once the grout was cured.

The increase in quantity of violent ejection failures in 1999/2000 at Brunswick Mine in Canada led to the urgent development of complete yielding support system [23]. The South African conebolts were modified to satisfy resin-grouting applications in Canada. Norand Inc. modified the conebolt head and added a blade for the purpose of resin mixing, and the new bolt was called Modified Cone Bolt (MCB). This new tendon can shear through the surrounding column of polyester resin grout. It is a smooth bar threaded at its outer end, with a forged cone and mixing blade at another end.

A close-up view of the rock burst support system installed at Brunswick Mine can be seen in Fig. 2. There was a distinct boundary in one drift (tunnel) that defined stable and unstable rock masses in Fig. 2. This boundary was called the "extreme edge" at the mine site. Beyond the extreme edge, there were only standard rock support systems installed. A series of rock burst events that occurred between October 13 and 17, 2000 severely damaged the rock mass where standard supports were installed, but the section which was supported by the rock burst support system suffered no damage.

The excellent performance of the MCB supported tunnel section allowed many people to speculate that the rock might not be prone to burst as the rest of the area. However, close on-site examination revealed that the MCB had fulfilled specific role in dissipating dynamic energy as some conebolts displaced as much as 180 mm [23]. Subsequent use of MCBs based rock support system at the mine site showed its excellent performance.

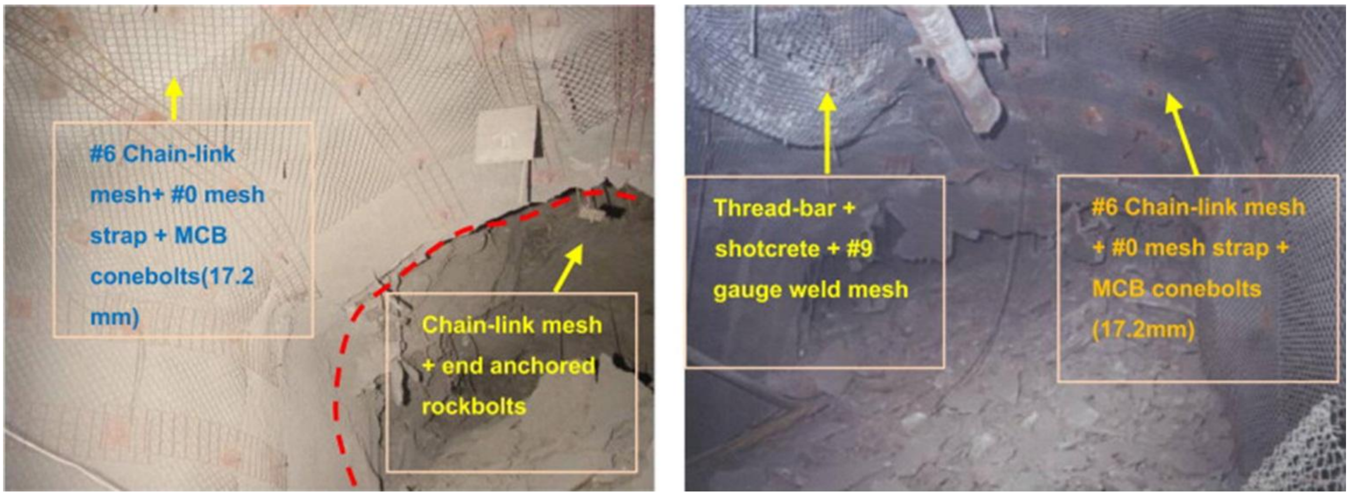

Fig. 2. Modified Cone Bolt (MCB) at Brunswick Mine

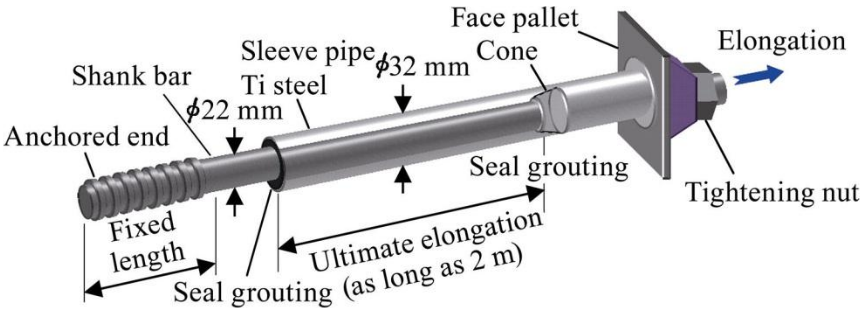

Fig. 3. Schematic of the three-dimensional view of CRLD bolt

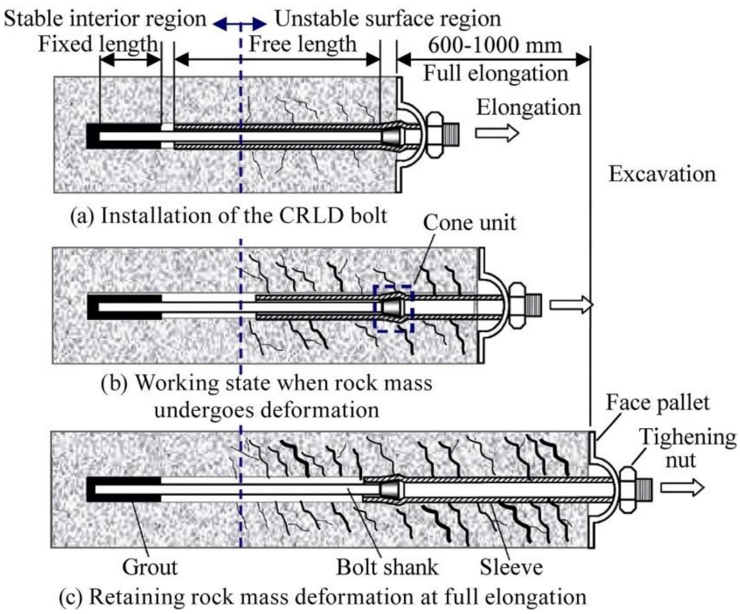

Fig. 4. Working principles of CRLD bolt

After the success at Brunswick Mine, MCBs have enjoyed slow but gradual acceptance by some Canadian mines having rock burst problems, and have been successfully applied in rock burst support systems.

3.2. CRLD bolt

Bolts provide a major method used in rock support in many practical situations. However, in high stressed rock masses and for large strain/deformation situations, bolts may be broken if they are not able to adapt to the induced large deformations [24, 25]. So, a new constant-resistance and large-deformation (CRLD) bolt was developed by GDUE to mitigate and control rock burst damage.

Fig. 3 shows schematically the structure of the CRLD bolt which consists of the following components: a piston-like cone installed on a bolt shank (rebar), sleeve pipe with its inner diameter slightly smaller than the large-end diameter of the cone, face plate and nut functioned as the retention device. The fixed length of the shank bar is bonded by grout.

Fig. 4 illustrates the supporting principle of the CRLD bolt over three different stages:

- Elastic deformation stage: at this stage, the deformation energy of the surrounding rocks impacts on the bolt rod in the bolt assembly through the baffle plate and inner anchorage segment. In the case of relative deformation of the surrounding rock where the axial force caused by the rock deformation is less than the rated constant resistance of the CRLD bolt, the bolt will not elongate. Instead, the bolt will resist the deformation and failure of the rock by solely relying on the elastic deformation of the constant-resistance element or bolt rod itself (Fig. 4a). In the figure, P_0 is generated by the cone-sleeve relative sliding and is the resistance of the bolt, pre-designed as function of elasticity of the sleeve and the structure of the cone.

– Structural deformation stage: at this stage, the axial force on the rod increases and may be equal to or greater than the rated constant resistance of the CRLD bolt. This leads to frictional-sliding displacement of the constant-resistant body along the sleeve track, i.e., the CRLD bolt elongates. While elongating, the bolt keeps the constant-resistant characteristics and the deformation and failure of the rock mass is contained by its elongation, i.e. structural deformation of the constant-resistant element occurs (Fig. 4b).

Ultimate deformation stage: at this stage, the deformation energy of the rock mass in the abutment to the stope is fully released. The external loads will be lower than the rated constant resistance, and the constant-resistant body will stop sliding due to frictional drag. By this way, the surrounding rock mass is stabilized once again (Fig. 4c).

During development, the CRLD bolt has been tested both in situ and in laboratory conditions. The maximum extension of the CRLD rockbolt is about 1000 mm which should be able to accommodate the displacement of the rock mass adjacent to the deep underground excavations. Compared to existing large-deformation bolts and anchors, the CRLD bolt (CRLDB) has much longer extension length under the same external pulling forces, while its maximum load-carrying capacity is much higher.

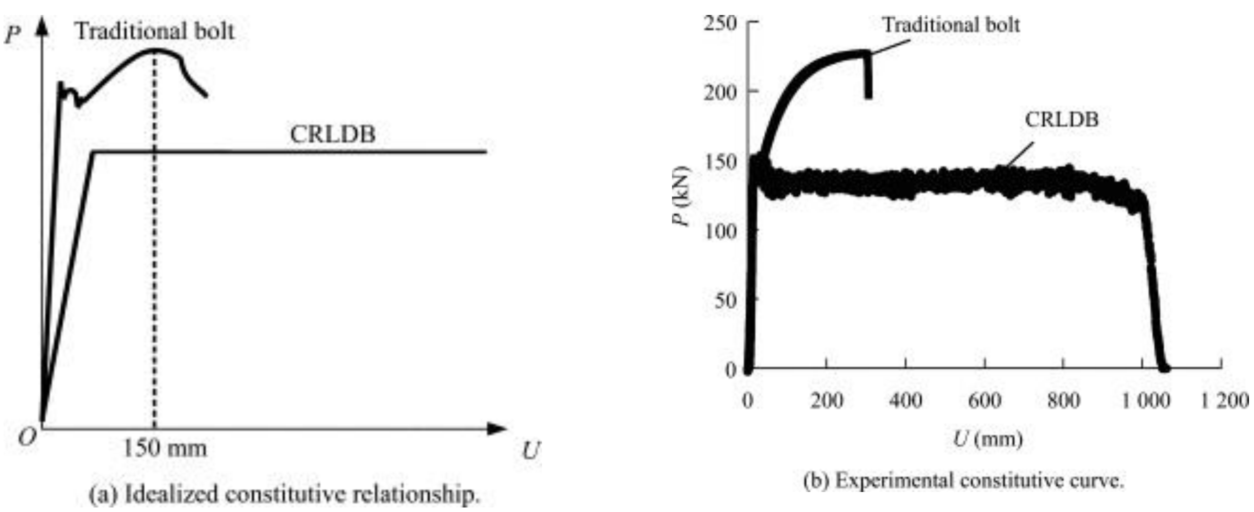

Fig. 5. Behavior of traditional bolt and CRLD bolt in tension tests

That is why the CRLDB is suitable for rocks and soils with large deformation. The built-in drag-adaptive regulator in the CRLDB can be adaptive to the external loading by preventing itself from being broken off in the case where the external load exceeds the allowable value. CRLDB demonstrates ideally elastoplastic behavior (Fig. 5a), and the behavior of the traditional bolt is also plotted herein for comparison. For detailed assessment of this new type of bolt, tension tests were carried out on a traditional bolt and CRLDB (Fig. 5b). At the same tensile loading level, the traditional bolt was broken with limited deformation length, whereas CRLDB showed much longer extensile length. CRLDB can bear shock for many times keeping good supporting performance. It is suitable for supporting in the burst-prone roadways [26].

4. Conclusion

This short review presents rock burst research status in the world, and highlights some of rock burst classification methods and novel energy-absorbing bolts for controlling rock burst.

Rock burst classification by type can be based on different parameters such as:

– Rock burst damage mechanism and damage severity;

– Rockburstmechanisms;

– Rockbursttriggeringmechanism; and

– Rock burst potential and the confinement effect.

Rock burst classification based on rock burst severity was introduced.

For rock burst control, new yieldable or energy absorbing bolt/cable (MCB conebolt and CRLD bolt) were developed which demonstrate constant resistance under static and dynamic loadings and have large elongation capacity. MCBs have proved their efficiency in resolving rock burst problems in Canada, and have been successfully applied worldwide. CRLD bolt was tested in a field experiment, and the experimental results demonstrated its good energy absorbing performance and the ability to contain large deformation of rock masses.

References

1. Amin M., Ming C. Numerical modeling of rock burst near fault zones in deep tunnels. Tunnelling and Underground Space Technology, 80, 2018, pp. 164-180.

2. Xiao Y. X., Feng X. T., Li S. J., Feng G. L., Yub Y. Rock mass failure mechanisms during the evolution process of rock burst s in tunnels. International Journal of Rock Mechanics & Mining Sciences, 83, 2016, pp. 174-181.

3. Man C. H., Fu Q. R., Dong Q. L., Rock burst mechanism research and its control. International Journal of Mining Science and Technology, 28, 2018, pp. 829-837.

4. Jian Z., Xi B. L., Ha S. M. Evaluation method of rock burst: State-of-the-art literature review. Tunnelling and Underground Space Technology, 81, 2018, pp.632-659.

5. Kaiser P. K., McCreath D., Tannant D. Rock burst research handbook, Vol. 2, 1996, pp.1990-1995.

6. Cai M., Champaigne D. Influence of bolt-grout bonding on MCB conebolt performance. International Journal of Rock Mechanics and Mining Sciences, 49, 2012, pp.165-75.

7. He M. C., Gong W. L., Wang J., Qi P., Tao Z. G., Du S., et al. Development of a novel energy-absorbing bolt with extraordinarily large elongation and constant resistance. International Journal of Rock Mechanics and Mining Sciences, 67, 2014, pp.29-42.

8. Colson C. M. Rock burst s. Masters Theses. Missouri S&T, 1950, pp. 43-49.

9. Ortlepp W. D. Rock fracture and rock burst s an illustrative study. Johannesburg, SAIMM Monogr., 1997, Ser. M9, 98.

10. Kaiser P. K., Tannant D. D., Mccreath D. R., Jesenak R. Rock burst damage assessment procedure. In: Kaiser, P.K., McCreath, D.R. (Eds.), Rock Support in Mining and Underground Construction. Balkema, Rotterdam, 1992,pp. 639-647.

11. Kaiser P. K., Tannant D. D., McCreath D. R. Canadian Rock burst Support Handbook.Geomechanics Research Centre, Laurentian University, Sudbury, Ontario, 1996, pp. 314.

12. Tang B. Y. Rock burst control using distress blasting (Ph.D. thesis). McGill University, Montreal, Canada, 2000.

13. He M. C., Xia H. M., Jia X. N., Gong W. L., Zhao F., Liang K.Y. Studies on classification, criteria and control of rock burst s. J. Rock Mech. Geotech. Eng., 4(2), 2012, pp. 97-114.

14. Castro L. A. M., Bewick R. P., Carter T.G. In: An Overview of Numerical Modelling Applied to Deep Mining. Innovative Numerical Modelling in Geomechanics. CRC Press, 2012, pp. 393-414.

15. Russenes B.F. Analysis of rock spalling for tunnels in steep valley sides. M.Sc. thesis, Norwegian Institute of Technology, Trondheim, Department of Geology, 1974.

16. Tan Y.A. Rock bursting characteristics and structural effects of rock mass. Sci. Chin., 1992, Ser. B, 35(8), pp. 981-990.

17. Brauner G. Rock burst in Coal Mines and Their Prevention. A. A. Balkema, Netherlands, 1994.

18. Kaiser P. K., Tannant D. D., McCreath D.R. Canadian Rock burst Support Handbook. Geomechanics Research Centre, Laurentian University, Sudbury, Ontario, 1996, pp. 314.

19. Chen B. R., Feng X. T., Li Q. P., Luo R. Z., Li S.J. Rock burst intensity classification based on the radiated energy with damage intensity at Jinping II hydropower station, China. Rock Mech. Rock Eng., 2013, 48(1), 289-303.

20. Cai M., Champaigne D. Influence of bolt-grout bonding on MCB conebolt performance. International Journal of Rock Mechanics & Mining Sciences, 49, 2012, pp. 65-175.

21. Jager A. J. Two new support units for the control of rock burst damage. Rock Support in Mining and Underground Construction; 1992, pp. 621-31.

22. Tannant D. D., Buss B. W. Yielding rockbolt anchors for high convergence or rock burst conditions. In: Proceedings of the 47th Canadian Geotechnical Conference; 1994.

23. Simser B., Andrieus P., Gaudreau D. Rock burst support at Noranda's Brunswick Mine, Bathurst, New Brunswick. In: Hammah R, Bawden W, Curran J, Telesnicki M, editors. Proc NARMS 2002, vol. 1.University of Toronto Press; 2002, pp. 805-13.

24. Manchao H., Chen L., Weili G., L.R.S., Shenglin L. Dynamic tests for a Constant-Resistance-Large-Deformation bolt using a modified SHTB system. Tunnelling and Underground Space Technology, 64, 2017, pp. 103-116.

25. He M. C., Gong W., Wang J., Qi P., Tao Z., Du S. Development of a novel energy-absorbing bolt with extraordinarily large elongation and constant resistance. Int. J. Rock Mech. Min. Sci., 67, 2014, pp. 29-42.

26. He M., Miao J., Li D., Wang C. Experimental study on rock burst processes of granite specimen at great depth. Chinese Journal of Rock Mechanics and Engineering, 2007, 26(5), pp. 865-876.

ORIGINAL PAPERS

DOI: 10.17073/2500-0632-2019-2-111-121

The Study of Regularities of Changing Melting Enthalpy of Intermetallides of Magnesium–Lantanoids Systems Rich in Magnesium

I. R Ismoilov[1], E. S. Dodkhoev[1], R. A. Ismoilov[2], S. Z. Nazhmudinov[3], A. B. Badalov[1]

[1]Tajik Technical University named after academician M. S. Osimi, Dushanbe, Republic of Tajikistan;

[2]State Scientific Institution "Center for the Study of Innovative Technologies" at the Academy of Sciences of the Republic of Tajikistan, Dushanbe, Republic of Tajikistan;

[3]Academy of Sciences of the Republic of Tajikistan, Dushanbe, Republic of Tajikistan, ✉Najmiddinovsh2018@mail.ru.

Abstract: Providing a reasonable forecast of the required properties of intermetallic compounds (hereinafter also referred as intermetallides or IM) is an important scientific and commercial problem, which may be solved by focusing scientific researches and permanent generation of knowledge in this field. To date, researches in chemistry and physics of IM have been developing empirically for a simple reason, due to the complexity of describing the relationship between the crystal structure and chemical bonds, and, therefore, between all the properties of IM. IM is mainly characterized by metal type of chemical bond, as well as specific metallic properties. At the same time, among IM, there are also salt-like compounds with ionic bond, i.e. valency compounds formed from elements of different chemical nature, being stoichiometric compounds. The examples of such compounds are compounds with intermediate bond type, i.e. ion-metal and covalently-metal, as well as covalent bond types (e.g., NaAu). In the series of compounds of Mg with elements of the IV subgroup, along with decreasing the difference in the electrochemical characteristics of the components, the change in the IM properties is observed, from those peculiar to ionic compounds (for example, Mg_2Si, Mg_2Ge) to the properties typical of metals (Mg_2Pb), etc. Due to the fact that lanthanides form the largest group of elements of the periodic system occurring in nature, and Mg is a relatively active chemical element in terms of IM formation (for example, it forms three IM with cadmium - Mg_3Cd, MgCd and $MgCd_3$), its oxides in slag provide decreasing average silicon content and increasing the stability of the silicon content in iron, being an important process indicator in the course of physicochemical reactions occurring in a blast furnace (for example, in the process of iron production). The presence of Si impurity (along with O, Au, Ti, V, Zr) produces the greatest effect on efficiency of solar cells, etc. [1–3]. Based on the foregoing, it is very important to study the state function, i.e. enthalpy of magnesium-lanthanide systems, rich in magnesium, and, based on the results of computer simulation, taking into account molecular dynamics method and other similar studies [4–8], to model regularities of changes in melting enthalpy of IM of the mentioned systems. The issue of modeling the pattern of change in melting enthalpy of IM of magnesium-lanthanide (Mg-Ln) magnesium-rich systems is considered based on systematic analyzing melting enthalpy of IM of Mg-Ln magnesium-rich system, including Mg_2Ln, Mg_3Ln and equimolar compound MgLn, implemented using semi-empirical method developed by N.S. Poluektov.

Keywords: regularity, intermetallides, correlation, lanthanides, magnesium, lanthanide composition, enthalpy of melting, electronic structure, semi-empirical method.

For citation: Ismoilov I. R, Dodkhoev E. S., Ismoilov R. A., Nazhmudinov S. Z., BadalovA. B. The study of regularities of changing melting enthalpy of intermetallides of magnesium–lantanoids systems rich in magnesium. *Mining Science and Technology*. 2019;4(2):111-121 (In Russ.). DOI: 10.17073/2500-0632-2019-2-111-121.

Моделирование закономерности изменения энтальпии плавления интерметаллидов систем магний-лантаноиды, богатых магнием

Исмоилов И. Р.[1], Додхоев Э. С.[1], Исмоилов Р. А.[2], Нажмудинов Ш. З.[3], Бадалов А. Б.[1]

[1]Таджикский технический университет имени академика М. С. Осими, Душанбе, Республика Таджикистан;

[2]Государственное научное учреждение «Центр исследования инновационных технологий» при Академии наук Республики Таджикистан, Душанбе, Республика Таджикистан;

[3]Академия наук Республики Таджикистан, Душанбе, Республика Таджикистан,
✉Najmiddinovsh2018@mail.ru

Аннотация: Обеспечение обоснованного прогноза необходимых свойств интерметаллидов (ИМ), являющегося важным направлением науки и определенных отраслей промышленности, достигается научно-исследовательскими работами и постоянной генерацией знаний в этом направлении. Проводимые до сегодняшнего дня исследования по химии и физике ИМ развиваются эмпирически по простой причине – в связи со сложностью описания взаимосвязи между кристаллическим строением и химическими связями, а следовательно, и между всеми свойствами ИМ. Для ИМ в основном характерны металлический тип химической связи, а также специфические металлические свойства. В то же время среди ИМ имеются также солеобразные соединения с ионной связью, т.е. валентные соединения, образующиеся из элементов различной химической природы, представляющие собой стехиометрические соединения. Примером таких соединений являются соединения с промежуточным характером связи, т.е. ионно-металлической и ковалентно-металлической, а также с ковалентной (например, NaAu). В ряду соединений Mg с элементами IV подгруппы вместе с уменьшением различия в электрохимических характеристиках компонентов наблюдается и изменение свойств ИМ – от характерных для ионных соединений (например, Mg_2Si, Mg_2Ge) до свойств, типичных для металлов (Mg_2Pb), и т.д. В связи с тем что лантаноиды образуют самую большую группу элементов периодической системы, находящихся в природе, а элемент Mg является относительно активным химическим элементом по образованию ИМ (например, с кадмием образует три ИМ – Mg_3Cd, MgCd и $MgCd_3$), – его оксиды в шлаке обеспечивают снижение среднего значения и повышение устойчивости содержания кремния в чугуне, – а это важный технологический показатель в ходе физико-химических реакций, происходящих в горне доменной печи (например, при выплавке чугуна). Наличие его примеси (наряду с O, Au, Ti, V, Zr) оказывает наибольшее влияние на эффективность солнечных элементов и т.д. [1–3]. Исходя из изложенного весьма важным является исследование функции состояния, т.е. энтальпии систем магний–лантаноиды, богатых магнием, и на основе полученных путем компьютерного моделирования результатов, с учетом метода молекулярной динамики и других подобных исследований [4–8], моделирование закономерности изменения энтальпии плавления ИМ упомянутых систем. Рассматривается вопрос моделирования закономерности изменения энтальпии плавления ИМ систем магний–лантаноиды (Mg–Ln), богатых магнием, путем системного анализа энтальпии плавления ИМ систем Mg–Ln, богатых магнием составов Mg_2Ln, Mg_3Ln и эквимолярного состава MgLn, проведенного с помощью полуэмпирического метода, разработанного Н.С.Полуэктовым.

Ключевые слова: закономерность, интерметаллиды, корреляция, лантаноиды, магний, состав лантанидов, энтальпия плавления, электронное строение, полуэмпирический метод.

Для цитирования: Исмоилов И. Р., Додхоев Э. С., Исмоилов Р. А., Нажмудинов Ш. З., Бадалов А. Б. Моделирование закономерности изменения энтальпии плавления интерметаллидов систем магний-лантаноиды, богатых магнием. *Горные науки и технологии.* 2019;4(2):111-121. DOI: 10.17073/2500-0632-2019-2-111-121.

Introduction Intermetallides (IM), the most important minerals of rare-earth metals (elements) in nature, are characterized by predominantly metallic bonding between atoms in the lattice, but at the same time, there are intermetallic compounds with ionic and covalent chemical bonds, as well as intermediate cases, i.e. ion-metallic and covalent-metallic bonding. This rather diverse bonding between atoms in the IM lattice provides them with: low to high hardness; chemical resistance, as well as an active chemical reactivity (for example, the reaction of zinc and nickel at a temperature above 1000 ° C is of explosive nature); higher melting point than the that of the source metals in a range from 804 °C for cerium and 1700 °C for lutetium); the formation of an eutectic alloy (based on the smallest crystals of two metals, each of which has an independent crystal lattice), which melts at lower temperature than these pure metals (for example, an eutectic alloy consisting of 24.4 atomic % Pb (melting point of 327 °C) and 75.6 atomic % Sn (melting point of 232 °C), melts at 181 °C); relatively lower plasticity than the source metals, but appropriate ductility; increased brittleness of the alloys in the structure of which the elements are included; semiconductor properties; shape memory (after hardening, the product can be deformed mechanically, but will take its original shape after heating a little); weakening the contact mechanical strength and deterioration of electrical characteristics (for example, in soldered joints); division into two groups based on their density (light, below 8 g/cm^3, and heavy, from 8.272 to 9.482 cm^3), etc. [9–15].

Thematic justification Despite the fact that the term lanthanides appeared about a century ago (in 1925 it was first used by V. Goldschmidt), the importance and relevance of the use of lanthanides (Ln) are still required expansion and deepening of studies to identify their thermomechanical and thermodynamic characteristics, and also prospecting and exploration of deposits to produce Ln concentrates. Lanthanides find growing application in modern industries, actively developing over the past 40 years, especially in Japan, China, and other industrialized countries. The published data show that the demand for rare earth elements (REE) from 1980 to the present has grown from 30,000 tons to 120,000 tons and the annual average rate of their consumption growth is projected at 4%, which in turn justifies the relevance of further research in this direction.

Review of the historical studies shows that light alloys based on magnesium, alloyed with rare-earth metals, in particular lanthanides, have important application characteristics. In turn, reliable information on the physicochemical and thermal characteristics of these alloys contribute to their widespread use in modern branches of science, engineering and technological processes. Phase equilibrium diagrams of magnesium-based systems (silicate systems), as well as Mg – Ln systems, have been studied by many researchers [16–30]. The findings of these and other studies, summarized in [31], indicate that MgLn, Mg_2Ln, Mg_3Ln, $Mg_{12}Ln$, and $Mg_{24}Ln_5$ intermetallides (IM) are formed in Mg – Ln systems. Currently, there is no published information on an important indicator of the system internal energy (state function) – melting enthalpy (EP) of these IM, which characterizes the thermal effect of the process proceeding at constant pressure.

This paper presents the findings of a systematic analysis of melting enthalpy of the IM of Mg – Ln systems, magnesium-rich compounds Mg_2Ln, Mg_3Ln, and the equimolar MgLn. The analysis was carried out using the semi-empirical method developed by N. S. Poluektov and et. al. [32, 33]. The calculation (hereinafter calculation 1) is produced using the following correlation equation:

$$A_{(\mathrm{Mg\ xLny})} = A_{(\mathrm{Mg\ xLay})} + \alpha N_f + \beta S + \gamma' L_{(\mathrm{Ce\text{-}Eu})}(\gamma'' L_{(\mathrm{Tb\text{-}Yb})}), \quad (1)$$

where coefficient α – takes into account the share effect of 4*f* electrons, β-spin (*S*) - and γ-orbital (*L*) moments of Ln atom motion (γ' for Ln-cerium and γ'' for Ln-yttrium subgroups) on the values of the IM melting enthalpy (ΔH_{melt}).

The mentioned method is widely used, and we have also successfully applied it for many Ln compounds [34–36].

Determined and/or refined values of the melting temperature of Mg–Ln system IM made it possible to determine melting enthalpy of IM of the above-mentioned compositions (hereinafter referred as Calculation 2) using the following equation [37, 38]:

$$\Delta H^0_{\text{пл},}\mathrm{Mg}_x\mathrm{Ln}_y = T_{\text{пл.}}^{\text{им}}(n\Delta H_{\text{пл.}}^{\text{Ln}}/T_{\text{пл.}}^{\text{Ln}} + m\Delta H_{\text{пл.}}^{\text{Mg}}/T_{\text{пл.}}^{\text{Mg}})/n+m. \quad (2)$$

The values of the coefficients of the correlation equation (1) given in Table 1 allow to determine the share effect of each component of the equation on the values of melting enthalpy of Mg–Ln system IM.

The most complete data obtained on melting enthalpy of intermetallides of the studied compositions are given in Table 2.

The data given in Table 2 show satisfactory coincidence of the melting enthalpy values obtained by the two methods. This indicates the validity of the applied semi-empirical methods and the reliability of the obtained results. The only exception is data for few MI. Perhaps this is due to some experimental conditions and insufficiently pure reagents.

Table 1

The values of the coefficients of equation (1) for the determination of melting enthalpy of intermetallides

IM	Parameter	α	β	γ'	γ''
MgLn	$\Delta H^0_{\text{пл}}$	−0.096	0.02	−0.127	0.410
Mg_2Ln	$\Delta H^0_{\text{пл}}$	−0.26	0.43	−0.09	0.005
Mg_3Ln	$\Delta H^0_{\text{пл}}$	−0.018	−0.365	0.1652	0.062

Table 2

The most complete information obtained on melting enthalpy of intermetallides of the studied compositions

IM	Mg_3Ln			Mg_2Ln			MgLn		
	$\Delta H^{\circ}_{\text{пл.}}$		Discrepancy, %	$\Delta H^{\circ}_{\text{пл.}}$		Discrepancy, %	$\Delta H^{\circ}_{\text{пл.}}$		Discrepancy, %
Ln	Calculation 1	Calculation 2		Calculation 1	Calculation 2		Calculation 1	Calculation 2	
La	10190	10190	–	9950	9950	–	10610	10610	–
Ce	10670	10410	2.4	9550	9370	1.9	9000	9560	5.8
Pr	10290	10520	2.1	8530	9130	6.6	8779	8910	1.47
Nd	9870	10560	6.5	8530	9000	5.2	8466	8530	0.75
Pm	9954	10360	3.91	9270	8590	7.3	9010	8440	6.3
Sm	9080	9990	9.1	9420	9000	4.4	8333	8640	3.55
Eu	7800	8110	3.8	9520	9520	–	7080	7140	0.8
Gd	9040	9040	–	9650	9650	–	10010	10010	–
Tb	9024	9120	1.0	8150	8900	8.4	11140	11140	–
Dy	9073	9400	3.4	9330	8410	9.8	11220	11750	4.5
Ho	9260	9630	3.8	8020	7930	1.1	11170	12050	7.5
Er	10190	9800	3.9	8260	7450	9.8	10906	11950	8.37
Tm	9260	9900	6.46	6820	6980	2.2	10767	11430	5.80
Yb	8156	8420	3.13	8980	8980	–	6790	7020	3.27
Lu	9940	9940	–	6530	6530	–	9270	9270	–

The obtained most complete values of melting enthalpy of the studied IM compounds made it possible to determine the regularities of changing the melting enthalpy depending on the nature of Ln. As seen from Fig. 1-3, the dependencies are complex in nature within the entire group and are divided into the Ln subgroups, cerium and yttrium, with the manifestation of the "tetrad effect". The following features should be noted:

–for IM of MgLn and Mg_2Ln compositions (cerium subgroup), the similar curves are observed. Increasing Ln atomic number within the subgroups leads to decreasing the IM melting enthalpy, with a minimum for the Pm compound.

For the IM of the composition Mg_2Ln (yttrium subgroup), increasing Ln atomic number leads to practically linear decreasing the IM melting enthalpy, with the exception of the ytterbium compound;

–the similar curve character is observed for IM of MgLn (yttrium subgroup) and Mg_3Ln (both subgroups) compositions. The curves have a bulge up with a maximum in the middle of the subgroups;

–the deviation of the characteristics of europium and ytterbium IM from the found regularities is due to the partial and complete filling by electrons of the 4*f* orbitals of these elements atoms.

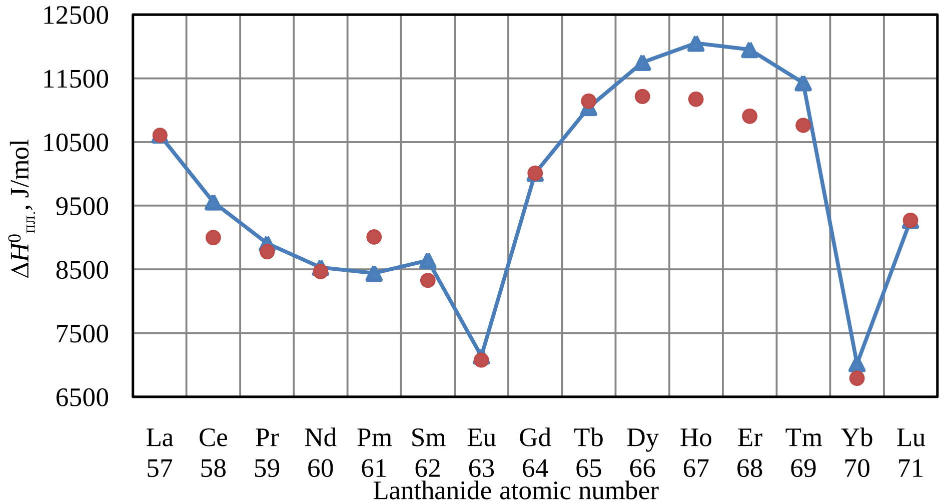

Fig. 1. Plot of melting enthalpy of intermetallides of MgLn composition as function of Ln sequence number. Hereinafter ● – calculation 1, ▲ – calculation 2

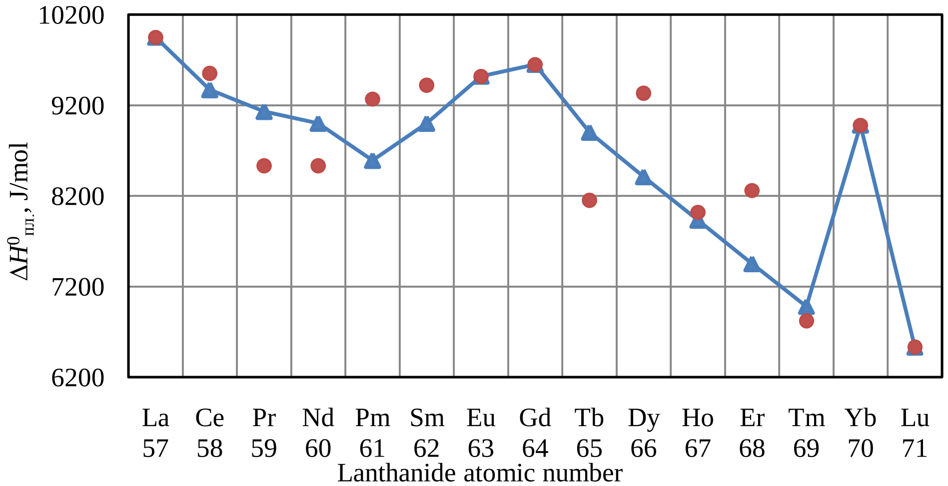

Fig. 2. Plot of melting enthalpy of intermetallides of Mg_2Ln composition as function of Ln sequence number

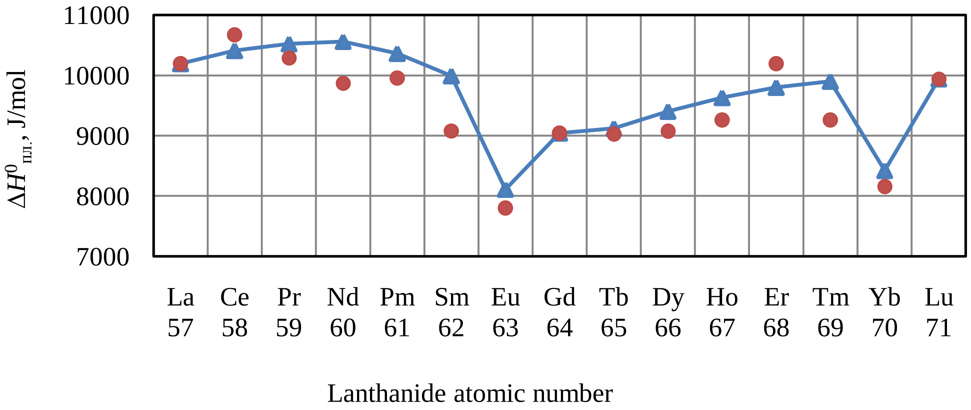

Fig. 3. Plot of melting enthalpy of intermetallides of Mg_3Ln composition as function of Ln sequence number

Table 3

The equations describing change of thermal characteristics of intermetallides depending on nature of lanthanides

IM composition	Parameter		Equation	R^{2*}
MgLn	$\Delta H^0_{пл.}$	(*a*)	$y = 0.1516x^2 - 1.4495x + 11.889$	0.9994
		(*b*)	$y = -0.2726x^2 + 2.1367x + 7.9771$	0.9412
Mg_2Ln	$\Delta H^0_{пл.}$	(*a*)	$y = 0.0763x^2 - 0.74x + 10.607$	0.9211
		(*b*)	$y = 0.019x^2 - 0.6581x + 10.23$	0.998
Mg_3Ln	$\Delta H^0_{пл.}$	(*a*)	$y = -0.0748x^2 + 0.492x + 9.751$	0.9806
		(*b*)	$y = -0.0145x^2 + 0.2826x + 8.7071$	0.9782

Notes: (*a*) – cerium; (*b*) – yttrium subgroups; R^2 is the degree of confidence; x is atomic number of a metal; y is melting enthalpy of an IM.

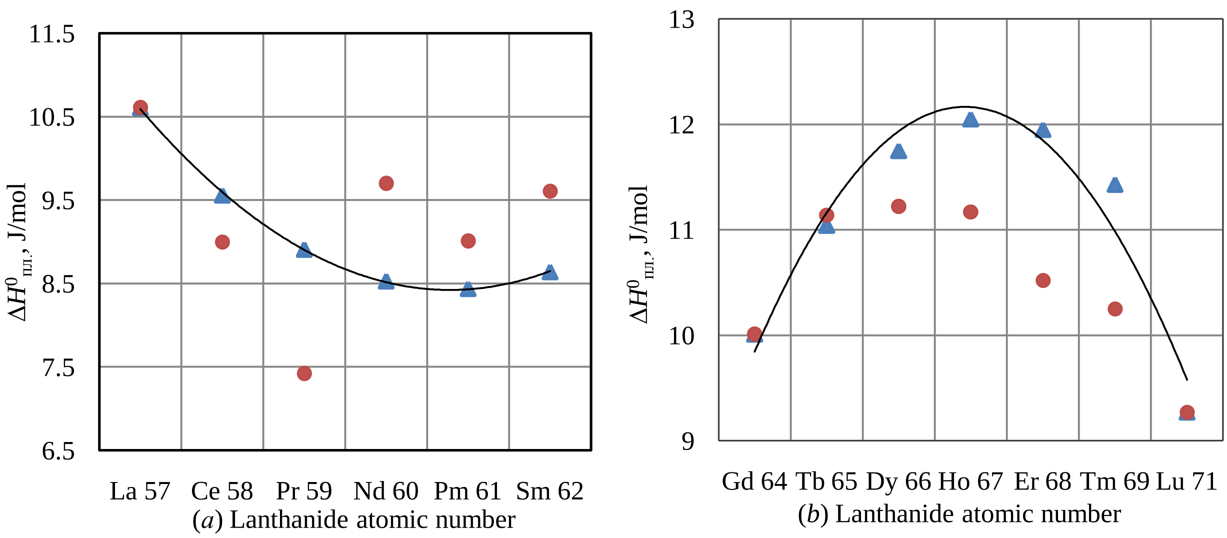

Fig. 4. Plot of melting enthalpy of intermetallides as function of the nature of lanthanides: – trend line

Table 4

The equations describing change of ΔH^0_{melt} of intermetallides depending on their composition

Lanthanide	Trend equation	Lanthanide	Trend equation
La	$y = 450x^2 - 2010x + 12170$	Gd	$y = -125x^2 + 15x + 10120$
Ce	$y = 285x^2 - 305x + 9020$	Tb	$y = 740x^2 - 5210x + 15610$
Pr	$y = 325x^2 + 135x + 6960$	Dy	$y = -230x^2 - 1200x + 12650$
Nd	$y = 1255x^2 - 4935x + 13380$	Ho	$y = 2195x^2 - 9735x + 18710$
Pm	$y = -340x^2 + 1280x + 8070$	Er	$y = 2095x^2 - 8545x + 16970$
Sm	$y = -75x^2 + 35x + 9650$	Tm	$y = 2715x^2 - 11575x + 19110$
Eu	$y = -2080x^2 + 8680x + 480$	Yb	$y = -2250x^2 + 8940x + 100$
		Lu	$y = 3075x^2 - 11965x + 18160$

***Notes to Table 4**: $R^2 = 1$ – for all the IM; $x = m : n$ and is determined based on $Mg_{(m)}Ln_{(n)}$ composition of IM; y – IM melting enthalpy ΔH^0_{melt}

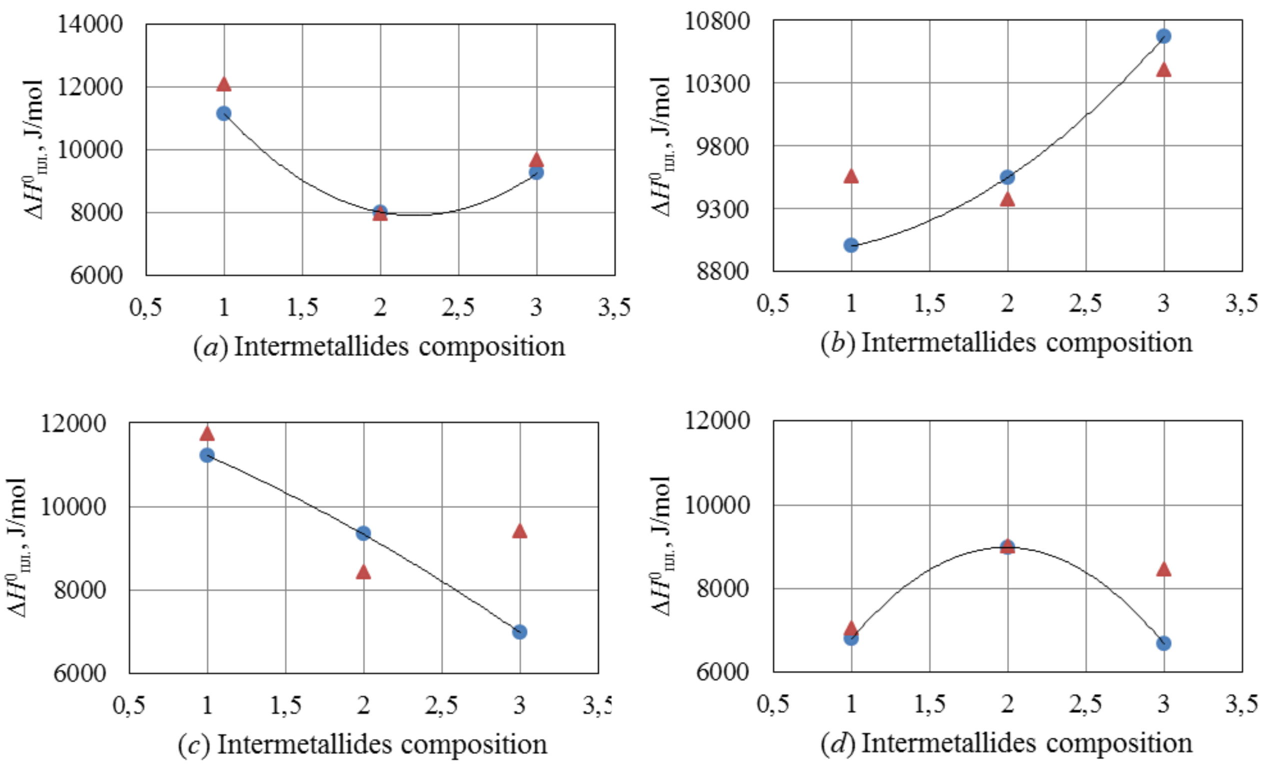

Fig. 5. Plot of melting enthalpy (ΔH^0_{melt}) of intermetallides of $Mg_{(m)}Ln_{(n)}$ system as function of their composition (m/n): — trend line

Mathematical modeling of the IM melting enthalpy for the studied compositions of Mg–Ln system was carried out using the standard Microsoft Excel program. The calculation results are given in Table 3. The data processing was performed separately for cerium and yttrium Ln subgroups. The calculations did not take into account the melting enthalpy values for europium and ytterbium IM.

Fig. 4 shows the characteristic curves of the IM melting enthalpy depending on the nature of Ln for the subgroups: 4 (*a*) – cerium, 4 (*b*) – yttrium.

Equations of the IM ΔH^0_{melt} dependence on the IM composition and the characteristic curves reflecting the IM melting enthalpy in Mg-Ln system depending on their composition are given in Table 4 and in Fig. 5, respectively.

The graphs present the melting enthalpy curves for the lanthanide IM of: 5 (*a*) – yttrium subgroups, 5 (*b*) – Ce, Pr, and Nd; 5 (*c*) – Pm, Sm, and Eu; 5 (*d*) – La, Gd, and Lu. The changes in the properties of the IM of La, Gd, and Lu are mainly due to the linear nature of electron replenishment of 4*f* orbitals (N_f Eq. (1)), the similarity of the electronic structure, and the possibility of 4f electron transfer to 5d orbitals in these atoms. In other subgroups, spin (*S*)-orbital (*L*) interactions have a decisive effect.

Conclusion

Analytical and graphical interpretations of the study results using the above methods and mathematical modeling of the IM compounds melting enthalpy allowed drawing the following conclusions:

1. Based on the use of the semi-empirical method, the values of the correlation equation coefficients were determined, enabling determining the share effect of each component on melting enthalpy of the Mg–Ln system IM.

2. The most complete data have been obtained on the melting enthalpy of the Mg – Ln system IM of the studied compositions, showing a fairly satisfactory convergence of the melting enthalpy values obtained by two methods, indicating the validity of the applied semi-empirical methods and the reliability of the study results (with the exception of few IM, large discrepancy for which was possibly connected with some experimental conditions and insufficiently pure reagents).

3. The regularities of changing the calculated IM melting enthalpy depending on Ln nature were determined: within the whole group, the regularities are of complex nature, with division into Ln subgroups, cerium and yttrium, with the "tetrad effect" manifestation, and with the following features: for the cerium group (IM of MgLn and Mg_2Ln composition), the similar curve shape is observed. Increasing Ln atomic number within the subgroups leads to decreasing the IM melting enthalpy, with a minimum for the Pm compound.

3.1. For the IM of Mg_2Ln composition (yttrium subgroup), increasing Ln atomic number leads to practically linear decreasing the IM melting enthalpy, with the exception of the ytterbium compound.

4. The determination of the regularities of changing the melting enthalpy of the Mg – Ln system IM (rich in Mg) depending on Ln nature, taking into account their important application characteristics, expands a database on: prognostic properties of the IM of different their structures and compositions; physicochemical and thermal characteristics of IM; as well as allows simplifying and refining system analyzes and solving other important applied problems.

References

1. Goncharov B. F., Solomakhin I. S. Production of pig iron. Moscow, Metallurgy Publ., 1965, 368 p. (in Russ.).

2. Vasiliev V. E. Blast furnace smelting based on stable slags. Kiev, State Publishing House for Technical Literature, 1956, 260 p. (in Russ.).

3. Parkhomenko Yu. N. Physics and technology of photonics instruments: solar energy and nanotechnologies. Textbook. / Parkhomenko Yu. N. Polisan A. A. Moscow, MISiS Publishing House, 2013, 142 p. (in Russ.).

4. Anastasiou N., Fiuchaur D. Programs for the dynamic simulations of liquids and solids. II MDIONS: Rigid ions using the Evalid sum // Comp. Phys. Commun. 1982, no. 25, pp. 158–176.

5. Woodcock L. V., Angell K. A., Cheeseman P. Molecular dynamics studies of the vitreons state: Simple ionics systems and silica // The Gournal of Chemical Physics, 1976, no. 65, pp. 1565–1577.

6. Belashchenko D. K., Ostrovski O. I., Skvortsov L. V. Molecular dynamics simulation of binary CaO–FeO, MgO–SiO_2, FeO–SiO_2, CaO–SiO_2 and ternary CaO–FeO–SiO_2 systems // Termochimica Acta. 2001, vol. 372, pp. 153–163.

7. Zhang L., Jahanshahi S. Review and modeling of viscosity of silicate melts. Part I. Viscosity of binary and ternary silicates containing CaO, MgO and MnO // Meter. Trans. B. 1998. vol. 29, no. 1, pp. 177–186.

8. Gutierres J., Romero-Serrano A., Plascencia G., Chaves F., Vargas R. Thermodynamical model of ternary silicate systems // ISIJ Int. 2000, vol. 40, no. 7, pp. 664–669.

9. Kornilov I. I., Matveeva N. M., Pryakhina L. I., Polyakova R. S. Metallochemical properties of the periodic system elements. Moscow, Nauka Publ., 1966, 272 p. (in Russ.).

10. Skakov Yu.A. Intermetallides. Chemical Encyclopedia in 5 volumes. Knunyants, I. L. (Ch. Ed.). M., Soviet Encyclopedia Publ., 1990, v. 2: Duff-Copper, 671 p. (in Russ.).

11. Intermetallides. Kazakhstan, National Encyclopedia. Almaty, *Kazak encyclopediyasy* [Kazakh Encyclopedia] Publ., 2005, v. II (in Russ.).

12. Kripyakevich P. I. Structural types of intermetallic compounds. Moscow, 1977 (in Russ.).

13. Teplyakov F. K., Oskolskikh A. P., Kaluzhsky N. A. [et al.]. About mechanism of formation of intermetallic compounds and their transformation in the process of preparation and use of Al – Ti – B and Al – Ti master alloys. Tsvetnye Metally [Nonferrous Metals], 1991, no. 9, p. 54. (in Russ.).

14. Sidelnikov S. B., Dovzhenko N. N, Voroshilov D. S. [et al.]. The study of the metal structure and evaluation of the properties of test samples of Al – REM system alloy, obtained by combined casting/pressing methods. Bulletin of Magnitogorsk State Technical University named after G.I. Nosov, Magnitogorsk, 2012, no. 1, pp. 51-55. (in Russ.).

15. Belopukhov S. L., Starykh S. E. Physical and colloidal chemistry. Basic terms and definitions. Textbook. M., Prospect, 2018, 256 p. (in Russ.).

16. Klyucharov Ya. V., Chen-Di-Jian. On phase equilibrium in MgO – Cr_2O_3 – Fe_2O_3 system. (in Russ.).

17. Strott A. J. Prod. Engng, 1960, no. 43.

18. Ryschkewitsch E. Oxide ceramics: Phisical chemistry and Technology. New-Jork–London, 1960.

19. Atlas L., Journal. Geol., 1952, vol. 60, no. 2, p. 127.

20. Boyd F. R., J. L. England, Carnegie Inst. Washington, year book 59, 47, 1959–1960.

21. Boyd F. R., J. L. England, Carnegie Inst. Washington, year book 60, 115, 1960–1961.

22. Davis B. T. C., J. L. England, Carnegie Inst. Washington, year book 62, 119, 1962–1963.

23. Morimoto N., Carnegie Inst. Washington, year book 58, 197, 1958 – 1959.

24. Ringwood A.E., Journal. Geophysics Rea., 67, № 10, 4005, 1962.

25. Ringwood A.E., M. Seabrook, Nature, 196, № 4857, 883, 1962.

26. Physico-chemical properties of elements. Handbook. Ed. Samsonova G. V. Kiev, 1965, 806 p. (in Russ.).

27. Vozdvizhensky V. M. Forecast of binary phase equilibrium diagrams. M., Metallurgy Publ., 1975, 222 p. (in Russ.).

28. Burylyov B. P. Thermodynamics of metallic interstitial metal solutions. Rostov-on-Don, Rostov University Publ., 1984, 160 p. (in Russ.).

29. Vozdvizhensky V. M. General patterns in the structure of phase equilibrium diagrams of metal systems. M., Nauka Publ., 1973, 144 p. (in Russ.).

30. Budanova G. M., Volodarskaya, R. S., Kanaev, N. A. Analysis of aluminum and magnesium alloys. Moscow, Metallurgy Publ., 1966, 360 p. (in Russ.).

31. Phase equilibrium diagrams of binary metal systems / Ed. N. P. Lyakisheva. Moscow: Mashinostroenie (Machine Building) Publ., 1996, 1997, 2001, v. 1-3, 992 p., 1024 p., 1320 p. (in Russ.).

32. Poluektov N. S., Meshkova S. B., Korovin Yu. V., Oksinenko, I. I. Correlation analysis in physical chemistry of compounds of trivalent lanthanide ions. DAN USSR, 1982, v. 266, no. 5, pp. 1157-1159. (in Russ.).

33. Meshkova S. B., Poluektov N. S., Topilova Z. M., Danilkovich M. M. Gadolinium “dog-leg” in row of trivalent lanthanides. Coord. Chemistry, 1986, v. 12, Issue. 4, pp. 481-484 (in Russ.).

34. Badalov A. B., Gafurov B. A., Mirsaidov I. U., Hakerov I. Thermal stability and thermodynamic properties of this tetrahydrofuranates lanthanide boro-hydrides. Inter. J. of Hydrogen energy, 2011, vol. 36, iss. I, pp. 1217-1219.

35. Ismoilov I. R., Umedov Sh. T., Akramov M. Yu., Badalov A. Thermochemical properties of intermetallic compounds of Mg_2Ln composition (Ln-lanthanides). Proceedings of Tajikistan scientific-practical conference devoted to the 10th anniversary of Mining and Metallurgical Institute of Tajikistan. Chkalovsk, 2016, pp. 36-37 (in Russ.).

36. Ismoilov I. R., Dodkhoev E. S., Obidov Z. R., Badalov A. Regularities of changing temperature and enthalpy of melting of intermetallic compounds of MgLn and Mg_2Ln composition (Ln-lanthanides). Proceedings of Tajikistan scientific-practical conference "Problems of Materials Science in the Republic of Tajikistan." IKh AN RT Publ., 2016, pp. 149-152 (in Russ.).

37. Bayanov A. P., Slavkina V. I. On thermodynamics of liquid rare-earth metal alloys with strong chemical interaction of components. Proceedings of the conference devoted to the centenary of the All-Union Chemical Society named after D.I. Mendeleev. Novokuznetsk, 1969, pp. 25-39 (in Russ.).

38. Bayanov A. P. Calculation of formation enthalpy of rare-earth elements compounds based on crystallochemical characteristics. Proceedings of the USSR Academy of Sciences, Neorgan. Mater., 1973, vol. 9, no. 6, pp. 959-963 (in Russ.).

Библиографический список

1. Гончаров Б. Ф., Соломахин И. С. Производства чугуна. М.: Металлургия, 1965. 368 с.

2. Васильев В. Е. Доменная плавка на устойчивых шлаках. Киев: Государственное издательство техн. литературы, 1956. 260 с.

3. Пархоменко Ю. Н. Физика и технология приборов фотоники: солнечная энергетика и нанотехнологии: учеб. пособие / Ю. Н. Пархоменко, А. А. Полисан. М.: Изд. Дом МИСиС, 2013. 142 с.

4. Anastasiou N., Fiuchaur D. Programs for the dynamic simulations of liquids and solids. II MDIONS: Rigid ions using the Evalid sum // Comp. Phys. Commun, 1982, no. 25, pp. 158–176.

5. Woodcock L. V., Angell K. A., Cheeseman P. Molecular dynamics studies of the vitreons state: Simple ionics systems and silica // The Gournal of Chemical Physics, 1976, no. 65, pp. 1565–1577.

6. Belashchenko D. K., Ostrovski O. I., Skvortsov L. V. Molecular dynamics simulation of binary CaO–FeO, $MgO–SiO_2$, $FeO–SiO_2$, $CaO–SiO_2$ and ternary $CaO–FeO–SiO_2$ systems // Termochimica Acta, 2001, Vol. 372, pp. 153–163.

7. Zhang L., Jahanshahi S. Review and modeling of viscosity of silicate melts. Part I. Viscosity of binary and ternary silicates containing CaO, MgO and MnO // Meter. Trans. B. 1998, vol. 29, no. 1, pp. 177–186.

8. Gutierres J., Romero-Serrano A., Plascencia G., Chaves F., Vargas R. Thermodynamical model of ternary silicate systems // ISIJ Int. 2000, vol. 40, no. 7, pp. 664–669.

9. Корнилов И. И., Матвеева Н. М., Пряхина Л. И., Полякова Р. С. Металлохимические свойства элементов периодической системы. М.: Наука, 1966. 272 с.

10. Скаков Ю. А. Интерметаллиды // Химическая энциклопедия: в 5 т / И. Л. Кнунянц (гл. ред.). М.: Советская энциклопедия. 1990. Т. 2: Даффа–Меди. 671 с.

11. Интерметаллиды // Казахстан. Национальная энциклопедия. Алматы: Қазақ энциклопедиясы, 2005. Т. II.

12. Крипякевич П. И. Структурные типы интерметаллических соединений. М., 1977.

13. О механизме образования интерметаллидов и их превращения в процессе приготовления и использования лигатур Al–Ti–B и Al–Ti / Ф. К. Тепляков, А. П. Оскольских, Н. А. Калужский [и др.] // Цветные металлы, 1991. № 9. С. 54.

14. Исследование структуры металла и оценка свойств опытных образцов из сплава системы $Al–P_3M$, полученных совмещенными методами литья и обработки давлением / С. Б. Сидельников, Н. Н. Довженко, Д. С. Ворошилов [и др.] // Вестник Магнитогр. гос. техн. ун-та имени Г.И. Носова. Магнитогорск, 2012. № 1. С. 51-55.

15. Белопухов С. Л., Старых С. Э. Физическая и коллоидная химия. Основные термины и определения: учеб.пособие. М.: Проспект, 2018. 256 с.

16. Ключаров Я. В., Чен-Ди-Цзянь. О фазовом равновесии в системе $MgO–Cr_2O_3–Fe_2O_3$.

17. Strott A. J. Prod. Engng, 1960. No. 43

18. Ryschkewitsch E. Oxide ceramics: Phisical chemistry and Technology. New-Jork–London, 1960.

19. Atlas L., Journal. Geol., 1952, vol. 60, no. 2, p. 127.

20. Boyd F. R., J. L. England, Carnegie Inst. Washington, year book 59, 47, 1959–1960.

21. Boyd F. R., J. L. England, Carnegie Inst. Washington, year book 60, 115, 1960–1961.

22. Davis B. T. C., J. L. England, Carnegie Inst. Washington, year book 62, 119, 1962–1963.

23. Morimoto N., Carnegie Inst. Washington, year book 58, 197, 1958–1959.

24. Ringwood A.E., Journal. Geophysics Rea., 67, № 10, 4005, 1962.

25. Ringwood A.E., M. Seabrook, Nature, 196, № 4857, 883, 1962.

26. Физико-химические свойства элементов. Справочник / Под ред. Г.В. Самсонова. Киев, 1965. 806 с.

27. Воздвиженский В. М. Прогноз двойных диаграмм состояния. М.: Металлургия, 1975. 224 с.

28. Бурылёв Б. П. Термодинамика металлических растворов внедрения. Ростов-на-Дону: Ростовский университет, 1984. 160 с.

29. Воздвиженский В. М. Общие закономерности в строении диаграмм состояния металлических систем. М.: Наука, 1973. 144 с.

30. Буданова Г. М., Володарская Р. С., Канаев Н. А. Анализ алюминиевых и магниевых сплавов. М.: Металлургия, 1966. 360 с.

31. Диаграммы состояния двойных металлических систем / Под ред. Н.П. Лякишева. М.: Машиностроение, 1996, 1997, 2001, т.1─3, 992 с., 1024 с., 1320 с.

32. Полуэктов Н. С., Мешкова С. Б., Коровин Ю. В., Оксиненко И. И. Корреляционный анализ в физикохимии соединений трёхвалентных ионов лантаноидов. ДАН СССР, 1982. Т. 266. № 5. С. 1157-1159.

33. Мешкова С. Б., Полуэктов Н. С., Топилова З. М., Данилкович М. М. Гадолиниевый излом в ряду трёхвалентных лантаноидов. Коорд. химия, 1986. Т. 12. Вып. 4. С. 481-484.

34. Badalov A. B., Gafurov B. A., Mirsaidov I. U., Hakerov I. Thermal stability and thermodynamic properties of this tetrahydrofuranates lanthanide boro-hydrides. Inter. J. of Hydrogen energy, 2011, vol. 36, iss. I, pp. 1217-1219.

35. Исмоилов И. Р., Умедов Ш. Т., Акрамов М. Ю., Бадалов А. Термохимические свойства интерметаллидов состава Mg_2Ln (Ln-лантаноиды). Материалы респ. науч.-практ. конф., посвященной 10-летию Горно-металлургического института Таджикистана. Чкаловск, 25.02.2016. С. 36-37.

36. Исмоилов И. Р., Додхоев Э. С., Обидов З. Р., Бадалов А. Закономерности изменения температуры и энтальпии плавления интерметаллидов составов MgLn и Mg_2Ln (Ln-лантаноиды). – Сб. матер. респ. науч.-практ. конф. «Проблемы материаловедения в Республике Таджикистан». ИХ АН РТ, 2016. С. 149-152.

37. Баянов А. П., Славкина В. И. К термодинамике жидких сплавов редкоземельных металлов с сильным химическим взаимодействием компонентов. Материалы конф., посвященной столетию Всесоюзного химического общества им. Д.И. Менделеева. Новокузнецк, 1969. С. 25-39.

38. Баянов А. П. Расчет энтальпии образования соединений редкоземельных элементов на основе кристаллохимических характеристик. Известия АН СССР, Неорган. матер. 1973. Том 9. № 6. С. 959-963.

Information about the authors

Ismoil R. Ismoilov – senior lecturer of the Department of Metallurgy of Tajik Technical University named after academician M. S. Osimi, Dushanbe, Republic of Tajikistan, krypton_89@bk.ru;

Eradzh S. Dodkhoev – senior lecturer of the Department of Electric Power Engineering of the Technical College of the Tajik Technical University named after academician M.S. Osimi, Dushanbe, Republic of Tajikistan, dodkhoev1984@mail.ru;

Rizo A. Ismoilov – researcher of the state scientific institution "Center for research of innovative technologies" at the Academy of Sciences of the Republic of Tajikistan, Dushanbe, Republic of Tajikistan, rizo.ismoilov@mail.ru;

Sarafidin Z. Nazhmudinov – Cand Sci. (Tech.), Headof the laboratory of Energy and energy saving of the Institute of water problems, hydropower and ecology of the Academy of Sciences of the Republic of Tajikistan. Najmiddinovsh2018@mail.ru;

Badalov Abdulhair – Dr. Sci. (Chem.), prof., Department "General and inorganic chemistry" of the Tajik Technical University named after academician M.S. Osimi, Dushanbe, Republic of Tajikistan,badalovab@mail.ru.

Информация об авторах

Исмоилов Исмоил Ризоевич – ст. преподаватель кафедры «Металлургия» Таджикского технического университета имени академика М.С. Осими, Душанбе, Республика Таджикистан, krypton_89@bk.ru;

Додхоев Эрадж Сарабекович – ст. преподаватель кафедры «Электроэнергетика» Технического колледжа Таджикского технического университета имени академика М.С. Осими, Душанбе, Республика Таджикистан, dodkhoev1984@mail.ru;

Исмоилов Ризо Ахмадович – научный сотрудник государственного научного учреждения «Центр исследования инновационных технологий» при Академии наук Республики Таджикистан. Соискатель, +992 935 60 67 69, e-mail: rizo.ismoilov@mail.ru;

Нажмудинов Шарофидин Зоирович – канд. техн. наук, зав. лабораторией Энергетики и энергосбережения Института водных проблем, гидроэнергетики и экологии Академии наук Республики Таджикистан, Душанбе, Республика Таджикистан, Najmiddinovsh2018@mail.ru;

Бадалов Абдулхаир – д-р хим. наук, проф. каф. «Общая и неорганическая химия» Таджикского технического университета им. акад. М.С. Осими, Душанбе, Республика Таджикистан, badalovab@mail.ru.

MINING SCIENCE AND TECHNOLOGY
ГОРНЫЕ НАУКИ И ТЕХНОЛОГИИ
VOL. 4, № 2 (2019)
MISIS National University of Science and Technology

ORIGINAL PAPERS

DOI: 10.17073/2500-0632-2019-2-122-131

Assessment of Effectiveness of Methods and Techniques for Degassing Methane-containing Coal Seams

S. N. Shirjaev
LLC "Raspadskaya Coal Company", Novokuznetsk, Russia, ✉sn_shir@mail.ru

Abstract: The findings of review of promising methods and techniques providing increasing effectiveness of degassing of coal seams containing methane in the process of their underground mining are presented. Based on the review findings, traditional methods and techniques of degassing were identified, the effectiveness of which is 12–25 %, as well as unconventional methods providing methane degassing of up to 40%. As a classification feature of the unconventional methods and techniques of gaseous methane liberation, a condition of decreasing pressure and increasing temperature of coal matrix containing solid gas hydrate has been adopted. The conditions for methane transition from gas hydrate to free gas taking into account actual mining and technogenic conditions of the mines have been identified. Given the difficulty of supplying additional thermal energy into a coal seam, as the main way to reduce pressure in the seam, unloading of the rock mass relative to the initial stress state, and disruption of coal and rocks in the course of transition from their elastic deformation to elastic-plastic and out-of-limit deformation are accepted.

Keywords: coal seam, methane, colliery, degassing, gas hydrate, rock pressure, desorption, filtration, rock disruption, gas content, coal matrix.

For citation: Shirjaev S. N. Assessment of effectiveness of methods and techniques for degassing methane-containing coal seams. *Mining Science and Technology*. 2019;4(2):122-131 (In Russ.). DOI: 10.17073/2500-0632-2019-2-122-131.

Оценка эффективности способов и средств дегазации углеметановых пластов

Ширяев С. Н.
ООО «Распадская угольная компания», Новокузнецк, Россия, ✉sn_shir@mail.ru

Аннотация: Представлены результаты анализа перспективных способов и технических средств, обеспечивающих повышение эффективности дегазации углеметановых пластов при их подземной разработке. По результатам анализа выделены традиционные способы и средства дегазации, эффективность которых составляет 12–25 %, и нетрадиционные способы с эффективностью десорбции метана до 40 %. В качестве классификационного признака нетрадиционных способов и средств десорбции метана газа принято условие снижение давления и повышение температуры угольной матрицы твёрдого газового гидрата. Выявлены условия перехода метана из газогидратного состояния в свободное с учётом реальных горнотехнических и техногенных условий шахт. Учитывая сложность подачи дополнительной тепловой энергии в угольный пласт, в качестве основного способа снижения давления в пласте принята разгрузка массива горных пород относительно исходного напряжённого состояния и дезинтеграция угля и пород при переходе от упругого их деформирования к упруго-пластичному и запредельному.

Ключевые слова: угольный пласт, метан, шахта, дегазация, газогидрат, горное давление, десорбция, фильтрация, дезинтеграция пород, газоносность, угольная матрица.

Для цитирования: Ширяев С. Н. Оценка эффективности способов и средств дегазации углеметановых пластов. *Горные науки и технологии*. 2019;4(2):122-131. DOI: 10.17073/2500-0632-2019-2-122-131.

Introduction

Coal deposits in Russia and abroad, as a rule, are highly methane-bearing, and during their development, an average of 18.6 m^3/t of methane is produced per tonne of coal mined [1–3] that is a limitation of the productivity of modern highly productive equipment. The abundant release of methane into mine workings at a certain combination of geological, mining, and organizational factors leads to incidents and dangerous production gas-dynamic situations in the form of gas pollution of mine workings, explosions of methane-air mixtures.

Effective management of the interacting technological, geomechanical and gas-dynamic processes in a modern coal mine requires solving a set of scientific and practical problems, including the development and implementation of mine process flow sheets that are adaptive to wide range of geological, geotechnical, and mining conditions of coal deposits and operating modes of high-performance mining facilities.

The work of many scientists and practitioners has been devoted to the development and implementation of high-performance technologies for the preparation and development of methane-bearing coal seams. However, the main urgent problems have not yet been solved: theoretical studies on the release (desorption) of methane have not been brought to practical use (efficiency of gas drainage of 0.12–0.40 has been achieved); the role of methane in a sudden coal burst as a complex physical-chemical-mechanical phenomenon has not been unambiguously identified; the parameters of methane breakthroughs from satellite seams, geological dislocations, and worked-out space have not been determined. A promising way for increasing the intensity of methane release from coal, including from the gas-hydrate state, is the creation and implementation of active combined degassing methods, providing for stage-by-stage coal disintegration and decreasing rock pressure.

In this regard, the need has arisen for the creation and implementation of active combined methods and means of phased degassing of an inhomogeneous coal-rock mass and worked-out space to ensure efficient and safe underground mining of highly gas-bearing coal seams. To this end, the effectiveness of traditional technologies for methods and means of degassing methane-bearing coal seams was assessed with the aim of developing, substantiating the parameters and introducing active combined methods and means of multi-stage degassing of an inhomogeneous coal-rock mass and the worked-out space for efficient and safe mining of methane-bearing coal seams.

The main idea of creating active combined methods and means of multi-stage degassing of methane-bearing coal seams consists in using the identified patterns of interaction of technological, gas-dynamic and geomechanical processes in a coal-rock mass to control the coal matrix disintegration, reduce pressure in it, and ensure the transition of methane from a hydrated state to gaseous one taking into account real mining conditions at mines.

To achieve this goal, the following problems are being solved:

– the synthesis of alternative options of active combined methods for the artificial disintegration of coal seams for their multi-stage degassing;

– identification of the patterns of methane desorption in wide range of mining and geological conditions of coal mines based on the results of mine research;

– identification of effective variants of active combined methods of multi-stage degassing of an inhomogeneous coal-rock mass based on the results of computer simulation and mine experiments;

– substantiation of technological parameters and the implementation of active combined methods and means of multi-stage degassing of high-gas-bearing coal seams.

The research methods. Analysis of the effectiveness of traditional methods and means for mine degassing; mine experiments; computer simulation of interacting technological, gas-dynamic and geomechanical processes; statistical assessment and ranking of options for active combined multi-stage degassing methods; synthesis of process flow options for the preparation and development of gas-bearing coal seams.

The study findings. Based on the analysis of the effectiveness of traditional methods and means of coal seam degassing [1, 3-5, etc.], the following was found:

– the annual volume of methane recovered in the period 1990–2009 in the Kuzbass by means of degassing amounted to 60–330 mln m^3, gas suction, 120–410 mln m^3, ventilation, 470–600 mln m^3;

– the proportion of mines which applied seam degassing in the period of 1990–2009 in the Kuzbass amounted to 0.18–0.33; work-out space degassing, 0.21–0.28; gas suction, 0.28–0.39;

– the effectiveness of degassing at the Kuzbass mines is 3–44 % and does not exceed 28 % on average,

– combined degassing methods are most effective. For example, the simultaneous use of gas suction and degassing allow achieving efficiency of gas drainage of 0.55, whereas degassing under similar conditions only provides 0.28;

– the use of combined ventilation schemes ensures the achievement of efficiency of gas drainage of 0.55;

– the use of boreholes drilled from the earth's surface ensures maximum methane drainage: efficiency of gas drainage reaches 0.85, whereas that for seam degassing under the same conditions provides 0.20 only.

The presented methane drainage indicators for different methods confirm not only the relatively low efficiency of the methods and means of methane-bearing coal seams degassing, but also the lack of methods for predicting methane release parameters in specific mining & geological and geotechical conditions, since the design and actual values of efficiency of gas drainage differ by 2–3 times. To develop new methods for predicting degassing parameters, it is necessary to identify and use the patterns of methane adsorption and desorption, the disintegration of coal matrix under the influence of pressure and temperature above the equilibrium parameters of gas hydrates that ensures the change of methane from hydrate to gaseous state, taking into account the actual mine conditions.

The following impacts on a coal mass are considered as alternatives to active combined methods of multistage degassing of an inhomogeneous coal-rock mass: electropulsed, periodic plasma-pulsed, vibrovawe, disintegration by fluid, vacuum degassing, etc. [6, 7, 11, 12]. The theoretical foundations of the coal matrix formation are described in [10, 13, 16]. According to the findings of these studies, methane gas in a coal seam can be in three forms: free gas in the pore and fracture spaces of coal or rocks; methane in adsorbed or gas hydrate state. Gas hydrates are solid crystalline substances, containing water and gas molecules.

Phase equilibrium diagram of solid coal-gas solutions (SCGS) containing methane is presented in Fig. 1.

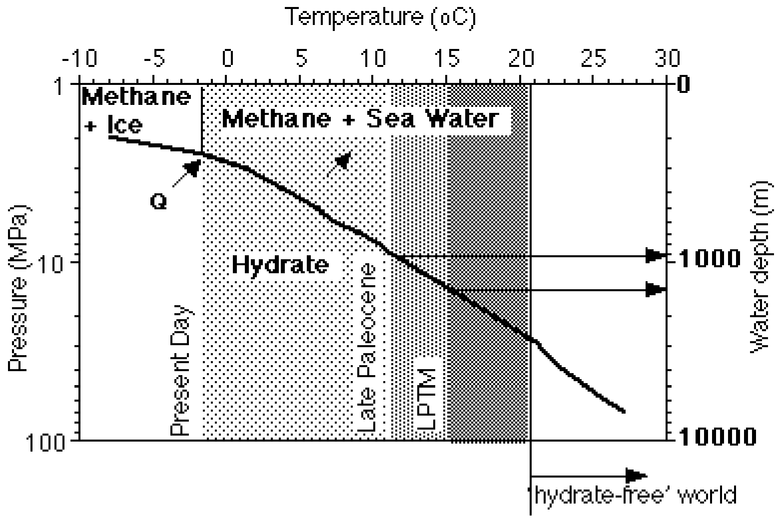

Fig. 1. Phase equilibrium diagram of methane in coal matrix [18]

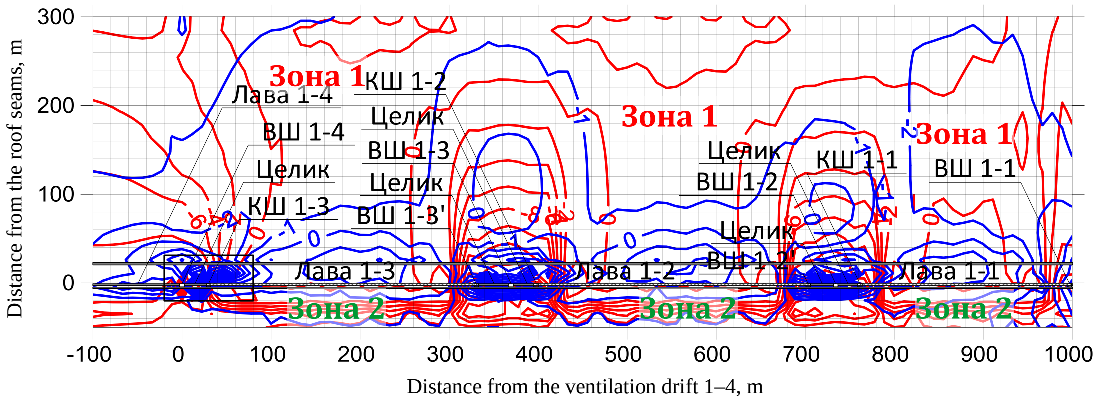

Fig. 2. Vertical (red lines) and horizontal (blue lines) stresses (MPa) in the zone of influence of goaf of three extraction districts

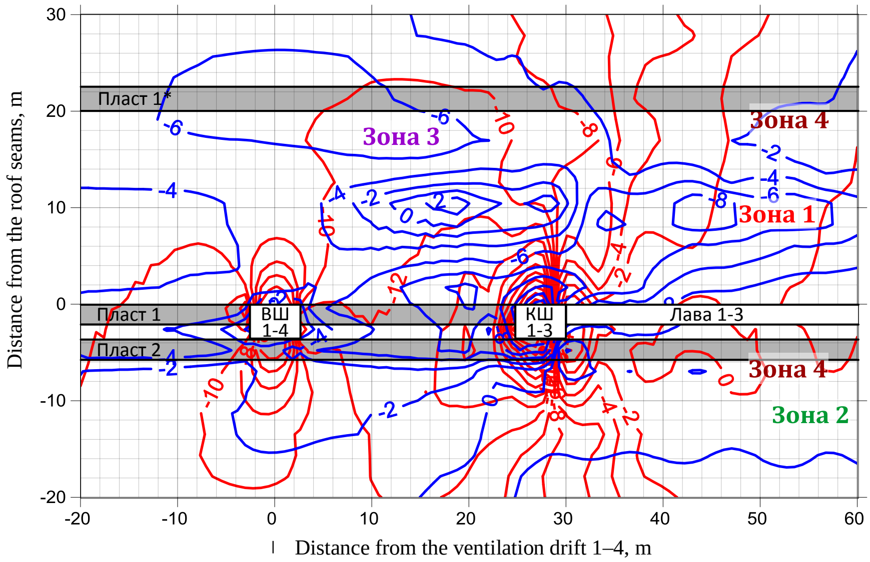

Fig. 3. Vertical (red lines) and horizontal (blue lines) stresses (MPa) in the zone of influence of goaf of three extraction districts, a portion of Fig. 2

According to the diagram, the transition of methane from solid coal-gas solutions and the adsorbed state to a gaseous state is possible at decreasing pressure and increasing temperature of the coal matrix. The possibility of increasing temperature of coal seams is limited in the mine by fire safety requirements and sanitary rules [19, 20]. Therefore, the main parameter providing the intensification of the methane transition to the gaseous state is reduction of mechanical stress, which is accompanied by the decomposition of solid coal-gas solutions (SCGS) and increasing methane pressure in natural and man-made fractures. There are several hypotheses for the transition of methane to the gaseous state and its migration through fractures and pores. However, the efficiency of these mechanisms realization in practice is not always confirmed [5, 9, 11, 12, 14–16].

Fig. 2 shows the results of numerical simulation of the distribution of vertical and horizontal stresses after mining-out three extraction districts in the conditions of the Yerunakovsky deposit in the Kuzbass. The thickness of the mined seam 1 is 2.48 m, that of undermined seam 1* (in the mined seam bottom) and seam 2 (in the mined seam roof) for the simulation is taken to be 2 m.

Fig. 3 shows a fragment of Fig. 2 in the form of a cutout on a large scale with the purpose of detailed description of the nature of the stress distribution in the rock mass near the ventilation drift 1–4, conveyor drift 1–3 and the stope worked-out space of extraction districts 1–3. The signs of stresses in Fig. 2 and 3 are as follows: compression $\sigma < 0$; tensile $\sigma > 0$.

According to the results of the analysis of vertical and horizontal stresses in the rock massif under the mutual influence of the worked-out space of several adjacent extraction districts separated by coal pillars, the following zones were identified, within which we should expect decreasing mechanical stresses and intensive decomposition of gas hydrates with the release of free methane:

1) The unloading zone (Zone 1 in Figs. 2 and 3) of undermined rock layers and coal seams. The transition of solid coal-gas solutions into the gaseous state in these zones is confirmed by the value of efficiency of gas drainage up to 0.85 when using boreholes drilled into the mined-out space from the earth's surface or underground workings [5].

2) The unloading zone (Zone 2 in Figs. 2 and 3) of rocks in the mined seam bottom. The intensity of the transition of methane from SCGS to the adsorbed state is confirmed in practice by periodic breakthroughs of methane from the mine working bottom that is accompanied by fractures of bottom rocks and increasing methane concentration.

3) Zone of partial horizontal stress drop in the edge sections of the mined seam (Zone 3 in Figs. 2 and 3), as evidenced by coal sloughing on the face, roof fall and increasing methane release. A feature of this zone is the deformation of rock layers and coal seams along their natural contacts and technogenic fractures. Under the influence of tangential and alternating-sign normal stresses in these zones, blocks and oblique fractures are formed along which methane migrates.

4) The zone of vertical stress drop (Zone 4 in Figs. 2 and 3), arising due to the expansion of undermined or bottom coal seams. Since the tensile strength of coal is 10–15 less than its compressive strength, intensive crushing of coal and the transition of methane to free gas state takes place, according to the diagram in Fig. 1.

5) The zone of alternating-sign stresses and deformations arising under the influence of geological dislocations/faults, the boundaries of geotectonic blocks [21].

6) The zone of migration of methane-air mixture between the mined-out spaces of the adjacent extraction pillars. According to Fig. 2, zones of tensile horizontal stresses and great compressive stresses arise above the coal pillars between adjacent extraction districts. Under the influence of alternating-sign stresses and strains, the formation of technogenic fractures occurs, along which the methane-air mixture migrates to the workings of the extraction pillar.

As follows from the diagram in Fig. 1 and the nature of the stress distribution in the rock mass in Figs. 2 and 3, in coal seams outside the zone of influence of mine workings or geological dislocations, one should not expect intense methane release, since all the mechanical stresses are compressive, that is, they reduce the coal porosity and the intensity of methane filtration. This is confirmed in practice in a seam degassing, where the average efficiency of gas drainage is 0.20.

With the aim of increasing the intensity of seam degassing using a borehole system, some authors [3, 7, 11, 12] propose various methods for coal crushing and increasing permeability. At the stage of experimental verification, the following methods for impacting a rock mass are tested: electropulsed, periodic plasma-pulsed, vibration microwave, fluid disruption, vacuum degassing, etc. However, according to the calculations from paper [14], with increasing porosity of coal mass without mechanical stress drop, filling of voids with gas and increasing pressure in the coal matrix occurs. In this case, it is necessary to create a surface to be free of mechanical stresses, through which methane flows into mine workings or boreholes.

According to the graphs in Fig. 4 and research [6] at the first stage after connecting a borehole to the degassing system, the degassing intensity is high, and after a few days it gradually decreases.

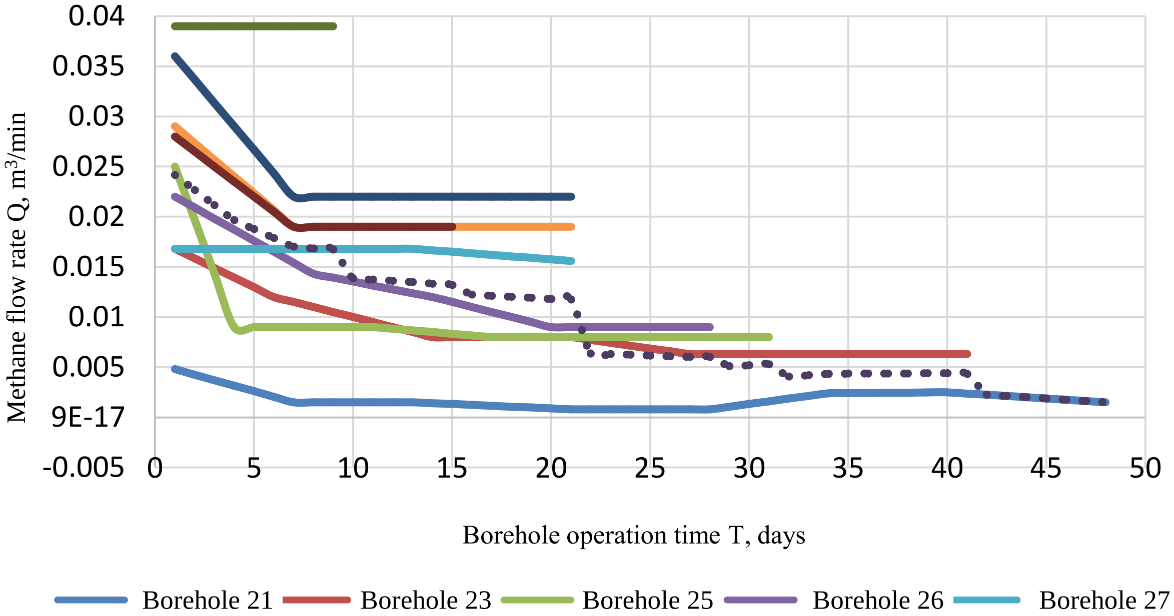

Fig. 4. Plot of methane flow rate from degassing boreholes during seam degassing as function of the borehole operation, seam 16, Abashevskaya mine, Kuzbass

The reasons for the decrease in the borehole methane flow rate are coal crushing with the borehole filling. At the C.M. Kirov Mine, experiments were conducted to enhance degassing in the vicinity of boreholes by means of anthropogenic impact on the boreholes; however, the results do not differ significantly from those shown in Fig. 4.

New technological solutions for methane recovery from coal-rock mass were proposed in a paper of scientists of the Republic of Kazakhstan [17]. The authors argue that the use of several technogenic impacts on rocks through boreholes drilled from the earth's surface does not provide the design flow rate of methane. Of the 150 boreholes in the Karaganda coal basin, only few boreholes produced gas encroachment rate of 3–4 thousand m^3 per day. High labor and energy intensity of the application of seam hydraulic fracturing is noted, at low efficiency of the method. The reasons for decreasing gas recovery factor after the hydraulic fracturing is blocking of methane in the pores and locking of the fractures with swelling clay particles.

Thus, the traditional methods of degassing coal seams, regulated by applicable documents, do not ensure effective degassing of the seams above 0.4.

Therefore, it is proposed to expand scientific research for the development of a new direction in order to create and implement combined methods of phased degassing using methods of reducing mechanical stresses in a coal matrix with preliminary increasing its porosity.

In connection with the above, a research program has been developed including the following types of work:

1) Plasma-pulsed impact on coal seams through boreholes drilled from the earth's surface [22]. The technology is based on the effect of a strong compression wave on rocks, resulting from the intense expansion of a plasma channel formed between special electrodes. As a result of the conductors closing, an explosion occurs, a strong shock wave is formed, compressing and tensioning the environment. Microfractures arise, which are filled with methane.

This method is implemented when performing early degassing in the conditions of the Yerunakovsky Vostochny area of the Yerunakovskaya-VIII Mine in the Kuzbass. Four vertical boreholes were drilled from the surface. The depth of vertical boreholes for the conditions under consideration is up to 700 m. Coal seams 48 and 45 of the Lenin suite ($P2_{ln}$) of medium thickness, with a gas content of about 25 m^3/ t dry ash-free mass. The target scope of drilling is presented in Table 1.

Table 1

Scope of drilling

Borehole	Target depth, m	Borehole purpose	Drilling method	Within extraction district outline
1	580	Degassing	Noncore	48–5
2	550	Degassing	Noncore	48–5
3	600	Degassing	Noncore	48–6
4	630	Degassing	Noncore	48–6

2) Plasma-pulsed impact on coal seams through boreholes drilled from the earth's surface and/or from underground workings. The technology is being developed relating to the possibility of using technical means in underground conditions.

3) Directional drilling of long (up to 1200 m) degassing boreholes for preliminary degassing of coal seams in the outline of extraction pillars planned. The method is implemented at the Kuzbass mines.

4) Drilling of degassing boreholes along a seam dip with the introduction of a polyethylene pipe into the borehole to its entire depth for dewatering the borehole and the gas recovery from the borehole bottom (increasing the gas mixture movement speed occurs).

The implementation of the combined methods of phased degassing using methods of reducing mechanical stresses in a coal matrix with preliminary increasing its porosity allows increasing methane yield up to 90 %.

Conclusions

The analysis of methods and directions of increasing the efficiency of coal seam degassing showed that:

1) The traditional methods and means of degassing, regulated by the applicable specification documents, ensure the achievement of efficiency of gas drainage in the range of 0.03–0.44, no more than 0.28 on average in the Kuzbass; using combined degassing methods with simultaneous gas suction and seam degassing increases this figure up to 0.55; applying boreholes drilled from the earth's surface raises efficiency of gas drainage to 0.85.

2) A promising direction for increasing the efficiency of methane-bearing coal seam degassing is the development of the theory and practice of combined phased crushing of coal matrix in order to create conditions for the transition of methane from hydrate to gaseous state through reducing mechanical stresses in the rock mass.

3) The main directions of increasing the efficiency of coal seam degassing in the coming years shall be: plasma-pulsed impact on coal seams through boreholes drilled from the earth's surface and/or from mine workings; coal seam degassing through long boreholes (up to 1200 m) using polyethylene pipes inserted in them for dewatering the boreholes and the gas recovery from the borehole bottom.

References

1. Ruban A. D. Preparation and excavation of coal seams with high gas content. / Ruban A.D., Artemyev V. B., Zaburdyaev V. S. [et al.]. Moscow, Gornaya Kniga [Mining Book] Publ., 2010, 500 p. (in Russ.).

2. Klishin V. I. [et al.]. Safety problems and new technologies for underground coal mining [Text]. Ed. Malyshev, Yu.N. Novosibirsk, "Novosibirsk Writer" Publishing House, 2011, 524 p. (in Russ.).

3. Remezov A. V. et al. Methane liberation from coal seams and host rocks at Kuzbass mines. History. Present day. Future. Kemerovo, 2012, 848 p. (in Russ.).

4. Puchkov L. A. Extraction of methane from coal seams./ Puchkov, L.A., Slastunov, S.V., Kolikov K.S. Moscow, Publishing House of Moscow State Mining University, 2002, 383 p. (in Russ.).

5. Rodin R. I. Effectiveness of Kuzbass mines degassing. Bulletin of Scientific Center for Work Safety in Coal Industry, 2011, no. 2, pp. 116-119 (in Russ.).

6. Plaksin M. S. Gas-kinetic response of methane containing coal seam when producing fractures in it by fluid injection [Text]. / Plaksin M. S., Rodin R. I., Alkov V. I. High-end technologies for development and use of mineral resources. Collector of scientific articles, Novokuznetsk, SibGIU Publ., 2017, pp. 63 - 67 (in Russ.).

7. Pashchenko A. F. Plasma Pulse Technology for enhancing oil recovery: estimation of mechanical effect parameters [Text]. / Pashchenko A. F., Avdeev P. G. Science and technology in gas industry, no. 3 (63), 2015, pp. 17-26 (in Russ.).

8. Manakov A. Yu. Clathrate hydrates at high pressures: structure, composition, properties [Text]: Extended Abstract of Doctoral (Chemistry) Dissertation, Institute of Inorg. Chemistry of SB RAS, Novosibirsk, 2007, 33 p. (in Russ.).

9. Shuqiang G. Investigation of Interactions between Gas Hydrates and Several Flow Assurance Elements [Текст] / G. Shuqiang // Energy and Fuels, 22 (5), 3150-3153, 2008.

10. Makogon Yu. F. Gas hydrates: prevention of their formation and their use [Text]. Moscow, Nedra Publ., 1985, 232 p. (in Russ.).

11. Plaksin M. S. Features of dynamic gas shows during development working driving [Text]. / Plaksin M. S., Ryabtsev A. A. High-end technologies for development and use of mineral resources. Collector of scientific articles. Novokuznetsk. SibGIU Publ., 2017, pp. 67-73 (in Russ.).

12. Shepeleva S. A., Dyrdin V. V., Kim T. D, Smirnov V. G., Gvozdkova T. N. Methane and outburst hazard of coal seams [Text]. Tomsk, Publishing House of Tomsk University, 2015, 180 p. (in Russ.).

13. Ettinger I. L. Methane Solutions in Coal Seams [Text]. Solid State Chemistry, 1984, no. 4, pp. 28-35 (in Russ.).

14. Zhuravkov M. A., Polevshchikov G.Ya. Gas-dynamic response of rocks to construction of development workings. Bulletin of Scientific Center for Work Safety in Coal Industry, 2011, no. 2, pp. 39-52 (in Russ.).

15. Karkashadze G. G. Intensification of coal seam degassing based on its geotechnical conditions under nonsteady mechanical and sorption strains. /Karkashadze, G.G., Slastunov, S.V., Ermak, G.P., Mazanic, E.V. Coal, 2015, no. 11, pp. 62-65 (in Russ.).

16. Bespyatov G. A. Synergetics of outburst-prone mining environment [Text]. / Bespyatov G. A., Vylegzhanin V. N., Zoloyykh S. S. Novosibirsk, Nauka Publ., 1996, 191 p. (in Russ.).

17. Varekha Zh. P. Technological solutions for extraction of methane from coal-rock mass./ Varekha, Zh.P., Lis, S.N. Mining Journal of Kazakhstan, 2016, no. 2, pp. 6-9 (in Russ.).

18. Dickens G. R., O'Neil J. R., Rea D. K., and Owen R. M. Dissociation of oceanic methane hydrate as a cause of the carbon isotope excursion at the end of the Paleocene. Paleoceanography, 1995, No. 10, Pp. 965-971.

19. Federal rules and regulations for industrial safety "Instructions for prevention of endogenous fires and safe mining of coal seams prone to spontaneous combustion" Series 05. Number 46. Moscow, CJSC Scientific and Technical Center for Study of Industrial Safety Problems, 2016, 52 p. (in Russ.).

20. Composite authors. Forecasting technique using geophysical exploration methods and selection of measures to decrease endogenous fire hazard in inclined openings within coal seam. Kemerovo, SC VostNII Publ., 2007, 34 p. (in Russ.).

21. Petukhov I. M. Subsoil geodynamics [Text] / Petukhov, I.M., Batugina, I.M., Moscow, Nedra Communication LTD Publ., 1999, 256 p. (in Russ.).

22. Ageev P. G. Plasma Pulse Technology – innovative approach to the production of traditional hydrocarbons and unconventional approach to production of traditional and unconventional hydrocarbons and early degassing of coal seams./ Ageev P. G., Ageev N. P., Ageev D. P., Desyatkin A. S., Pashchenko A. F. Drilling and Oil, 2016, no. 7-8, pp. 34-40 (in Russ.).

Библиографический список

1. Рубан А. Д. Подготовка и разработка высокогазоносных угольных пластов / А. Д. Рубан, В. Б. Артемьев, В. С. Забурдяев [и др.]. М.: Горная книга, 2010. 500 с.

2. Проблемы безопасности и новые технологии подземной разработки угольных месторождений [Текст] / В. И. Клишин [и др.]; под ред. Ю. Н. Малышева. Новосибирск: Издательский дом «Новосибирский писатель», 2011. 524 с.

3. Дегазация газа метана из угольных пластов и вмещающих пород на шахтах Кузбасса. История. Действительность. Будущее // А. В. Ремезов [и др.] Кемерово, 2012. 848 с.

4. Пучков Л. А. Извлечение метана из угольных пластов / Л. А. Пучков, С. В. Сластунов, К. С. Коликов. М.: Издательство Московского государственного горного университета, 2002. 383 с.

5. Родин Р. И. Эффективность дегазации шахт Кузбасса / Р. И. Родин // Вестник Научного центра по безопасности работ в угольной промышленности. 2011. № 2. С. 116-119.

6. Плаксин М. С. Газокинетическая реакция углеметанового пласта при создании в нём трещин посредством нагнетания флюидов [Текст] / М. С. Плаксин, Р. И. Родин, В. И. Альков // Наукоёмкие технологии разработки и использования минеральных ресурсов: сб. науч. ст. Новокузнецк: СибГИУ, 2017. С. 63-67.

7. Пащенко А. Ф. Плазменно-импульсная технология повышения нефтеотдачи: оценка параметров механического воздействия [Текст] / А. Ф. Пащенко, П. Г. Авдеев // Наука и техника в газовой промышленности, 2015. № 3(63). С. 17-26.

8. Манаков А.Ю. Клатратные гидраты при высоких давлениях: структура, состав, свойства [Текст]: автореф. дис. … докт. хим. наук / А. Ю. Манаков; Институт неорг. химии СО РАН. Новосибирск: 2007. 33 с.

9. Shuqiang G. Investigation of Interactions between Gas Hydrates and Several Flow Assurance Elements [Текст] / G. Shuqiang // Energy and Fuels, 22 (5), 3150-3153, 2008.

10. Макогон Ю. Ф. Газовые гидраты, предупреждение их образования и использование [Текст] / Ю. Ф. Макогон. М.: Недра, 1985. 232 с.

11. Плаксин М. С. Особенности развития динамических газопроявлений при проведении подготовительной выработки [Текст] / М. С. Плаксин, А. А. Рябцев // Наукоёмкие технологии разработки и использования минеральных ресурсов: сб. науч. ст. Новокузнецк : СибГИУ, 2017. С. 67-73.

12. Метан и выбросоопасность угольных пластов [Текст] / С. А. Шепелева, В. В. Дырдин, Т. Д. Ким, В. Г. Смирнов, Т. Н. Гвоздкова. Томск: Изд-во Томского ун-та, 2015. 180 с.

13. Эттингер И. Л. Растворы метана в угольных пластах [Текст] / И. Л. Эттингер // Химия твердого тела. 1984. № 4. С. 28-35.

14. Журавков М. А. Газодинамическая реакция горных пород на проведение подготовительных выработок / М. А. Журавков, Г. Я. Полевщиков // Вестник Научного центра по безопасности работ в угольной промышленности. 2011. № 2. С.39-52.

15. Каркашадзе Г. Г. Интенсификация дегазации угольного пласта на основе учёта его геомеханического состояния в условиях нестационарных механических и сорбционных деформаций / Г.Г. Каркашадзе, С.В. Сластунов, Г.П. Ермак, Е.В. Мазаник // Уголь. 2015. №11. С. 62-65.

16. Беспятов Г.А. Синергетика выбросоопасной горной среды [Текст] / Г.А. Беспятов, В.Н. Вылегжанин, С.С. Золотых. Новосибирск: Наука, 1996. 191 с.

17. Вареха Ж. П. Технологические решения по извлечению метана из углепородного массива / Ж. П. Вареха, С. Н. Лис // Горный журнал Казахстана. 2016. №2. С. 6-9.

18. Dickens G. R., O'Neil J. R., Rea D. K., and Owen R. M. Dissociation of oceanic methane hydrate as a cause of the carbon isotope excursion at the end of the Paleocene. Paleoceanography, 1995, No. 10, Pp. 965-971.

19. Федеральные нормы и правила в области промышленной безопасности «Инструкция по предупреждению эндогенных пожаров и безопасному ведению горных работ на пластах угля, склонного к самовозгоранию». М.: ЗАО «Научно-технический центр исследования проблем промышленной безопасности», 2016. Сер. 05. Вып. 46. 52 с.

20. Методика прогнозирования с использованием геофизических методов исследований и выбора мер по снижению эндогенной пожароопасности наклонных вскрывающих выработок, проводимых по угольному пласту / Кол. авторов / Кемерово: НЦ ВостНИИ, 2007. 34 с.

21. Петухов И. М. Геодинамика недр [Текст] / И. М. Петухов, И. М. Батугина. М.: Недра коммюникейшн ЛТД, 1999. 256 с.

22. Агеев П. Г. Плазменно-импульсное воздействие – инновационный подход к добыче традиционных и нетрадиционный подход к добыче традиционных и нетрадиционных углеводородов и заблаговременной дегазации угольных пластов / П. Г. Агеев, Н. П. Агеев, Д. П. Агеев, А. С. Десяткин, А. Ф. Пащенко // Бурение и нефть. 2016. № 7-8. С. 34-40.

Information about the author

Sergey N. Shirjaev – Deputy Technical Director, LLC "Raspadskaya Coal Company", Novokuznetsk, Russia, sn_shir@mail.ru.

Информация об авторе

Ширяев Сергей Николаевич – первый заместитель технического директора ООО «Распадская угольная компания», Новокузнецк, Россия, sn_shir@mail.ru.

ORIGINAL PAPERS

DOI: 10.17073/2500-0632-2019-2-132-143

Selection of Material for Facing Drive Drum of Belt Conveyor

D. V. Hrydziushka, A. V. Bryzhevich, E. V. Piskun

Joint Stock Company "Soligorsk Institute of Resources Saving Problems with Pilot Production", Soligorsk, Minsk region, the Republic of Belarus, ✉onti@sipr.by

Abstract: It is known that conveyor operates in chemically aggressive and abrasive environments; for this reason the drive drum of belt conveyor wears out rather rapidly. It is noted that the lining of the conveyor drum increases coefficient of friction between the conveyor drum and the conveyor belt, reduces the belt wear rate, and also protects against corrosion and abrasive wear. The plot of the PU-60 polyurethane wear rate as function of load when rolling on steel is presented. It is noted that increasing the load increases the strength of adhesive junction between steel and polyurethane rollers; friction wear causes fatigue failure of surface layers of the materials. Besides, the plot of the PU-80 polyurethane wear rate as function of load when rolling on steel is presented. The plot of the polyurethanes wear rate as function of hardness of polyurethane is presented, which shows that the lowest wear rate is demonstrated by the hardest polyurethane, PU-80. The bar chart of static friction coefficient for PU-60 and PU-80 polyurethanes demonstrates that the optimal material for lining the drive drum of a conveyor belt is PU-80. The plot of the rubber wear rate as function of load at a speed of 1 m/s is presented. The plot shows that the wear rate increases with increasing the load. This is due to the effect of two factors: growing contact deformations of the surface layer of the rubber and increasing the contact area of mating parts. It is noted that IRP-1347 rubber is less susceptible to wear than "REMAGRIP" rubber. This allows using IRP-1347 rubber in aggressive environments. The bar chart of static friction coefficient for the rubber presented in the paper shows that the investigated IRP-1347 and REMAGRIP rubber grades have the required value of static friction coefficient for use as lining material for the drive drum. The plot of the wear rate as function of the rubber hardness and as function of the polyurethane hardness is presented. In practice, it is proved that the best material for lining the drive drum is PU-80.

Keywords: polyurethane, rubber, lining, wear resistance, static friction coefficient, belt conveyor, linear wear rate, drive drum, strength, elastomer.

For citation: Hrydziushka D. V., Bryzhevich A. V., Piskun E. V. Selection of material for facing drive drum of belt conveyor. *Mining Science and Technology*. 2019;4(2):132-143 (In Russ.). DOI: 10.17073/2500-0632-2019-2-132-143.

Выбор материала для облицовки приводного барабана ленточного конвейера

Гридюшко Д. В., Брижевич А. В., Пискун Е. В.

Закрытое акционерное общество «Солигорский Институт проблем ресурсосбережения с Опытным производством», Солигорск, Минская область, Республика Беларусь, ✉onti@sipr.by

Аннотация: Известно, что конвейер работает в химически активной и абразивной средах, по этой причине приводной барабан ленточного конвейера быстро изнашивается. Отмечено, что футеровка конвейерного барабана повышает коэффициент трения между конвейерным барабаном и транспортерной лентой, снижает скорость изнашивания ленты, а также защищает от коррозии и абразивного износа. Представлен график зависимости интенсивности изнашивания полиуретанов ПУ-60 от нагрузки при качении по стали. Показано, что с увеличением нагрузки увеличивается прочность адгезионных соединений между стальным и полиуретановым роликами, при трении материалы повреждаются вследствие усталостного разрушения поверхностных слоев. Также представлен график зависимости интенсивности изнашивания полиуретанов ПУ-80 от нагрузки при качении по стали. Представлена диаграмма зависимости интенсивности изнашивания от твердости полиуретана, на которой видно, что самая маленькая интенсивность изнашивания у самого твердого полиуретана ПУ-80. Проиллюстрирована гистограмма коэффициента трения покоя полиуретанов ПУ-60 и ПУ-80, из которой можно сделать вывод, что оптимальный материал для облицовки приводного барабана ленточного конвейера – это ПУ-80. Представлен график зависимости интенсивности изнашивания резины от нагрузки при скорости 1 м/с. Из графика видно, что интенсивность изнашивания возрастает с повышением нагрузки. Это обусловлено влиянием двух факторов: увеличением контактных деформаций поверхностного слоя резины и увеличением площади контакта сопрягаемых деталей. Отмечено, что резина ИРП-1347 в меньшей степени поддается изнашиванию по сравнению с резиной «REMAGRIP», что позволяет ей работать в агрессивных средах. Гистограмма коэффициента трения покоя для резины, представленная в работе, показывает, что исследуемые резины марок ИРП-1347 и «REMAGRIP» обладают необходимым значением коэффициента трения покоя для использования их в качестве футеровочного материала для приводного барабана. Представлена диаграмма зависимости интенсивности изнашивания от твердости резины и полиуретана. На практике доказано, что наилучшим материалом для облицовки приводного барабана является ПУ-80.

Ключевые слова: полиуретан, резина, облицовка, износостойкость, коэффициент трения покоя, ленточный конвейер, линейная интенсивность изнашивания, приводной барабан, прочность, резина, эластомер.

Для цитирования: Гридюшко Д. В., Брижевич А. В., Пискун Е. В**.** Выбор материала для облицовки приводного барабана ленточного конвейера. *Горные науки и технологии.* 2019;4(2):132-143. DOI: 10.17073/2500-0632-2019-2-132-143.

Introduction

Due to the fact that a conveyor operates in chemically aggressive and abrasive environments the drive drum of a belt conveyor wears out quickly [1]. In order to reduce the wear, the drum lining is required.

There are several types of lining material for drive drum. The selected material should have the following properties:

–high strength and hardness;

–resistance to chemical attack;

–increase the life of the conveyor belt;

–increase friction coefficient between the conveyor drum and the conveyor belt;

–protect against corrosion and abrasion.

Thus, in the course of the study, it is necessary to study the tribotechnical properties of the material proposed for lining the drive drum and determine the material that meets the requirements and has the necessary properties [2].

1. Lining of a conveyor belt drive drum. Drive drums are manufactured by welding with a shell of sheet steel or by iron casting. Regarding the drum shape, the drums are made with a cylindrical or convex (barrel-shaped) surface, smooth or with notches. The drive drum traction properties are improved by increasing the tension of the belt or the angle of the drive drum clasping by the belt, using highly friction lining with longitudinal or chevron ribs (which contributes to self-cleaning) [3].

Lining of a conveyor drum increases friction coefficient between the conveyor drum and the conveyor belt, reduces the belt wear rate, and also protects against corrosion and abrasion.

Lining is installed on the conveyor drum using special adhesives. The lining plates significantly reduce the belt switch and slipping, as well as the ingress of cargo onto the drum surface. This all significantly improves conveyor operation and increases the operation technical and economic indicators.

The ribbed surface of the drive drum provides an increase in coefficient of adhesion of the belt to the drum and the drive traction factor, while reducing the required belt tension [4], increasing service life of the belt and its abutting joints.

The main material used for a drive drum lining is rubber.

A positive property of rubber is its very high elasticity. Rubber is amenable to large deformations, which are almost completely reversible [5]. In addition, rubber is characterized by high tensile and abrasion resistance, gas and water impermeability, chemical resistance, good electrical insulation properties, low density, low compressibility, and low thermal conductivity.

Rubber, as a structural material, in a number of its properties significantly differs from metals and other materials. Distinctive features of rubber are: the ability to withstand significant deformations without fracture under the influence of an external load; small values of shear modulus, modulus of tension, compression modulus; strong influence of the duration of the applied load and the temperature factor on the stress – strain relationship; almost constant volume during deformation; almost complete reversibility of deformation; significant mechanical losses in the process of cyclic deformation.

However, rubber has low abrasion resistance, low operation temperature range, low modulus of elasticity, and low hardness in relation to other materials [6].

Polyurethanes are the most versatile materials available in practical use.

Products made of polyurethane are up to 50 times more wearproof than rubber, plastics, in some applications, nonferrous and ferrous metals. This durability often means that polyurethane parts require less material amount for manufacture and less maintenance, resulting in significant cost savings.

Polyurethane is one of the most rigid (Shore 30–95) and the most abrasion-resistant elastomers, which are not subject to fracture under loads [7]. It has high tensile strength and resistance to incision advancement, resistance to chopping shocks. Products made of polyurethane retain their shape and mechanical properties after cyclic loads.

Products made of polyurethane well withstand multiple bends without breaking.

The product operation temperature range is from −50 to +80 °C, for a short time up to +100 °C. Polyurethane remains flexible at very low temperatures and has good resistance to thermal shock.

Polyurethane has high allowable shear load, good adhesion to most materials, good chemical resistance to oils, petroleum, organic solvents.

The use of polyurethane allows reducing the product weight by up to 50 %, reducing the level of vibration and system noise of operating mechanisms in comparison with metals [8].

2. Polyurethane wear test._With the aim of determining whether polyurethane can work as a lining material for a conveyor belt drive drum, tests were conducted to determine its mechanical and frictional properties.

The essence of the testing is to determine friction coefficient of the material under study against a counterbody made of steel, as well as wear under different loading conditions and speed modes.

For testing, a SMT-1 friction machine was used [9].

Fig.1 shows the test arrangement.

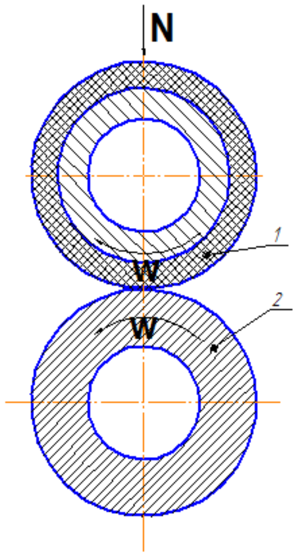

Fig. 1. Arrangement of the tribological technical tests:
1 – polyurethane roller; *2* – Steel 45 roller

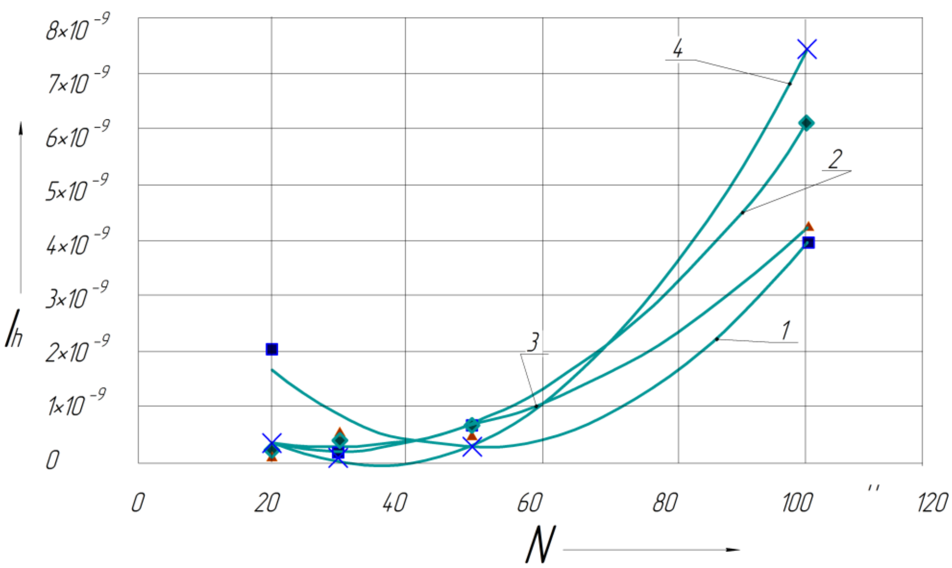

Fig. 2. The plot of PU-60 polyurethane wear rate as function of load when rolling on steel:
1 – 1.25 m/s; *2* – 0.4 m/s; *3* – 0.7 m/s; *4* – 1 m/s

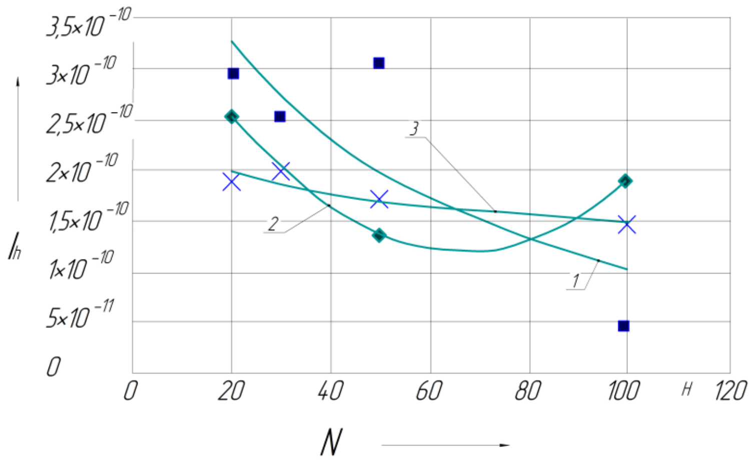

Fig. 3. The plot of PU-80 polyurethane wear rate as function of load when rolling on steel:
1 – 0.25m/s; *2* – 0.4 m/s; *3* – 1 m/s

The testing was performed on samples of PU-60 and PU-80 polyurethane of sizes: D_{inner} = 16 mm; D_{outer} = 40 mm; h = 10 mm. The testing device was a steel roller covered with the testing material.

As a counterbody, a roller made of Steel 45 40 mm in diameter was used.

The tests were carried out at speeds of 0.25 m/s, 0.4 m/s, 0.7 m/s, 1 m/s and loads of 20N, 30N, 50N, 100N for each speed.

After testing, the mass difference of the samples before and after the tests was calculated.

The linear wear rate was determined using formula

$$I_h = \frac{\Delta m}{\rho A S}, \qquad (1)$$

where Δm – mass difference before and after the test, kg;

ρ – density of the test material (1715.74 кг/м^3);

A – friction surface area, m^2;

S – slip path length, m.

3. The influence of loading conditions on the friction and wear of polyurethane.

It can be seen from the graph (Fig. 2) that with increasing the load, the strength of adhesive joints between the steel and polyurethane rollers increases. During friction, materials are damaged due to fatigue failure of surface layers [10]. The destruction occurs by separation, which is due to the gradual destruction of the macromolecule chains under the action of non-critical loads.

Due to the fact that the speed increases, the temperature at the contact spots increases too that leads to increasing the strength of the formed adhesion joints. This explains the higher wear rate at higher speed.

It is seen from the graph (Fig. 3) that on curves 1 and 3, the wear rate decreases. This is due to the fact that, as the load increase, a shift in the inner layers of polyurethane occurs. Internal elastic deformations arise [11], which do not reach the surface that leads to gradual decrease in the wear rate.

Curve 1 (Fig. 3) decreases at a large angle due to the fact that the temperature effect affects to a lesser extent.

On curve 2 (Fig. 3), the dependence of the wear rate on the load is presented by a curve with a minimum. The wear rate decrease, same to curves 1 and 3, is due to the displacement of the inner layers. Increasing wear rate is connected with increasing temperature in the contact zone.

To select polyurethane suitable for drive drum lining, tribotechnical characteristics of the polyurethanes under study should be compared.

It is seen from the graph (Fig. 4) that the lowest wear rate is demonstrated by the hardest PU-80 polyurethane. This is due to the fact that in solid polyurethane has stronger molecular bonds that does not allow breaking at high speeds and loads.

4. Determination of static friction coefficient of polyurethane. Operation of a belt conveyor is based on the transfer of traction force by friction. The traction element of belt conveyors is a belt, which is also a load-carrying surface. Throughout the whole length the belt is supported by stationary rollers. Traction due to the adhesion of the belt with the drum is transmitted to the belt by a drive drum, rotation of which provided by an electric motor through a gearbox [12, 13]. The tensioning device provides the belt tension, which is extremely important for adhesion of the belt to the drum, to prevent slipping of the belt on the drive drums and to limit the sag between the roller bearings.

The movement of the belt on the drive drum surface should occur at optimum static friction coefficient value. This condition is required to minimize the conveyor belt wear. To determine the optimal value of static friction coefficient, tests were carried out, results of which are given in Table 1 [14].

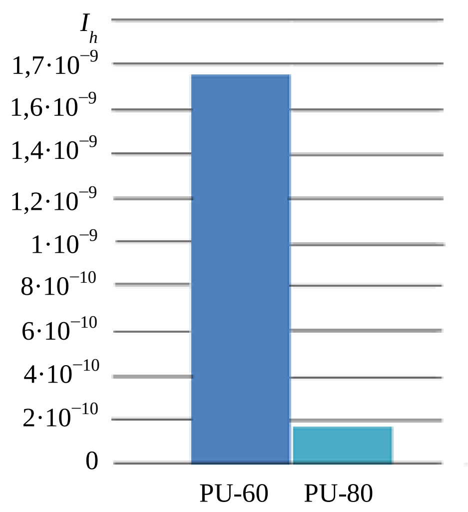

Fig. 4. The plot of wear rate as function of the polyurethane hardness

Table 1

Data of tests for measuring static friction coefficient

Polyurethane grade	Static friction coefficient
PU-60	1.04
PU-80	0.67

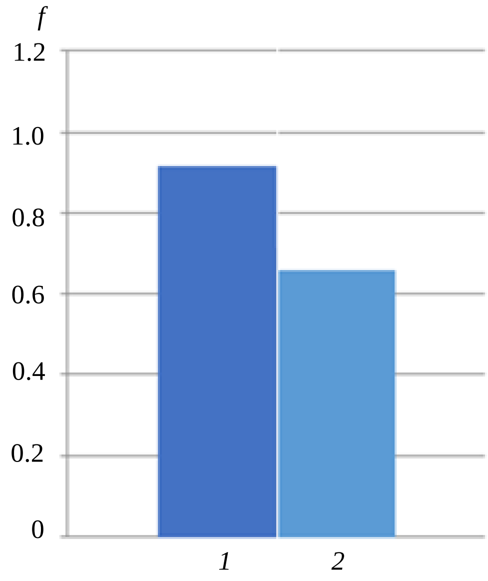

Fig. 5. The bar chart of static friction coefficient for the polyurethane grades:
1 – PU-60; 2 – PU-80

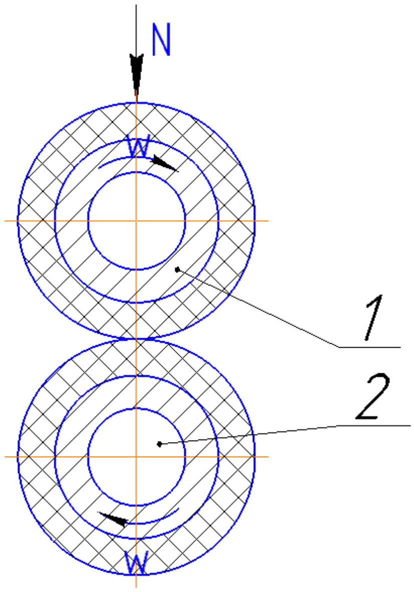

Fig. 6. Arrangement of the tribological technical tests:
1 – rubber roller; *2* – conveyor belt roller

Table 2

Rubber performance indicators

Rubber compound grade	**Performance indicators**	
	Operating temperature range, °C	**Shore hardness, A**
IRP-1347	from −50 to 80	47…57
REMAGRIP	from −30 to 80	63 ± 5

The histogram of the polyurethane static friction coefficient (Fig. 5) shows that the studied polyurethanes have the required value of static friction coefficient for the use as a lining material for a drive drum. Static friction coefficient value of PU-80 [15] is sufficient to use this material in the drive drum lining.

Based on this we can conclude that the optimal material for the conveyor belt drive drum lining is PU-80. This polyurethane is durable. It demonstrated high hardness and wear resistance.

5. Rubber wear testing. The testing was performed on samples of the testing material of sizes: D_{inner} = 16 mm; D_{outer} = 40 mm; h = 10 mm, representing a roller (Fig. 6).

As the testing samples, we used rubber grades presented in table 2 [8, 16].

A roller 40 mm in diameter from the conveyor belt was used as counterbody.

The tests were carried out 3 times at a speed of 1 m/s; the applied loads amounted to 20N; 30H; 50H. After the testing, the arithmetic average of all the wear rate values was calculated and comparative charts were built.

6. The influence of loading conditions on friction and wear of rubber

It is seen from the graph (Fig. 7) that the wear rate increases with increasing the load. This is due to the influence of two factors [17]:

–contact deformations of the surface rubber layer increase and, as a result, the probability of fatigue failure of this layer increases.

–the contact area of the mating parts increases and a larger number of adhesive bonds is formed, accompanied by an increase in the friction coefficient. As a result, adhesive wear of rubber proceeds more intensively.

As the speed increases, the temperature in the contact also increases that leads to the growth of the contribution of both wear types.

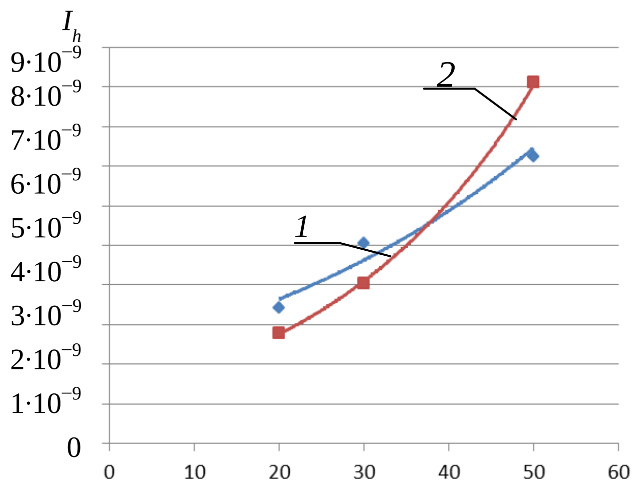

Fig. 7. The plot of the rubber grade wear rate as function of load at a speed of 1 m/s:
1 – IRP-1347 rubber; *2* – "REMAGRIP" rubber

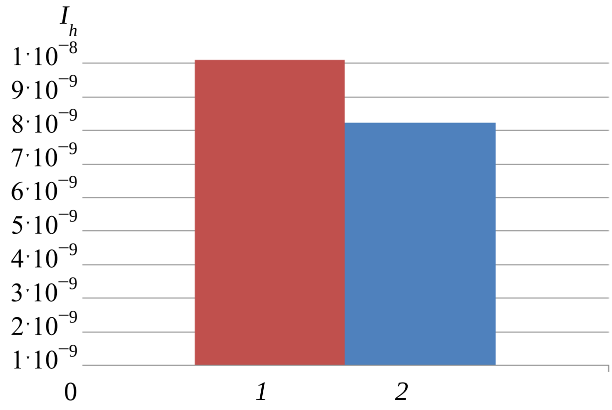

Fig. 8. The plot of wear rate as function of the rubber grade hardness:
1 – REMAGRIP rubber; *2* – IRP-1347 rubber

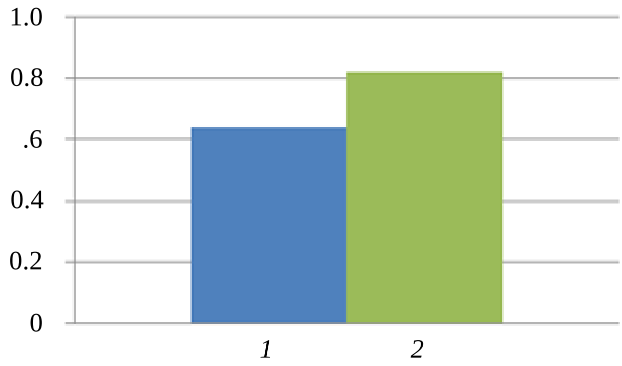

Fig. 9. The bar chart of static friction coefficient for the rubber grades:
1 – IRP-1347; *2* – "REMAGRIP"

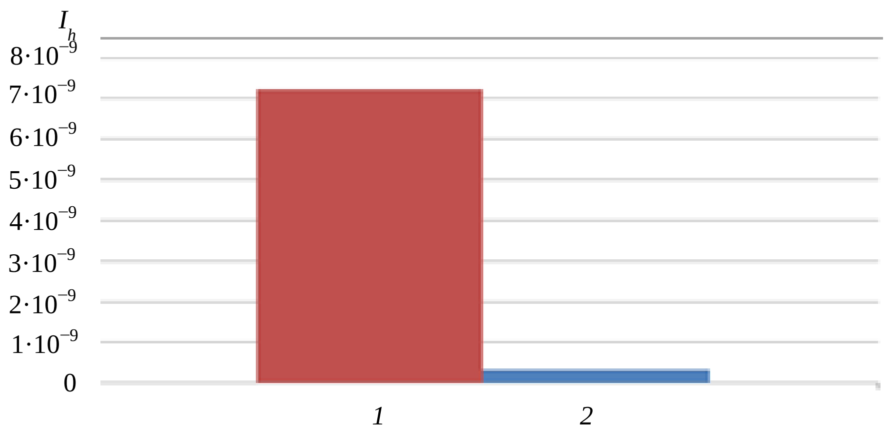

Fig. 10. The plot of wear rate as function of the rubber hardness and as function of the polyurethane hardness :
1 – IRP-1347 rubber; *2* – PU-80

It is seen from the graph (Fig. 8) that the lowest wear rate is demonstrated by IRP-1347 rubber. This means that this rubber is less susceptible to wear than REMAGRIP rubber. This allows using IRP-1347 rubber in aggressive environments.

The histogram of the rubber static friction coefficient (Fig. 9) shows that the studied rubbers have the required value of static friction coefficient for their use as the lining material for a drive drum. The static friction coefficient of IRP-1347 rubber is sufficient for using this material for drive drum lining [18].

7. Comparison of tribotechnical characteristics of rubber and polyurethane. As shown above, PU-80 polyurethane and IRP-1347 rubber used for lining the conveyor belt drive drum are less susceptible to wear.

The diagram (Fig. 10) shows that polyurethane demonstrates the lowest wear rate. This is due to the highest resistance to increasing temperature and load. PU-80 can operate at the load of above 50 N, while IRP-1347 rubber at the load of above 50 N starts to deteriorate.

Comparison the values of static friction coefficient of the studied materials shows that PU-80 has the lowest static friction coefficient.

Thus, the best material for lining the drive drum is PU-80.

The use of the polyurethane as a lining material allows to increase the maximum load on the product up to 4 times, and resistance to abrasive wear up to 10 times as compared to the rubber. Polyurethanes are among of the most abrasion resistant materials [19, 20].

Conclusion

1. Among all the tested polyurethane types, the maximum wear resistance is demonstrated by PU-80 grade polyurethane, which has the highest hardness, that ensures minimal contact deformations. Besides, this material has the required value of static friction coefficient.

2. Of all the tested rubber types, the maximum wear resistance is demonstrated by IRP-1347 rubber.

3. The comparison of the polyurethane and rubber showed that the best material for lining a conveyor belt drive drum is PU-80, since this material has the lowest wear rate compared to rubber, as well as the lowest static friction coefficient. Thus, PU-80 is the most suitable material that allows to recommend it for use for drive drum lining.

References

1. Alkhovik M. V. Mixture compositions containing secondary polyurethane. In: Alkhovik M. V., Kasperovich O. M., Petrushenya A. F. Disposal, recycling and processing of industrial waste. 2017, pp. 14-16 (in Russ.).

2. Sutkowsky W. W. Thennogravimetric study of rubber-waste polyurethane composites / W. W. Sutkowsky, A. J. Danch // Therm. Anal. and Calorim. 2004, vol. 78, iss. 3, pp. 905-921.

3. Katryuk I. S. Stream-flow transportation facilities. Designs, engineering, and operation. Textbook: Katryuk I. S., Musiyachenko E. V., Krasnoyarsk: KSTU Publ., 2006, 266 p. (in Russ.).

4. Czuprynski M. Elastomery poliuretanowe napelniane granulatem gumowy / M. Czuprynski // Polimery. 2004, vol. 49, no. 92, pp. 110-113.

5. Gadzhieva R. Sh. Problems and solutions of technological compatibility of polymer mixtures of polyamide, polyurethane and acrylonitrile-butadiene-styrene copolymer / Gadzhieva R. Sh., Kahramanov N. T., Guliyev A. M. Azerbaijan Chemical Journal, 2013, no. 4, pp. 80-86 (in Russ.).

6. Giles C. H. A general treatment and classification of the solute adsorption isotherm / C. H. Giles, D. Smith, A. Huitson // J. Colloid Interface Sci., 1974, vol. 47(3), p. 755.

7. Pat. USA 12/994692 (2013).

8. Vulcanized rubbers for articles working in liquid corrosive media. Technical requirements. GOST 071-76. Enacted as of 01/01/80. Moscow: USSR State Committee for Product Quality Management and Standards. State Standard of the USSR, 1976, 12 p. (in Russ.).

9. Kuzmina A. S. Composite materials made of waste rubber and polyurethane binders. / Kuzmina A. S., Balakin V. M., Litvinets Yu. I. / Plenary papers and abstracts of the 11th International Conference of undergraduate and graduate students "Synthesis, study of properties, modification, and processing of high-molecular-weight compound". Kazan, May 24-25, 2005, p. 224 (in Russ.).

10. Potentially improved and toughened polymeric products from fine metal powder – filled castor oil-based polyurethanes / Srivastava Anil, Singh Paramjit // 38th Macromolecular IUPAC Sumposium, Warsaw, 9-14 July, 2000: Book Abstr., vol. 3, Warsaw, 2000, p. 1200.

11. Golovanova K. V. Synthesis and physicochemical properties of aqueous polyurethane dispersions. / Golovanova K. V. [et al.]. Bulletin of the Technological University, 2017, v. 20, no. 13, pp. 18-22 (in Russ.).

12. Yagnyatinskaya E. Ya. Manufacturing technique, properties and features of use of rubber with fibrous fillers in industrial rubber goods./ Yagnyatinskaya E. Ya., Goldberg B. B., Leonov V. V. et al. M., TsNIITEneftekhim Publ., 1979, 54 p. (in Russ.).

13. Kim, B.K. Polym. Sei 54. 12 / B.K. Kim, Y.M. Lee, J. Appl. 1994. Pp. 1809-1815.

14. Levchenko N. I. Partnership of Polymers / N. I. Levchenko, S. A. Sukhorukova, T. V. Travinskaya // Churchill College, Univ. of Cambridge, 1996, pp. 195-200.

15. Kozhevnikova I. V. Polyurethane blend compounds containing waste dehumidifiers based on mineral oxides. Cand.Sci. (05.17.06 Engineering) Dissertation. Kazan, 2015, 178 p. (in Russ.).

16. LNK COMPANY [Electronic source]. Available at: http://www.lnkcom.ru/catalog/protective_coatings /lining_materials/lining_and_coating_of_driving_dr/remagrip_lining_tip_top_/). (acc. 07.11.2017).

17. Synthesis of polyether-based polyurethane-silica nanocomposites with high elongation property / Lee Sung-Il, Hahn Yoon Bong, Nahm Kee Suk, Lee Youn-Sik // Polym. Adv. Technol., 2005, Vol. 16, no. 4, pp. 328-331.

18. Varghese S. Morphology and mechanical properties of layered silicate reinforced natural and polyurethane rubber blends produced by latex compounding / S. Varghese, 1C0 Gatos., A.A. Apostolov, J. Karger-Kocsis // J. Appl. Polym. Sci. 2004, vol. 92, Nno. 21, pp. 543-551.

19. PC Polymer [Electronic source]. Access mode: http:/polimer-ug.com) (acc. 30.10.2017).

20. Ivanov E. I. Stelpant polyurethane lacquer coatings for corrosion protection in metallurgy. / Ivanov E. I., Ivanova A. E. Technology of wheeled and tracked vehicles, 2013, no. 3 (7), pp. 34-40 (in Russ.).

Библиографический список

1. Альховик М. В. Смесевые композиции с использованием вторичного полиуретана / М. В. Альховик, О. М. Касперович, А. Ф. Петрушеня // Обезвреживание, утилизация и переработка промышленных отходов. 2017. С. 14-16.

2. Sutkowsky W. W. Thennogravimetric study of rubber-waste polyurethane composites / W. W. Sutkowsky, A. J. Danch // Therm. Anal. and Calorim. 2004, vol. 78, iss. 3, pp. 905-921.

3. Катрюк И. С. Машины непрерывного транспорта. Конструкции, проектирование и эксплуатация: учеб. пособие / И. С. Катрюк, Е. В. Мусияченко. Красноярск: ИПЦ КГТУ, 2006. 266 с.

4. Czuprynski M. Elastomery poliuretanowe napelniane granulatem gumowy / M. Czuprynski // Polimery, 2004, vol. 49, no. 92, pp. 110-113.

5. Гаджиева Р. Ш. Проблемы и решения технологической совместимости полимерных смесей полиамида, полиуретана и акрилонитрил-бутадиен-стирольного сополимера / Р. Ш. Гаджиева, Н.Т. Кахраманов, А.М. Гулиев // Азербайджанский химический журнал. 2013. № 4. С. 80-86.

6. Giles C. H. A general treatment and classification of the solute adsorption isotherm / C. H. Giles, D. Smith, A. Huitson // J. Colloid Interface Sci., 1974, vol. 47(3), p. 755.

7. Pat. USA 12/994692 (2013).

8. Резины для изделий, работающих в жидких агрессивных средах. Технические требования: ГОСТ 071–76. Введ. 01.01.80. М: Государственный комитет СССР по управлению качеством продукции и стандартам: Государственный стандарт союза ССР, 1976. 12 с.

9. Кузьмина А. С. Композиционные материалы из отходов резины и полиуретановых связующих/ А. С. Кузьмина, В. М. Балакин, Ю. И. Литвинец / 1 Пленарные доклады и тезисы докладов 11 Международной конференции студентов и аспирантов «Синтез, исследование свойств, модификация и переработка ВМС». Казань, 24-25 мая, 2005. С. 224.

10. Potentially improved and toughened polymeric products from fine metal powder – filled castor oil-based polyurethanes / Srivastava Anil, Singh Paramjit // 38th Macromolecular IUPAC Sumposium, Warsaw, 9-14 July, 2000: Book Abstr., vol. 3, Warsaw, 2000, p. 1200.

11. Голованова К. В. Синтез и физико-химические свойства водных полиуретановых дисперсий / К. В. Голованова [и др.] // Вестник технологического университета. 2017. Т 20. № 13. С. 18-22.

12. Ягнятинская Е. А. Технология изготовления, свойства и особенности применения резин с волокнистыми наполнителями в РТИ / Е. А. Ягнятинская, Б. Б. Гольдберг, В. В. Леонов и др. М.: ЦНИИТЭнефтехим, 1979. 54 с.

13. Kim, B.K. Polym. Sei 54. 12 / B.K. Kim, Y.M. Lee, J. Appl., 1994, pp. 1809-1815.

14. Levchenko N. I. Partnership of Polymers / N. I. Levchenko, S. A. Sukhorukova, T. V. Travinskaya // Churchill College, Univ. of Cambridge, 1996, pp. 195-200.

15. Кожевникова И. В. Полиуретановые композиции, содержащие отходы осушителей на основе минеральных оксидов: дис. … канд. техн. наук: 05.17.06 / И. В. Кожевникова. Казань, 2015. 178 с.

16. LNK COMPANY [Электронный ресурс]. Режим доступа: http://www.lnkcom.ru/ catalog/protective_coatings/lining_materials/lining_and_coating_of_driving_dr/remagrip_lining_tip_top_/. Дата доступа 07.11.2017.

17. Synthesis of polyether-based polyurethane-silica nanocomposites with high elongation property / Lee Sung-Il, Hahn Yoon Bong, Nahm Kee Suk, Lee Youn-Sik // Polym. Adv. Technol., 2005, vol. 16, no. 4, pp. 328-331.

18. Varghese S. Morphology and mechanical properties of layered silicate reinforced natural and polyurethane rubber blends produced by latex compounding / S. Varghese, 1C0 Gatos., A.A. Apostolov, J. Karger-Kocsis // J. Appl. Polym. Sci., 2004, vol. 92, no. 21, pp. 543-551.

19. ПК Полимер [Электронный ресурс]. Режим доступа: http://polimer - ug.com /. Дата доступа 30.10.2017.

20. Иванов Е. И. Полиуретановые лакокрасочные покрытия Stelpant для защиты от коррозии на предприятиях металлургии / Е. И. Иванов, А. Е. Иванова // Технология колесных и гусеничных машин. 2013. № 3(7). С. 34-40.

Information about the Authors

D. V. Hrydziushka – Head of Experimental Shop (post-graduate student of Grodno State University named after Y. Kupala); Joint Stock Company «Soligorsk Institute of Resources Saving Problems with Pilot Production»; Soligorsk, Minsk region, the Republic of Belarus.

A. V. Bryzhevich – Deputy Head of Experimental Workshop (post-graduate student of Grodno State University named after Y. Kupala), Joint Stock Company «Soligorsk Institute of Resources Saving Problems with Pilot Production»; Soligorsk, Minsk region, the Republic of Belarus.

E. V. Piskun – Engineer of Scientific and Technical Information (post-graduate student of Belarusian State University of Transport), Joint Stock Company «Soligorsk Institute of Resources Saving Problems with Pilot Production»; Soligorsk, Minsk region, the Republic of Belarus, onti@sipr.by.

Информация об авторах

Гридюшко Д. В. – начальник опытно-экспериментального цеха (аспирант Гродненского государственного университета им. Я. Купалы), Закрытое акционерное общество «Солигорский Институт проблем ресурсосбережения с Опытным производством», г. Солигорск, Минская область, Республика Беларусь.

Брижевич А. В. – заместитель начальника опытно-экспериментального цеха (аспирант Гродненского государственного университета им. Я. Купалы), Закрытое акционерное общество «Солигорский Институт проблем ресурсосбережения с Опытным производством», г. Солигорск, Минская область, Республика Беларусь.

Пискун Е. В. – инженер по научно-технической информации (аспирантка Белорусского государственного университета транспорта), Закрытое акционерное общество «Солигорский Институт проблем ресурсосбережения с Опытным производством», г. Солигорск, Минская область, Республика Беларусь, onti@sipr.by.

ORIGINAL PAPERS

DOI: 10.17073/2500-0632-2019-2-144-149

Operating Load of Belt Conveyor as a Reflection of Actual Planogram of Coal Shearer Operation in Integrated-Powered Face

V. M. Yurchenko

«Kuzbass State Technical Universitynamed after T. F. Gorbachev» (KuzSTU),
Kemerovo, Russia, ✉yvm@kuzstu.ru

Abstract: Conveyor transport at a modern coal mine is the main link that determines the overall performance of the enterprise. For safe operation of belt conveyors, it is important to ensure that shift output per face doesn't produce average and maximum minute material flows, which exceed strength margin of the belt, power margin of the drive, and receiving capacity. Such situation, as a rule, may arise due to the strive of workers to compensate for underproduction caused by long downtimes of a face for any reason. In the paper, a method is proposed that enables determining the maximum shift output per face. According to the technique described in the "Basic Provisions for Designing Underground Transport of New and Existing Coal Mines," the average minute material flow, which determines the operational load on a belt conveyor, depends on the material feed time factor. Accepting the assumption that a coal shearer works the entire shift in a face, the limiting value of the material feed time factor is equal to 1. To determine the actual value of this factor, it is proposed to determine the face operating (production) time using actual planogram. The shift time is spent for preparatory and finishing operations, the face equipment and conveyor line troubleshooting and failure recovery, auxiliary service operations and, finally, operational and organizational downtimes. On the actual planogram, these time intervals are displayed by straight-line portions. Thus, the shift time minus downtime for any reason, represents the face production time. The ratio of these values represents the operation factor. Applying the operation factor allows to determine the maximum limiting face production, not only taking into account the volume of coal mined per cycle, but also based on coal cuttability and technical specifications of the face equipment. This enables us to determine the face production load that ensures safe operation of the belt conveyor.

Keywords: belt conveyor, output per face, average and maximum minute material flows, material feed factor, conveyor operating load, operation factor, down-time.

For citation: Yurchenko V. M. Operating load of belt conveyor as a reflection of actual planogram of coal shearer operation in integrated-powered face. *Mining Science and Technology*. 2019;4(2):144-149 (In Russ.). DOI: 10.17073/2500-0632-2019-2-144-149.

Эксплуатационная нагрузка ленточного конвейера как отражение действительной планограммы работы комбайна в комплексно-механизированной лаве

Юрченко В. М.

«Кузбасский государственный технический университет имени Т. Ф. Горбачева» (КузГТУ),
Кемерово, Россия, ✉yvm@kuzstu.ru

Аннотация: Конвейерный транспорт на современной угольной шахте является главным звеном, определяющим эффективность работы предприятия в целом. Для безопасной эксплуатации ленточных конвейеров важно, чтобы от сменной нагрузки на лаву не возникали средний и максимальный минутные грузопотоки, при которых не обеспечиваются запас прочности ленты, запас мощности привода и приемная способность. Такая ситуация, как правило, возникает при стремлении работающих компенсировать потерю добычи после длительных простоев лавы по любой причине. В рамках статьи предложен инструментарий, позволяющий определять максимальную сменную нагрузку на лаву. Согласно методике, изложенной в «Основных положениях по проектированию подземного транспорта новых и действующих угольных шахт», средний минутный грузопоток, определяющий эксплуатационную нагрузку на ленточный конвейер, зависит от коэффициента времени поступления груза. Если принять допущение, что комбайн в лаве работает всю смену, предельная величина коэффициента времени поступления груза равна единице. Для определения действительной величины этого коэффициента предлагается определять время работы лавы по добыче по действительной планограмме. Время смены тратится на выполнение подготовительно-заключительных операций, на устранение неисправностей и отказов оборудования лавы и конвейерной линии, на выполнение вспомогательных операций по обслуживанию и, наконец, на эксплуатационные и организационные простои. На действительной планограмме эти промежутки времени отражены прямолинейными участками. Таким образом, время смены за вычетом времени простоев по любым причинам, представляет время работы лавы по добыче. Отношение этих величин представляет собой коэффициент эксплуатации. Использование коэффициента эксплуатации позволяет определять предельную нагрузку на лаву не только с учетом объема угля, добываемого за цикл, но и с учетом сопротивляемости угля резанию, с учетом технических параметров забойного оборудования. Это дает возможность определять эксплуатационную нагрузку, обеспечивающую безопасную работу ленточного конвейера.

Ключевые слова: ленточный конвейер, нагрузка на лаву, средний и максимальный минутный грузопотоки, коэффициент поступления груза, эксплуатационная нагрузка на конвейер, коэффициент эксплуатации, время простоев.

Для цитирования: Юрченко В. М. Эксплуатационная нагрузка ленточного конвейера как отражение действительной планограммы работы комбайна в комплексно-механизированной лаве. *Горные науки и технологии.* 2019;4(2):144-149. DOI: 10.17073/2500-0632-2019-2-144-149.

Conveyor transport, being the core transport facility, determines mine effectiveness. Rational and safe operation of conveyor transport is ensured only with a shift load meeting that given in the "Face operation certificate of excavation section." However, in a real-life situation, a need arises to increase a face load per shift to compensate for losses of production due to long downtime for any reason [1, 3–11]. Therefore, the maximum allowable face load per shift should be determined, the excess of which leads to emergency conditions when operating conveyor transport.

This paper proposes an instrumentarium allowing determining the maximum face load per shift, which ensures safe operation of conveyor transport. For this, two conditions must be observed:

– the maximum minute flow of a coal shearer should not exceed the receiving capacity of a belt conveyor,

– the belt conveyor operational load due to the face load per shift, should provide strength margin of the belt and power margin of the drive.

The belt conveyor operational load depends not only on the face load per shift, but also on the time during which the load arrives on the conveyor. According to the methodology [2], the operational load is determined by the formula, t/h,

$$Q_э = 60 a_{1(n)1} k_t ,$$

where $a_{1(n)1} = \dfrac{A_{см}}{60 T_{см} k_п}$ – is the average minute load flow, t/min; k_t – the estimated load factor, taking into account the uneven load flow during the load passage along the entire length of the conveyor; $k_п$ – the load (material) feed time factor (governed by time of feeding the material on a belt conveyor).

The load is fed on a belt conveyor mainly during coal cutting and face cleanup during a shearer operation by one-sided scheme; therefore, factor $k_п$ is determined by the formula

$$k_{\text{п}} = \frac{t_{\text{п}} + t_{\text{з}}}{60T_{\text{см}}} N_{\text{ц}} \leq 1.$$

In the case when an attempt is made to increase the face load per shift in order to compensate for production losses due to unforeseen downtime, the load feed (on a belt conveyor) time factor can be taken equal to unity. It should be borne in mind that the shift time cannot be fully used for a face production time. The shift time is spent for preparatory and finishing operations, the face equipment and conveyor line troubleshooting and failure recovery, auxiliary service operations and, finally, operational and organizational downtimes. On an actual planogram, these time intervals are recorded in rectilinear horizontal sections (Fig. 1).

Thus, the shift time minus downtime for any reason represents a face production time

$$T_{\text{рл}} = T_{\text{см}} - T_{\text{пз}} - T_{\text{ун}} - T_{\text{во}} - \ldots - T_{\text{эо}}\text{, min.}$$

The ratio of a face production time per shift to the shift time is called the factor of an integrated-powered face and the conveyor line equipment operation $k_{\text{экс}}$: $k_{\text{экс}} = T_{\text{рл}}/T_{\text{см}}$ or $k_{\text{экс}} = T_{\text{рл}} N_{\text{см}}/T_{\text{сут}}$.

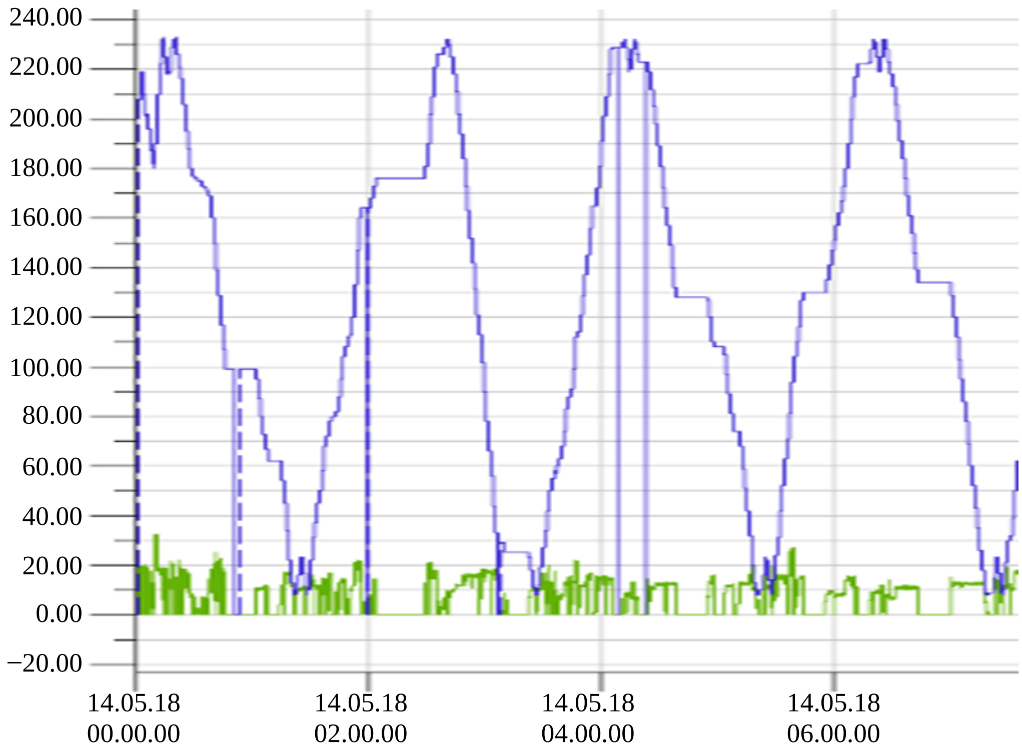

Fig. 1. Actual planogram of face operation

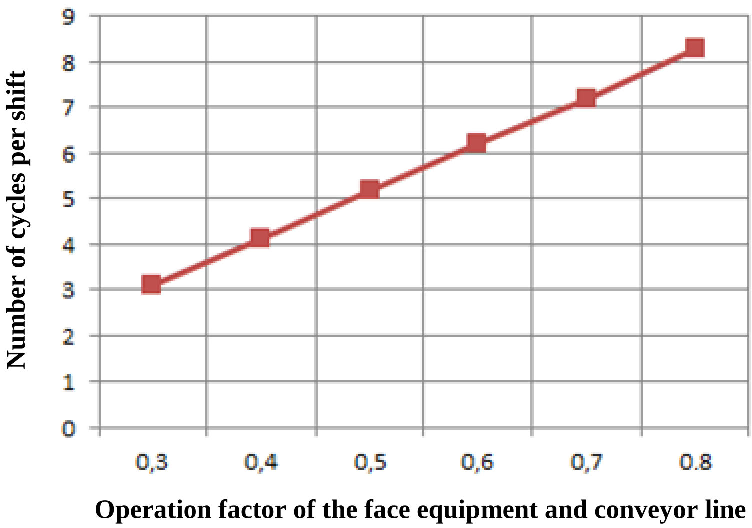

Fig. 2. The dependence of the number of cycles per shift on the operation factor $k_{экс}$ at the cycle time of 65.2 minutes by the example of 52-13 face

The operation factor obtained by this way reflects not only mining and geological conditions (seam thickness, coal density in the solid, coal cuttability, face length), but also the equipment technical specifications (working width, power of electric motors of the shearer's working members, the possible feed rate when cutting and at cleanup. In addition, the equipment condition (downtime due to failures, time spent on troubleshooting, as well as the staff skills and competence (the time spent for face preparatory and finishing operations and operational and organizational downtimes).

Based on these assumptions, we obtain the expression

$$1 = \frac{t_п + t_з}{60 T_{см} k_{экс}} N_ц,$$

which allows determining the number of cycles per shift based on the time of a cycle performed by a shearer:

$$N_{цт} = \frac{60 T_{см} k_{экс}}{t_п + t_з}.$$

The obtained dependence, taking into account the real-life factor of the integrated-powered face and conveyor line specific equipment operation, allows to accurately plan a shift load.

At the same time, technologists, planning the face load per shift, determine the number of cycles per shift based on the amount of coal per cycle

$$N_{цу} = \frac{A_{см}}{m b L_{оз} \gamma_ц}.$$

Ultimately, in order for the calculations to reflect reality, it is necessary to comply with the condition

$$N_ц = N_{цт} = N_{цу}.$$

The achievement of this equality is facilitated by using the operation factor obtained based on treatment of the actual planogram (see Fig. 1).

Based on this equality, the actual load per shift should be determined by the formula, t,

$$A_{см} = \frac{60 T_{см} k_{экс} m b L_{оз} \gamma_ц}{t_п + t_з}.$$

Conclusions

Applying the operation factor obtained based on treatment of the actual operation planograms for integrated-powered face and conveyor line equipment allows to accurately determine and plan a maximum face load per shift, taking into account:

– volume of coal mined per cycle,

– coal cuttability,

– technical specifications of the face equipment,

– staff competence,

– achieved workflow management sophistication level.

This enables determining the face production load that ensures safe operation of the belt conveyor.

References

1. Yurchenko V. M. Features of the joint operation of face equipment and conveyor transport. Mining Informational and Analytical Bulletin (magazine) 2016, no. 9, pp. 165-171 (in Russ.).

2. Basic Provisions for Designing Underground Transport of New and Existing Coal Mines. M. IGD named after A. A. Skochinsky, 1986, 355 p. (in Russ.).

3. Kopylov K. N., Kubrin S. S., Zakorshmenniy I. M., Reshetniak S. N. Reserves of increase of efficiency of coal extraction sections of coal mines Ugol, 2019, (3), pp. 46-49.

4. Gładysiewicz L., Król R., Kisielewski W. Measurements of loads on belt conveyor idlers operated in real conditions (2019) Measurement: Journal of the International Measurement Confederation, 134, pp. 336-344. DOI: 10.1016/j.measurement.2018.10.068.

5. Kruczek P., Polak M., Wyłomańska A., Kawalec W., Zimroz R. Application of compound Poisson process for modelling of ore flow in a belt conveyor system with cyclic loading. International Journal of Mining, Reclamation and Environment, 2018, 32(6), pp. 376-391. DOI: 10.1080/17480930.2017.1388335.

6. Comparison of the loading methods for the driving roller of a belt conveyor in finite element analysis. ACM International Conference Proceeding Series, 2018, pp. 73-77. DOI: 10.1145/3230876.3230879.

7. Mrazek, J., Dynyby, V., Stary, F. Adaptive control of the belt conveyor preloading. Applied Mechanics and Materials, 2014, 486, pp. 62-65. DOI: 10.4028/www.scientific.net/AMM.486.62.

8. Ianăşi A. C., Mihuţ N. M. Mechanical and geometrical characterization of the conveyors belts from mineral resources exploitation. Advanced Materials Research, 2014, 837, pp. 99-104. DOI:10.4028/www.scientific.net/AMR.837.99.

9. Hou Y.-F., Meng Q.-R. Dynamic characteristics of conveyor belts. Journal of China University of Mining and Technology, 2008, 18(4), pp. 629-633. DOI: 10.1016/S1006-1266(08)60307-7.

Библиографический список

1. Юрченко В. М. Особенности совместной эксплуатации забойного оборудования и конвейерного транспорта // Горный информационно-аналитический бюллетень (журнал). 2016. № 9. С. 165-171.

2. Основные положения по проектированию подземного транспорта новых и действующих угольных шахт. М.: ИГД им.А.А. Скочинского, 1986. 355 с.

3. Kopylov K. N., Kubrin S. S., Zakorshmenniy I. M., Reshetniak S. N. Reserves of increase of efficiency of coal extraction sections of coal mines Ugol, 2019, (3), pp. 46-49.

4. Gładysiewicz L., Król R., Kisielewski W. Measurements of loads on belt conveyor idlers operated in real conditions (2019) Measurement: Journal of the International Measurement Confederation, 134, pp. 336-344. DOI: 10.1016/j.measurement.2018.10.068.

5. Kruczek P., Polak M., Wyłomańska A., Kawalec W., Zimroz R. Application of compound Poisson process for modelling of ore flow in a belt conveyor system with cyclic loading. International Journal of Mining, Reclamation and Environment, 2018, 32(6), pp. 376-391. DOI: 10.1080/17480930.2017.1388335.

6. Comparison of the loading methods for the driving roller of a belt conveyor in finite element analysis. ACM International Conference Proceeding Series, 2018, pp. 73-77. DOI: 10.1145/3230876.3230879.

7. Mrazek, J., Dynyby, V., Stary, F. Adaptive control of the belt conveyor preloading. Applied Mechanics and Materials, 2014, 486, pp. 62-65. DOI: 10.4028/www.scientific.net/AMM.486.62.

8. Ianăşi A. C., Mihuţ N. M. Mechanical and geometrical characterization of the conveyors belts from mineral resources exploitation. Advanced Materials Research, 2014, 837, pp. 99-104. DOI:10.4028/www.scientific.net/AMR.837.99.

9. Hou Y.-F., Meng Q.-R. Dynamic characteristics of conveyor belts. Journal of China University of Mining and Technology, 2008, 18(4), pp. 629-633. DOI: 10.1016/S1006-1266(08)60307-7.

Information about the author

Vadim M. Yurchenko – Cand. Sci. (Tech.), Assistant Professor of the Department of Mining Machines and Complexes, «Kuzbass State Technical University named after T. F. Gorbachev» (KuzSTU), Kemerovo, Russia, yvm@kuzstu.ru

Информация об авторе

Юрченко Вадим Максимович – канд. техн. наук, доцент кафедры горных машин и комплексов, «Кузбасский государственный технический университет имени Т. Ф. Горбачева» (КузГТУ), Кемерово, Россия, yvm@kuzstu.ru.

ORIGINAL PAPERS

DOI: 10.17073/2500-0632-2019-2-150-156

Пути снижения потерь электроэнергии в питающих горные предприятия линиях

Анциферов Н. С.

«СК КаскадСтрой», Москва, Россия, ✉nikita-anciferov@rambler.ru

Аннотация: Электрическая энергия является наиболее удобным и универсальным видом энергии. Ее можно производить в больших количествах вблизи источников энергии, передавать на большие расстояния, легко распределять между потребителями и преобразовывать в механическую, тепловую и световую энергии. Обеспечение надежного и экономичного энергоснабжения электроэнергией заданного качества предприятий горной промышленности при наиболее эффективном использовании энергетических ресурсов является одной из важнейших задач, стоящих перед энергетиками страны. В Российской Федерации достигнута высокая степень концентрации мощностей на электрических станциях. Основные мощности сосредоточены на электростанциях с установленной мощностью более 1 млн кВт. Высокий уровень значимости электроэнергетики определяется инфраструктурным характером отрасли и прямой зависимостью между экономическим ростом страны и уровнем эффективности ее развития. Одной из наиболее актуальных проблем современного электроснабжения является проблема обеспечения качества электроэнергии. Основная причина ухудшения качества электроэнергии – широкое распространение нелинейных нагрузок, создающих при своей работе токи несинусоидальной формы, несимметрия напряжений. Несимметрия напряжений вызывается чаще всего наличием несимметричной нагрузки. Несимметричные токи нагрузки, протекающие по элементам системы электроснабжения, вызывают в них несимметричные падения напряжения. Вследствие этого на выводах ЭП появляется несимметричная система напряжений. Отклонения напряжения у ЭП перегруженной фазы могут превысить нормально допустимые значения, в то время как отклонения напряжения у ЭП других фаз будут находиться в нормируемых пределах. Кроме ухудшения режима напряжения у ЭП, при несимметричном режиме существенно ухудшаются условия работы как самих ЭП, так и всех элементов сети, снижается надежность работы электрооборудования и системы электроснабжения в целом. В статье рассматриваются вопросы снижения потери напряжения питающих электрических сетей посредством улучшения качества электроэнергии.

Ключевые слова: качество электроэнергии, энергоэффективность, нелинейная нагрузка, высшие гармоники, несимметрия нагрузки, потери мощности, отклонения напряжения.

Для цитирования: Анциферов Н. С. Пути снижения потерь электроэнергии в питающих горные предприятия линиях. *Горные науки и технологии.* 2019;4(2):150-156. DOI: 10.17073/2500-0632-2019-2-150-156.

Ways to Reduce Power Losses in Mining Power Supply Lines

N. S. Antsiferov

Leading Design Engineer "SK Kaskadstroy", Moscow, Russia, ✉nikita-anciferov@rambler.ru

Abstract: Electric energy is the most common and universal form of energy. It can be produced in large quantities near energy sources, transmitted to large distances, easily distributed between consumers and converted into mechanical, thermal, and light energy. Ensuring reliable and economical quality electric energy supply to mining enterprises with the optimal use of energy resources is one of the most important tasks facing the country's energy sector. In the Russian Federation, high degree of concentration of generating capacities at power plants has been achieved. The main capacities are concentrated in power plants with installed capacity of more than 1 million kW. High importance of the electric power industry is determined by the infrastructural nature of the industry and the direct relationship between the country's economic growth and the level of its development effectiveness. One of the most pressing problems of modern electricity supply is the problem of ensuring the quality of electric energy. The main reason for the deterioration in the electricity quality is widespread non-linear loads that create non-sinusoidal currents and voltage unbalance during their operation. The voltage unbalance is most often caused by the presence of an unbalanced load. Unbalanced load currents flowing through the elements of the power supply system cause unbalanced voltage losses in them. This results in appearance of unbalanced voltages on the terminals of electric apparatus. The voltage deviations at electric apparatus overdriven phase may exceed the normally acceptable values, while the voltage deviations at electric apparatus other phases may remain within the normal limits. In addition to the deterioration of the voltage mode at electric apparatus under the unbalanced voltage conditions, the operating conditions of both the electric apparatus and all the network elements are significantly worsened, and the reliability of the electrical equipment and the power supply system as a whole decreased. The paper considers the issues of reducing the voltage losses in power supply networks by improving quality of electric power.

Keywords: quality of electric power, energy performance, nonlinear load, higher harmonics, load unbalance, power losses, voltage deviation.

For citation: Antsiferov N. S. Ways to reduce power losses in mining power supply lines. *Mining Science and Technology*. 2019;4(2):150-156 (In Russ.). DOI: 10.17073/2500-0632-2019-2-150-156.

Высокий уровень значимости электроэнергетики определяется инфраструктурным характером отрасли и прямой зависимостью между экономическим ростом страны и уровнем эффективности ее развития. В РФ сложилась неблагоприятная ситуация с потреблением энергоресурсов: по данным Международного энергетического агентства, энергоемкость ВВП (внутренний валовой продукт) России в 2,5 раза выше среднемирового уровня и в 2,5–3,5 раза выше, чем в развитых странах: в целом по стране около 35–40 % всех потребляемых топливно-энергетических ресурсов (ТЭР) расходуется без отдачи, неэффективно: только прямые потери топливно-энергетических ресурсов достигают 25–30 %. Вследствие этого возрастает себестоимость производимой продукции, снижается ее конкурентоспособность, увеличиваются ежегодные затраты на поддержание в работоспособном состоянии и развитие ТЭК, возрастают издержки населения, бюджетной сферы и производственного сектора на потребляемые топливно-энергетические ресурсы. Все это приводит к снижению энергоэффективности экономики в целом [10].

Если ранее источники искажения качества электроэнергии, кроме частоты и отклонения напряжения, были присущи только промышленным потребителям и потребителям, приравненным к ним, то сейчас они активно появляются и у других видов потребителей [2].

Одним из эффективных мероприятий по энергосбережению, позволяющих экономить до 40–50 % электроэнергии, является использование частотно-регулируемых приводов в котельных, насосных, в том числе и систем горячего водоснабжения зданий, сооружений, а также в технологических установках предприятий, осуществляющих регулируемые виды деятельности [11].

Низкое качество электроэнергии – потенциал энергосбережения. Общеизвестно, что низкое качество электроэнергии приводит к увеличению потерь электроэнергии, а следовательно, к снижению энергетической эффективности электрических сетей. Необходимо определить, насколько велика доля потерь электроэнергии от низкого качества электроэнергии и есть ли смысл рассматривать их как потенциал энергосбережения. В электрических сетях среднего напряжения с мощными источниками высших гармоник технические потери мощности в силовых трансформаторах связи с энергосистемой существенно увеличиваются [4]. При коэффициенте искажения синусоидальности кривой напряжения, равном 5 % у коммунально-бытовых потребителей, питающихся от сети 0,4 кВ, они составляют 15 % нагрузочных потерь в силовом трансформаторе, а при коэффициенте искажения синусоидальности кривой напряжения 10 % эти потери увеличиваются от 20 до 60 %.

В качестве примера в табл. 1 приведены значения дополнительных потерь в силовом трансформаторе ТДН-16000/110 при следующих значениях показателя качества электрической энергии (ПКЭ): $K_{2U} = 4$ %; $K_{U5} = 5$ %; $K_{U7} = 7$ %; $K_{U11} = 3$ %; $K_{U13} = 1$ %. Потери определялись по методике, приведенной в [4]. Здесь указана доля дополнительных потерь (в %) относительно номинальных потерь [3].

Таблица 1

Дополнительные потери при искажении качества электрической энергии в силовом трансформаторе

Additional losses due to distortion of the quality of electric power in a power transformer

Параметр качества электроэнергии	Нагрузочные потери		Потери холостого хода		Суммарные потери	
	%	кВт	%	кВт	%	кВт
Несимметрия напряжения	14,5	12,325	0,16	0,03	11,9	12,355
Несинусоидальность напряжения	8,86	7,53	0,84	0,16	7,39	7,69

В синхронных и асинхронных двигателях – доля таких потерь может достигать 15–20 % в зависимости от соотношения показателей качества электроэнергии. Приведенные примеры свидетельствуют о том, что дополнительные технические потери электроэнергии, вызываемые низким качеством электроэнергии, можно рассматривать в качестве потенциала энергосбережения [2].

Низкое качество электроэнергии приводит и к появлению дополнительных метрологических потерь электроэнергии, которые не учитываются в оценке экономической эффективности при установке приборов учета электроэнергии. Как известно, в зависимости от расположения источника несинусоидальности или несимметрии напряжений и токов в сети возможен как недоучет, так и переучет отпущенной или потребленной электроэнергии.

Последовательность решения задачи повышения энергоэффективности электрических сетей путем улучшения качества электроэнергии [1]

Первым этапом ее решения является выявление источников искажения качества электроэнергии и мест их расположения. Это возможно сделать следующими путями: энергоаудитом, контролем качества электроэнергии, расчетно-аналитическим путем. Затем по типу источников искажения определяются параметры качества электроэнергии и показатели качества электроэнергии, которые их описывают, либо измерениями, либо расчетом [7].

Производится расчет потенциала энергосбережения, обусловленного низким качеством электроэнергии в зависимости от его структуры. Далее выбираются узлы сети для реализации мероприятий по улучшению качества электроэнергии. Для выбранных узлов вначале определяется возможность применения организационных мероприятий как малозатратных, выбираются организационные мероприятия, набор которых зависит от показателей качества электроэнергии, не удовлетворяющих требованиям действующего стандарта на качество электроэнергии, производится оценка их экономической эффективности и определяется доля реализованного потенциала энергосбережения, т.е. процент снижения потерь от низкого качества электроэнергии [1].

Для тиражирования мероприятий, направленных на повышение энергоэффективности сетей с низким качеством электроэнергии, целесообразно разработать типовые мероприятия по аналогии с существующим перечнем типовых мероприятий по энергосбережению и повышению энергетической эффективности и создать библиотеку таких мероприятий [8].

Каждое мероприятие рекомендуется описывать в следующем порядке: аннотация, назначение мероприятия, тип мероприятия, область применения, краткая характеристика мероприятия, нормативные документы, методика оценки экономической эффективности, инструкция к применению [3].

Производство электрической энергии (ЭЭ) во всём мире неуклонно повышается, что обусловлено всё возрастающим её потреблением в различных отраслях хозяйственной деятельности человечества. Так, к 2020 г. количество производимой в мире ЭЭ должно вырасти до 30 трлн кВт·ч, что соответствует темпам роста производства до 2,5–3 % в год в среднем.

Современная система электроснабжения является довольно сложным физико-техническим объектом и неотъемлемой частью Единой энергетической системы страны, регионов. В нынешней экономической ситуации вопрос рационального использования топливно-энергетических ресурсов стоит особо остро. При этом для получения наибольшей эффективности их использования необходимо рассмотреть весь процесс – от добычи первичных энергоресурсов до их потребления.

Электрическая энергия как сертифицируемая продукция обладает целым рядом особенностей, в числе которых неразрывность и одновременность процессов производства и потребления, когда искажающее влияние на показатели качества электроэнергии может быть оказано как электроприёмниками потребителя, так и принесено извне в виде кондуктивной электромагнитной помехи, распространяемой по общей электрической сети.

Учёт электроэнергии состоит из определения произведённого её количества, количества электроэнергии, потреблённой электроприёмниками, а также количества электроэнергии, потерянной при её передаче.

Электроэнергия является единственным видом продукции, транспортировка которой осуществляется за счёт расхода определённой части самой продукции, то есть потери электроэнергии при её передаче неизбежны.

Первоочередной задачей экономии ТЭР электроэнергетики является снижение потерь электроэнергии в электрических сетях, которые достигают 15–20 % от общего отпуска электроэнергии.

Анализ структуры потерь электроэнергии в действующих электрических сетях показывает, что потери в линиях 0,38 кВ составляют 31,33 % от общих потерь. С учётом потерь электроэнергии в трансформаторах 10/0,4 кВ потребительских ТП потери в электрических сетях 0,38 кВ составляют более 50 % от общих потерь. Поэтому снижение потерь электроэнергии в сетях 0,38 кВ позволит добиться снижения общих потерь в электрических сетях.

Исследованиями установлено, что в сетях с коммунально-бытовыми и смешанными нагрузками возникает значительная несимметрия токов, т.е. режимы работы сельских сетей 0,38 кВ являются объективно несимметричными. Несимметрия токов в сети вызывает несимметрию напряжений на зажимах трёхфазных электроприёмников, которая во многих случаях превышает в 2–2,5 раза допустимое ГОСТ 13109–97 значение. При величине коэффициентов несимметрии токов обратной и нулевой последовательности в сети, равной 25–30 %, потери мощности и электрической энергии в линиях 0,38 кВ и трансформаторах потребительских ТП возрастают на 30–50 % по сравнению с симметричным режимом работы.

Кроме того, несимметрия токов и напряжений в сетях приводит к увеличению в узлах нагрузки отклонения напряжения от допустимого значения, сокращению срока службы электродвигателей агропромышленного комплекса и другим негативным явлениям в сетях и приёмниках электроэнергии.

Работа распределительных сетей с постоянной несимметрией нагрузки является причиной довольно значительного ущерба в хозяйственной деятельности. Это определяется дополнительными потерями электроэнергии в сетях и нагрузке, с одной стороны, и снижением эффективности использования оборудования и сокращением срока службы электрических установок – с другой.

Анализ проблемы несимметрии в сетях 0,38 кВ показал, что существующие методы расчёта показателей несимметрии и потерь электроэнергии в этих сетях не позволяют установить закономерности их изменения от параметров нагрузки и сети, провести анализ потерь при различных режимах работы электроприёмников и разработать наиболее эффективные способы и средства снижения несимметрии и обусловленных ею потерь, так как в этих методах несимметрия токов в сетях учитывается приближёнными способами. Кроме того, большинство научных работ не рассматривают проблему качества электрической энергии в целом. Так, например, повышение качества напряжения за счёт снижения уровня несимметрии напряжений рассматривалось в отрыве от проблемы снижения потерь мощности и энергии в сети, и, наоборот, вопросы снижения потерь не затрагивали проблему несимметрии напряжений. Вместе с тем, до настоящего времени не разработаны общие методы расчёта сетей с несимметричными рассредоточенными нагрузками. Отсутствие комплексности в подходе к решению проблемы несимметрии приводило в отдельных случаях к недостаточно верным выводам и рекомендациям по способам и средствам для снижения потерь электроэнергии в сетях 0,38 кВ, обусловленных несимметрией токов.

Недостаточность знаний об уровне несимметрии токов и напряжений в низковольтных сетях 0,38 кВ, а также о способах и технических средствах её снижения, не позволяют составить достоверной картины о действительном характере изменения потерь электрической энергии в этих сетях, а без этого невозможно разработать и применить на практике мероприятия по снижению потерь электрической энергии и повышению её качества.

Таким образом, решение задач энергосбережения и улучшения качества электрической энергии в низковольтных сетях 0,38 кВ тесно связано с проблемой снижения несимметрии токов в этих сетях. Поэтому актуальным и своевременным является рассмотрение вопросов, связанных с разработкой способов снижения несимметрии токов и подготовкой практических рекомендаций по эффективности использования МСП.

Выводы

1. Показана целесообразность использования в качестве типовых мероприятий, направленных на повышение энергоэффективности электрических сетей, мероприятия по улучшению качества электроэнергии.

2. Разработан порядок реализации потенциала энергосбережения в электрических сетях, обусловленного низким качеством электроэнергии.

3. Предложено создать библиотеку типовых мероприятий по повышению энергоэффективности электрических сетей путем улучшения качества электроэнергии, и показана методика ее реализации.

Библиографический список

1. Sidea D. Weather-based assessment of the overhead line conductors thermal state // PowerTech. IEEE Eindhoven, 2015, pp. 1-6.

2. Mir V. Ali. Evolution of heating units: from Ingalls to Jinmao // Electronic J. of Structural Engineering, 2001, vol. 1, no. 1, pp. 2-14.

3. Ignotas A. Lithuanian legal and regulatory framework for district heating. Presented at IEA workshop «District heating policy in transition economies», Prague, February 2004, 167 p.

4. Georgiadis M. C., Kikkinides E. S., Pistikopoulo E. N. Energy Systems Engineering // WILEY-VCH, Weinheim-2008, 337 p.

5. McGranagham M., Blevins J., Samotyj M. Оптимальное решение для качества электроэнергии и повышения надёжности // Transmission & Distribution World, 2004, no. 2, С. 48-52.

6. Ананичева С. С., Мызин А. Л. Схемы замещения и установившиеся режимы электрических сетей: уч. пос.; 6-е изд., испр. Екатеринбург: УрФУ. 2012. 80 с.

7. Латыпов И. С., Сушков В. В. Снижение потерь электроэнергии в распределительной сети напряжением 6–35 кВ в системе электроснабжения потребителей нефтегазовой отрасли // Культура, наука, образование: проблемы и перспективы: материалы 5-й Междунар. науч.-практ. конф. Нижневартовск. 2016. Ч. П. С. 107-111.

8. Вендин С. В., Щербинин И. А. К расчету распространения электромагнитного импульса при СВЧ обработке диэлектрических сред / Вестник Белгородского государственного технологического университета им. В. Г. Шухова. 2015. № 2. С. 204-206.

9. Виноградов А. А., Соловьев С. В. Математические задачи электроэнергетики / Методические указания к выполнению курсовой работы для студентов направления 140400 // Электроэнергетика и электротехника. Белгород: БГТУ им Шухова. 2013. 37 с.

10. Повышение эффективности воздушных линий электропередачи напряжением 110–220 кВ в гололедных районах: монография / Г. Г. Угаров, Н. Ю. Шевченко, Ю. В. Лебедева, А. Г. Сошинов. М.: Перо, 2013. 186 с.

11. Электрические системы. Т. 2. Электрические сети: уч. пос. / Под ред. В. А. Веникова. М.: Высш. шк., 1971. 440 с.

12. Электрические системы. Режимы работы электрических систем и сетей: уч. пос. / Под ред. В. А. Веникова. М.: Высш. шк., 1975. 344 с.

13. Блок В. Н. Электрические сети и системы: уч. пос. М.: Высш. шк.. 1986. 430 с.

14. Электрические системы и сети: уч. пос. / Под ред. Г. И. Денисенко. Киев: Вища школа, 1986. 82 с.

15. Frichtel I. S. Influence of electric power quality on avionic design and weapon system effectivness // Power Cond. Specialists Conf. Rec. (Pasadena, Cal., 1971). New York, 1971, p. 173.

16. Sciubidio E. Spadke napiecia i straty mocy czynnj w liniach 4-przewodowych niskiego napiecia przy niesymetrycznym obciazeniu // Energetyka (DHL). 1975, 29, no. 2, pp. 63-64.

17. Айзенберг Б. Л. Влияние неравномерности нагрузки фаз городской сети 0,4 кВ на напряжение в установках потребителей и его экономическая оценка. – В кн.: Регулирование напряжения в электрических сетях. М.: Энергия, 1968. С. 130-135.

18. Волков Э. П., Баринов В. А., Маневич А. С. Основные направления развития электроэнергетики России с учётом долгосрочной перспективы и совершенствования рыночных отношений. Изв. Академии наук – Энергетика, 2000. № 5. С. 3-40.

19. Вайнштейн Л. М., Жуков Л. А. Несимметрия напряжений в электрических системах и симметрирование режима. – В кн.: Регулирование напряжения в электрических сетях. М.: Энергия, 1968. С. 444-450.

20. Васильев В. Г., Ганиходжаев Н. Г., Васильева С. П. Регрессионный метод для оценки величины потерь электроэнергии в воздушных линиях сельских электрических сетей 0,38 кВ. – В сб.: Вопросы электрификации сельского хозяйства Уз. ССР. М., 19079. С. 101-119.

21. Goela S. C. Discussion on the Paper: Allowable output from a 3-phase induction motor connected to unsymmetrical supply by N. N. Roy. Author's reply. I.Inst. Eng. (India). Elec. Eng., Div. 1969. 49. Pt. 3. K. 6, pp. 812–816.

22. Frichtel I. S. Influence of electric power quality on avionic design and weapon system effectiveness // Power Cond. Specialists Conf. Rec. (Pasadena, Cal., 1971). New York, 1971, p. 173.

References

1. Sidea D. Weather-based assessment of the overhead line conductors thermal state // PowerTech. IEEE Eindhoven, 2015, pp. 1-6.

2. Mir V. Ali. Evolution of heating units: from Ingalls to Jinmao // Electronic J. of Structural Engineering. 2001, vol. 1. no. 1, pp. 2-14.

3. Ignotas A. Lithuanian legal and regulatory framework for district heating. Presented at IEA workshop «District heating policy in transition economies», Prague, February 2004, 167 p.

4. Georgiadis M. C., Kikkinides E. S., Pistikopoulo E. N. Energy Systems Engineering // WILEY-VCH, Weinheim-2008, 337 p.

5. McGranagham M., Blevins J., Samotyj M. Optimal solution for improving electric energy quality and reliability // Transmission & Distribution World. 2004. № 2. С. 48-52.

6. Ananicheva S. R., Myzin A. L. Substitution schemes and established modes of electrical networks: workbook; 6th ed., revised, Yekaterinburg, UrFU Publ., 2012, 80 p. (in Russ.).

7. Latypov I. S., Sushkov V. V. Reducing power losses in a power distribution network of 6–35 kV voltage in the power supply system for consumers in the oil and gas industry. Proc. of the 5th Int. scientific-practical conf. Culture, science, education: problems and prospects, Nizhnevartovsk, 2016, pp. 107-111 (in Russ.).

8. Vendin S. V., Shcherbinin I. A. On the calculation of the propagation of electromagnetic pulse in the process of microwave processing of dielectric media. Bulletin of the Belgorod State Technological University named after V. G. Shukhov, 2015, no. 2, pp. 204-206 (in Russ.).

9. Vinogradov A. A, Soloviev S. B. Mathematical problems of electric power industry. Methodological guidelines for course paper for students of discipline 140400. Electrical Power Engineering and Electrical Engineering. Belgorod, BSTU named after Shukhov, 2013, 37 p. (in Russ.).

10. Ugarov G. G., Shevchenko N. Yu., Lebedeva Yu. V., Soshinov A. G. Improving the efficiency of overhead power lines of voltage of 110-220 kV in icing areas. Moscow: Pero Publ., 2013, 186 p. (in Russ.).

11. Electrical systems. v. 2. Electrical power networks: work-book. Ed. Venikov V. A., Moscow, Vyshchaya Shkola Publ., 1971, 440 p. (in Russ.).

12. Electrical systems. Operating modes of electrical systems and networks. Ed. V.A. Venikov. Moscow, Higher school, 1975, 344 p. (in Russ.).

13. Block V. N. Electrical power networks and systems. Student training manual. Moscow, Vyshchaya Shkola Publ., 1986, 430 p. (in Russ.).

14. Electrical systems and networks. Student training manual. Ed. Denisenko G. I. Kiev, Vyshchaya Shkola Publ., 1986, 82 p. (in Russ.).

15. Frichtel I. S. Influence of electric power quality on avionic design and weapon system effectivness // Power Cond. Specialists Conf. Rec. (Pasadena, Cal., 1971). New York, 1971. P. 173.

16. Sciubidio E. Spadke napiecia i straty mocy czynnj w liniach 4-przewodowych niskiego napiecia przy niesymetrycznym obciazeniu // Energetyka (DHL). 1975, 29, № 2, pp. 63-64.

17. Aizenberg B. L. Effect of uneven load on phases in a municipal network of 0.4 kV on consumer installation voltage and its economic assessment. In the book: Regulation of voltage in electrical networks. Moscow, Energiya Publ., 1968, pp. 130-135 (in Russ.).

18. Volkov, E. P., Barinov, V. A, Manevich, A. S. The main lines of electric power industry development in Russia, taking into account long-term prospects and improving market relations. Izvestiay Akademii Nauk – Energetika [Proceedings of the Russian Academy of Sciences – Power Engineering], no. 5, 2000, pp. 3-40 (in Russ.).

19. Wainstein L. M., Zhukov L. A. Voltage unbalance in electrical power systems and mode balancing. In the book: Regulation of voltage in electrical networks. Moscow: Energiya Publ., 1968, pp. 444-450 (in Russ.).

20. Vasiliev V. G., Ganikhodjaev N.G., Vasilieva S. P. Regression method for assessing the power losses of electricity in overhead lines of rural networks of 0.38 kV. In Composite Book: Problems of Electrification of Agriculture of Uzbeksky SSR. Moscow, 1979, pp. 101-119 (in Russ.).

21. Goela S. C. Discussion on the Paper: Allowable output from a 3-phase induction motor connected to unsymmetrical supply by N. N. Roy. Author's reply. I. Inst. Eng. (India). Elec. Eng., Div. 1969. 49. Pt. 3. K. 6, pp. 812–816.

22. Frichtel I. S. Influence of electric power quality on avionic design and weapon system effectiveness // Power Cond. Specialists Conf. Rec. (Pasadena, Cal., 1971). New York, 1971, p. 173.

Информация об авторе

Анциферов Никита Сергеевич – ведущий инженер-проектировщик «СК Каскадстрой», Москва, Россия, nikita-anciferov@rambler.ru.

Information about the Author

Nikita S. Antsiferov – Leading Design Engineer "SK Kaskadstroy", Moscow, Russia, nikita-anciferov@rambler.ru.